Carbohydrate-Derivatized Poly(Ethylene Oxide) Hydrogels For Hepatocyte Adhesion

by

Stephanie Therese Lopina

B.S., Chemical Engineering, University of Notre Dame, 1986
M.S., Chemical Engineering, Lehigh University, 1990

Submitted to the Department of Chemical Engineering
in Partial Fulfillment of the Requirements for the Degree of
Doctor Of Philosophy

at the
Massachusetts Institute Of Technology

February, 1996

Signature of Author

Stephanie T. Lopina

Certified by

Professor Linda G. Cima
Thesis Supervisor

Accepted by

Professor Robert E. Cohen
Chairman, Committee for Graduate Students

Carbohydrate-Derivatized Poly(Ethylene Oxide) Hydrogels For Hepatocyte Adhesion

by
Stephanie Therese Lopina

Submitted to the Department of Chemical Engineering on 28 September 1995
in partial fulfillment of the requirements for the degree of
Doctor Of Philosophy

Abstract

Poly(ethylene oxide) creates an scaffold for engineered biomaterials. PEO has been shown to be resistant to nonspecific protein and cell adhesion; its hydroxyl endgroups provide a site for ligand attachment to promote specific hepatocyte adhesion. A series of radiation-crosslinked poly(ethylene oxide) (PEO) hydrogels which span a range of free chain end concentrations and tether lengths were synthesized, characterized and modified with bioactive ligands to create a scaffold for hepatocyte adhesion. The derivatized materials were seeded with hepatocytes to determine the cellular response.

Covalent crosslinks between polymer backbone chains are produced in aqueous PEO solutions through high energy electron beam irradiation, preserving endgroup functionality for further derivatization. Star PEO, with PEO chains emanating from poly(divinyl benzene) cores, was used to produce biomaterials with a large range of endgroup concentrations and tether arm lengths. Swelling and compression measurements confirmed that highly overlapping solutions of star PEO behave in a similar fashion to solutions of linear molecules. Irradiated solutions of high molecular weight linear PEO for hydrogel macrostructure and low molecular weight PEO oligomers for derivatizable endgroups produced hydrogels with many short ligand tethers. Irradiation crosslinked PEO hydrogels were shown to be biocompatible in that they are not functionalized by irradiation, they permit minimal protein adsorption, they do not allow nonspecific cell adhesion and they exhibit minimal inflammatory response *in vivo*.

The PEO hydroxyl endgroups were activated with tresyl chloride chemistry to provide a leaving group for efficient ligand coupling through amines or thiols. Bioactive ligands 1-amino-1-deoxy-ßD-galactose (ADGal) and arginine-glycine-aspartic acid (RGD) were uniformly coupled to activated hydrogels through terminal amino groups.

Hepatocytes adhere and spread on ADGal-modified PEO hydrogels in a concentration/tether length dependent manner, suggesting that spreading is achieved when multiple binding sites are activated on the asialoglycoprotein receptor (ASGP-R), unique to hepatocytes. Hepatocytes did not adhere to unmodified hydrogels or to glucose-modified hydrogels (a negative control). Cells cultured on ADGal-modified PEO hydrogels exhibit normal morphology and function. Cytometry experiments confirm that mechanical forces are transferred to the cytoskeleton through the ASGP-R.

Acknowledgments

While working on my thesis, I have been aided and influenced by many people. I could not possibly thank everyone by name, but will use this space to acknowledge some of the contributions.

The work was funded in part by the National Institute of Health. PEO stars, the base material for most of the substratum produced for this thesis, were kindly donated by Paul Rempp, Pierre Lutz and Bertrand Schmidt of the Institut C Sadron, Strausbourg, France and Professor Edward Merrill of MIT. I enjoyed the many hours spent with Kenneth Wright of MIT's High Voltage Research Lab, who not only ran the 1950s vintage van de Graaf electron beam accelerator with expert skill, but also imparted bits of wisdom along the way. Hepatocyte isolations were completed by others who generously provided hepatocytes for our lab, including Kristen O'Neill of the Shriner's Burn Center (Cambridge, MA); Magali Fountaine, Matthias Kauffman, and Kaoru Sano of the Children's Research Hospital (Boston, MA); Mitsuo Miazawa and George Wu of the Cima lab.

I had the pleasure of working with many undergraduates, whose efforts greatly increased the quantity and quality of data I was able to generate. Thanks to Cynthia Blake-Powell, Scott Cohen, Stephanie DeWeese, Sooyoung Kim, James Quirk, and David Weisburg for the dedicated hours they spent on my projects. Special thanks to Son Nguyen, Raul Rodriguez and Karen Zee whose undying enthusiasm and probing questions kept the intellectual spark alive.

I appreciate the many conversations I had with graduate students Ed Perez, Sue Sofia Allgor, Philip Kuhl, Ann Park and George Wu where ideas were generated and bounced around. Tim Royappa also gave invaluable advice and assistance during his Post-Doctoral appointment in the lab. Working together in a synergistic effort paid large dividends for me.

Special effort was required this past year as I completed my thesis without a home base in Cambridge. I thank the many people who provided a bed or couch for me to sleep on including Sue and Russ Allgor, my former roommates Marie-José Bélanger and Heidi Wald, Mrs. Francis Elliot, Jaqui Lynch and Peter Nelson, Ann Park, Rae Simpson, and Stefan Winkler. I also appreciate the leg work carried out by Sue Sofia Allgor, Wendy Koegler, Ann Park and especially Liz Webb (and undoubtedly others).

Thanks to my lab buddies, Scott Borland, Sue Hobbs and Ann Park, who would always lend an ear when I needed to chat and would occasionally drag me out of the lab for a beer or Tosci's cone. Marie-José and Heidi were awesome roommates. They certainly made our little place on Harvard Street a home. We started out acquaintances and became good friends.

Most of all, I owe a huge debt of gratitude to my husband Tom. He was always at my side through the good and bad; my emotional support all the way. Thanks for believing in me no matter what.

Table of Contents

List of Tables

List of Figures

1. Introduction and Literature Review

1.1 Background and Motivation

Biomaterials - substances other than food or drugs contained in therapeutic or diagnostic systems that are in contact with tissue or biological fluids (Peppas, 1994) - have been used for many decades. The development of polymeric biomaterials has traditionally evolved on a trial and error basis as need arose. Existing materials which exhibit properties suitable for a biomedical need have been implanted and the resulting biological response observed. Optimization has proceeded along the same trial and error scheme, with some success. Table 1-1 lists some such biomaterials presently in clinical use.

Table 1-1. Biomaterials

Polymer	Application
Cellulose	Dialysis membranes
Poly(methyl methacrylate)	Bone cement
Polyurethanes	Catheters, pacemakers
Polytetrafluoroethylene (Teflon)	Catheters, vascular grafts
Polyester (Dacron)	Vascular grafts
Silicone rubber	Catheters, tubing

The ability to specifically engineer a material to meet the precise needs of a biomedical application has obvious benefits. The explosion of knowledge in molecular biology in recent years, coupled with advances in surface chemistry and materials science, provides the foundation to achieve the goal of developing ideal biomaterials designed to meet specific needs. Researchers in the biomaterials community recognize the potential for combining disciplines to develop materials of the future (Peppas, 1994; Ratner, 1993).

One of the goals in the field of biomaterials is development of synthetic implantable materials with surfaces which remain bland and inert towards the adsorption of proteins and cells. Such materials are sought for a wide range of applications including vascular grafts, drug delivery devices, and cell encapsulation membranes. Elucidation of molecular-level events involved in receptor-mediated cell interactions with their natural

environments has made such "inert" materials even more sought after as substratum for immobilizing ligands which foster highly specific cell interactions and precise control of cell behavior from the substrate. Such ligand-modified materials have the potential to enable or facilitate selective migration and growth of cells *in vivo*, thus expanding therapeutic options for regenerating tissues as diverse as bone, nerve, and liver. The biomaterial model for this thesis is the development of a scaffold for hepatocyte (liver cell) transplantation, a proposed alternative to whole organ transplantation.

Presently, whole organ liver transplantation is the only viable option for end-stage liver disease. The need for liver donors continues to grow and far exceeds the available supply. From 1987 to 1992 the number of people on the liver transplant waiting list grew more than 268%, with approximately one quarter of these patients being children under 10 years of age (UNOS, 1992). If hepatocytes can be made to grow on an implantable scaffold while maintaining differentiated function, the available organs could be expanded since only a portion of the liver would be used for each transplant. Increasing the number of transplants would lead to earlier intervention and better tissue matches.

A common theme in the development of inert materials is the incorporation of polyethylene oxide (PEO) as a bulk or surface component. In such composite materials, accumulating experimental evidence supports a positive correlation between the amount of PEO at the surface and resistance to interaction with the biological milieu. The question for implantable biomaterials becomes how to achieve sufficient ethylene oxide (EO) density at the surface of a device. For simple abhesion, only EO segment density matters. The constraints on materials used for ligand immobilization, though, are greater – in addition to high EO segment density, the surfaces must possess a sufficient surface density of free chain ends for ligand attachment, and the bond of the PEO chain to the bulk material must be strong enough to withstand forces exerted by the cells pulling the free end bearing the ligand. A host of considerations – including the number of receptors and their affinity for the ligand, the quantity of receptors which must be occupied to obtain the desired cell response, the spacing between receptors once bound to ligand, and the mobility of the ligand when bound to the substrate – govern the optimal ligand concentration for any given cell type and receptor-ligand system. Ligand surface densities ranging from 50-100,000 ligands/μm^2 (or 10-20,000 nm^2/ligand) have been reported as necessary for achieving appropriate interactions between cells and immobilized ligands in various systems (Weigel, 1978; 1979; Schnaar, 1978; 1989; Guarnaccia 1982a,b; Oka, 1986; Raja, 1986; Kobayashi, 1988; Brandley, 1990; Massia, 1991a,b; Weisz, 1991a,b; Ito, 1992).

One way to meet the constraints of sufficient EO density and strongly-bonded chains as well as general *in vivo* biocompatibility is to employ covalently crosslinked networks comprising primarily EO. Two general approaches for forming PEO networks are endlinking and backbone crosslinking via radiation-induced free radical processes. Several such networks have been described and applied for various applications in biomaterials where abhesion is desired. A major limitation of the network approach, however, is that few chain ends remain available for ligand modification.

A guiding issue in developing inert biomaterials, where the ligands are essentially tethered via PEO chains, is that the concentration of ligand accessible at the surface of the gel is not necessarily the only determinant of cell response to the ligand. It has been demonstrated, for example, that adhesion receptors for extracellular matrix molecules generate a different signal inside the cell when they are clustered together than when free (Kornberg, 1991). If interactions between two or more ligand receptors in the cell membrane are important, then ligand mobility, which is related to the length of the PEO "tether", also becomes a variable in describing the system.

The main thrust of this work is thus to synthesize and characterize a series of radiation-crosslinked hydrogels which spans a range of free chain end concentrations and modify these materials with bioactive ligands to create a scaffold for hepatocyte adhesion. Hydrogels with the structures shown in Figure 1-1 have been formed to vary both the mode and concentration of ligand presented to cells on a synthetic substrate. In gels of type A and B, a gel is formed from high molecular weight linear PEO. In gels of type B, a low molecular weight PEO oligomer is co-crosslinked to the backbone of the linear PEO gel. Most of the free chain ends in the resulting gel are ends of oligomer chains; thus the ligand is presented in closely-spaced groups of two with the spacing between ligands determined by the length of oligomer used. In gels of type C, PEO stars with a high degree of functionality are used to create gels in which the chain ends are more evenly distributed and the tethers are relatively long. Gels of type C are presumed to impart significantly more mobility to the ligand; allowing lower concentrations of ligand to be effective in eliciting a biological response in cases where receptor mobility is important. Some hydrogels are modified with the synthetic peptide arginine-glycine-aspartic acid (RGD), the sequence located within many cell adhesive proteins which is recognized as a ligand for integrin cell-surface adhesion receptors (Orlando, 1991; Kühn, 1994). Other hydrogels have been modified with carbohydrate ligands which interact with liver cells via the hepatic asialoglycoprotein receptor.

Figure 1-1. Hydrogel Variations

1.2 Cell Transplantation

Hepatocyte transplantation is a conceptually attractive alternative to whole organ liver transplants because it could allow early intervention in the treatment of liver disease and increase the donor pool to include living donors. Initial studies of hepatocyte transplantation involved injecting a suspension of hepatocytes directly into existing host tissues such as fat (Jirtle, 1980), liver (Matas, 1976), and spleen (Mito, 1979). The efficiency of this approach is generally low because the hepatocytes must adhere and form new tissue structures within the confines of existing mature tissue. Given these constraints, hepatocyte mass is unable to increase significantly from the original injected mass. Providing an artificial scaffold for the hepatocytes may permit greater hepatocyte growth. Demetriou and coworkers intraperitoneally injected hepatocytes attached to collagen-coated micro-carrier dextran beads (Demetriou, 1987; 1988; Moscioni, 1989). They were able to replace hepatic function in rats with 90% partial hepatectomy for 60 days. Others have examined use of a three-dimensional polymer scaffold on which to anchor cells (Thompson, 1989a; Cima, 1991).

Although some cell survival is seen, one of the key obstacles in obtaining survival and growth of the mass of cells required to have a metabolic impact is the bioreactivity of the material. Polymeric materials which have been employed in transplant devices include collagen-coated dextran beads (Demetriou, 1987; 1988; Moscioni, 1989), polylactic and polyglycolic acids (Cima, 1991), polytetrafluoroethylene (Gore-Tex) (Thompson, 1989a; 1989b), and polyvinyl alcohol (Ivalon) (Soni, 1975; Jackson, 1984). While these materials are all biocompatible in the sense that they are nontoxic and are associated with a mild tissue response, they permit nonspecific protein adsorption and cell adhesion. Numerous studies have been undertaken to measure protein adsorption on various surfaces and identify the cause (Ratner, 1976; 1981; Mori, 1982; Castillo, 1985; Merrill, 1987; Lee, 1988; Jeon, 1991; Andrade, 1992; Norde, 1992; Prime, 1993). Protein adsorption is primarily due to hydrophobic and electrostatic interactions between proteins and the material surface (Andrade, 1992). A case study which carefully measured albumin adsorption and desorption under varying conditions onto surfaces with a range of hydrophilicities found adsorption to be entropically driven (Lee, 1988). Surfaces exhibiting minimal protein binding are amorphous, solvated by water, nonelectrolytic, and H-bond accepting (Merrill, 1987). When materials which permit nonspecific protein adsorption and cell adhesion are implanted, the hepatocytes seeded onto the transplant must compete with connective tissue cells to occupy the surface. Over time, the connective tissue encapsulates the device preventing adherent hepatocytes from

functioning properly. If a very large number of cells are implanted, this may not be a problem and the hepatocytes may dominate the surface. But clinically, it is more likely that a small number of cells will be implanted to grow and cover the surface, forming a new organ. This would not be possible if the device becomes overgrown with other cell types.

1.3 Poly(Ethylene Oxide) (PEO) as Biomaterial

Poly(ethylene oxide) (PEO) is a recognized biomaterial which has been approved by the Food and Drug Administration (FDA) for implantation. A common theme in the development of inert materials is the incorporation of poly(ethylene oxide) as a bulk or surface component. In such composite materials, accumulating experimental evidence supports a positive correlation between the amount of PEO at the surface and resistance to interaction with the biological milieu. The hydrophilicity and solubility properties of PEO produce surfaces which are in a liquid-like state with extremely flexible polymer chains. It is believed that the rapid movement of these chains influences the thermodynamics at the solution/polymer interface. A repulsive force may develop due to a loss of configurational entropy of the surface-bound PEO upon approach of a protein or other particle (Andrade, 1987; Jeon, 1991). Adsorption of proteins is actively prevented as the PEO chains sweep out a large excluded volume (Atha, 1981). The PEO-water interface also has a low interfacial free energy and thus provides a low driving force for protein adsorption – the proteins will not feel any greater effects from the surface than they do from the bulk solution (Andrade, 1973). Proteins adhere much more readily to materials with high surface free energy (Schakenraad, 1989). Andrade describes PEO as the ideal polymer from the perspective of low protein adsorption:

> (PEO) is a neutral molecule, and its weak hydrogen bonding characteristics can be easily satisfied by surrounding water molecules. Its low refractive index suggests that van der Waals interactions will be relatively low. Its stereochemical structure suggests that it tends to fit into the tetrahedral water lattice with minimal perturbation of water structure. It is perturbation of water structure, and particularly its enhanced structuring in the presence of hydrophobic solutes, that leads to the hydrophobic interaction. . . .
>
> PEO is infinitely soluble in water and has exceptionally low chain rigidity. It is a dynamic and mobile molecule in solution. It fits almost all of the criteria for a surface that has minimal interactions of any kind with protein and for a surface that would be of intrinsically high mobility and rapid dynamics, and is therefore optimum for steric exclusion.
> (p. 9, Andrade, 1992).

1.3.1. Grafted PEO

To take advantage of its inert characteristics, PEO is grafted onto potential implantation materials as well as enzymes, drugs and liposomes for use in drug delivery systems. The reticuloendothelial system (RES) rapidly clears drugs and liposomes from the blood, but therapeutic enzymes and liposomes with covalently grafted PEO chains have extended stability in blood circulation (Davis, 1980; Yoshioka, 1991; Needham, 1992). PEO-grafted lipids used in liposomes produced for drug delivery systems have been termed Stealth® lipids to describe their ability to avoid the RES (Needham, 1992).

Many different techniques have been used to graft PEO onto various materials in order to minimize the biological response (Table 1-2). A general trend is observed where an increase in the EO concentration on the surface is inversely proportional to the protein adsorption or platelet adhesion onto the material, but complete resistance to protein adsorption remains difficult to obtain due to constraints on segment densities which can be achieved by grafting. In fact, a low segment density can actually enhance platelet deposition and activation by solvating what would otherwise be a prohibitively hydrophobic substrate, making functional groups on the base material accessible to the biological milieu (Chaikof, 1992). The relationship between EO surface concentration and protein resistance has recently been cast in quantitative terms using an elegant experimental system comprising self-assembled monolayers (SAMs) of alkyl chains modified with EO oligomers of systematically varied length, where very high surface chain densities (and thus complete resistance to protein adsorption) can be achieved (Prime, 1993). SAMs are created when thiol-terminated alkyl or PEO chains adsorb in a tightly packed monolayer onto gold-coated substratum creating densely packed, pseudocrystalline arrays of predominantly trans-extended chains oriented with their sulfur termini at the gold-SAM interface (Nuzzo, 1990). The critical density of grafted chains required for complete protein resistance scaled as $n^{-0.4}$ (n is the number of monomers in the grafted chain), a scaling remarkably consistent with a power law for polymers attached to a surface by one end where the average number of monomer groups a distance R from the surface scales as $n^{0.4}$ (de Gennes, 1980). While SAMs did not spontaneously desorb from gold over several days in water at room temperature (Pale-Grosdemange, 1991) biological shear forces and forces exerted by cells may pull adsorbed moieties from the surface, making SAMs unsuitable for implantation. These studies suggest that implantable substratum could be made protein resistant given a sufficient PEO segment density.

Table 1-2. PEO Grafting Techniques

Grafting Technique	Substrate	Reference
adsorption	glass	Hiatt, 1971
	mica	Luckham, 1985
	quartz	Gasanov, 1991
di/tri-block adsorption		
PEO-co-PVC	PVC	Nagaoka, 1990
PEO-co-PPO, PEO-co-PBO	polyethylene	JH Lee, 1989
carbodiimide coupling	poly(L-lysine)	Sawhney, 1992
	cellulose	Kishida, 1992
cyanuric chloride activation	proteins	Abuchowski, 1977
	PET	Gombotz, 1989; Desai, 1991b
dithio-carbamate photo-grafting	PVC	Mori, 1982; Nagaoka, 1984; Nakao, 1986
epoxide reaction	polystyrene	Bergström, 1992
hexamethylene diisocyanate coupling	polyurethane	Han, 1989
photo-polymerization	glass	Tseng, 1992
radiation	silastic film	Sun, 1987
	PET	Merrill, 1990
surface-physical-interpenetrating-network	PET, PMMA, polyurethane	Desai, 1991a
2,4,6-trichloro-s-triazine activation	enzymes	Davis, 1980

PBO - poly(butylene oxide)
PEO - poly(ethylene oxide)
PET - poly(ethylene terephthalate)
PMMA poly(methyl methacrylate)
PPO - poly(propylene oxide)
PVC - poly(vinyl chloride)

1.3.2. PEO Networks

Given the difficulty in obtaining a pure PEO surface by covalently grafting PEO chains to implantable materials (Chaikof, 1986; Gombotz, 1989; JH Lee, 1989; Merrill, 1990; Desai, 1991a,b; Andrade, 1992; Prime, 1993; Drumheller, 1995), attention has turned to the formation of networks with PEO as an intrinsic component. The PEO component of non-covalent networks formed with block copolymers of PEO and poly(L-lactide) (PLLA) (Hu, 1993) or PEO and polysiloxane (Pekala, 1986a,b; Verdon, 1990) act to reduce protein adsorption and platelet activation from that observed with the base (PLLA or polysiloxane) material. Methoxy poly(ethylene glycol) monomethacrylates with PEO side chains of various lengths (MnG, where n equals the number of EO repeat units), can be polymerized with methylmethacrylate (MMA) to create covalently crosslinked hydrogels with inherent PEO characteristics (Nagaoka, 1984; JH Lee, 1990). In a similar manner, PEO-diacrylates photopolymerize with trimethylolpropane triacrylate (TMPTA) to create grafted semi-interpenetrating networks with a significant PEO component (Drumheller, 1995). Once again, enough PEO must be incorporated into the copolymer to mask the MMA or TMPTA. Platelet and protein adsorption were eliminated in a MMA-PEO copolymer with 35 wt% MnG of $n > 50$ (Nagaoka, 1984). A similar degree of PEO incorporation was required to prevent the adhesion of human foreskin fibroblasts (HFF) to TMPTA-PEO networks (Drumheller, 1995).

Networks consisting solely of PEO would presumably be exempt from concerns of biological interactions with copolymers or substratum. PEO networks can be prepared by the crosslinking reactions of PEO with plurifunctional isocyanates (Graham, 1984; Gnanou, 1987; Yoshikawa, 1989). The isocyanates become network junctions with PEO chains endlinked to consecutive junctions to form the macrostructure (Figure 1-2). While such a network produces a purely PEO material, few free chains are available for further derivatization and attachment of bioactive moieties. Although the isocyanates are extremely reactive and unlikely to be free after crosslinking, their presence in the hydrogel will create added concerns for FDA approval of a device manufactured in this manner.

A novel biodegradable PEO hydrogel which is formed by *in situ* photopolymerization was shown to eliminate thrombosis and preserve long-term patency after crushing rat carotid arteries. It was also shown to inhibit thrombosis and reduce long-term intimal thickening in rabbit arteries injured by balloon angioplasty (Hill-West, 1994). The polymer precursor combines the inert character of PEO (center chain) with the water lability of poly(lactic acid) (adjacent segments); and is capped with tetraacrylate termini

to provide polymerizability. This material shows promise for producing implantable inert hydrogel barriers, but no chain ends remain for further derivatization with bioactive moieties.

PEO networks with random links distributed along the polymer backbone, as opposed to being restricted to the chain ends, can be achieved through radiation crosslinking (Merrill, 1983; 1990; Minkova, 1989). This preserves hydroxyl endgroups for derivatization and ligand attachment while eliminating reagents needed for chemical crosslinking which may produce undesired reactions within the biological system (Figure 1-2). Irradiation of PEO in aqueous solution breaks down the water into hydrogen and hydroxyl radicals. PEO crosslinks are formed when the hydrogen radicals abstract hydrogens from the polymer backbone creating macroradicals. These macroradicals diffusion terminate by coupling to each other, forming the covalent carbon-carbon crosslink. Either gamma irradiation (Minkova, 1989), or high energy electron beam irradiation (Merrill, 1983; 1990) are effective in producing PEO hydrogels. Since PEO crosslink formation from macroradicals is a bimolecular reaction, the reaction rate should be proportional to the second power of macroradical concentration. Maximizing the radiation dose rate maximizes the concentration of macroradicals and favors crosslinking over degradation. Therefore, electron radiation, with a dose rate three orders of magnitude greater than gamma radiation, is the preferred source to optimize radiation crosslinking of PEO solutions (Merrill, 1990).

The hydroxyl groups present on the end of each PEO chain provide the only site for ligand coupling chemistry. A hydrogel of linear PEO (Figure 1–1 A) would have very few hydroxyl groups available for derivatization. The endgroup concentration in the gel can be increased by irradiating a solution which includes both high MW PEO to provide hydrogel macrostructure and low MW PEO oligomers which will increase the number of endgroups (Figure 1-1 B). Another option is to produce hydrogels from high functionality PEO stars. Rempp and coworkers have developed a star form of the polymer in which PEO "arms" are grafted onto an anionically polymerized divinyl benzene core, typically 10-60 arms per star (Gnanou, 1988; Merrill, 1990; Rempp, 1990). Radiation crosslinking of the stars into hydrogels provides a 5-30 fold increase in available hydroxyl groups over linear polymer hydrogels (Figure 1-1 C). Preliminary studies indicate that a "pure" PEO surface is presented, completely masking the divinyl benzene core (Merrill, 1990; Rempp, 1990).

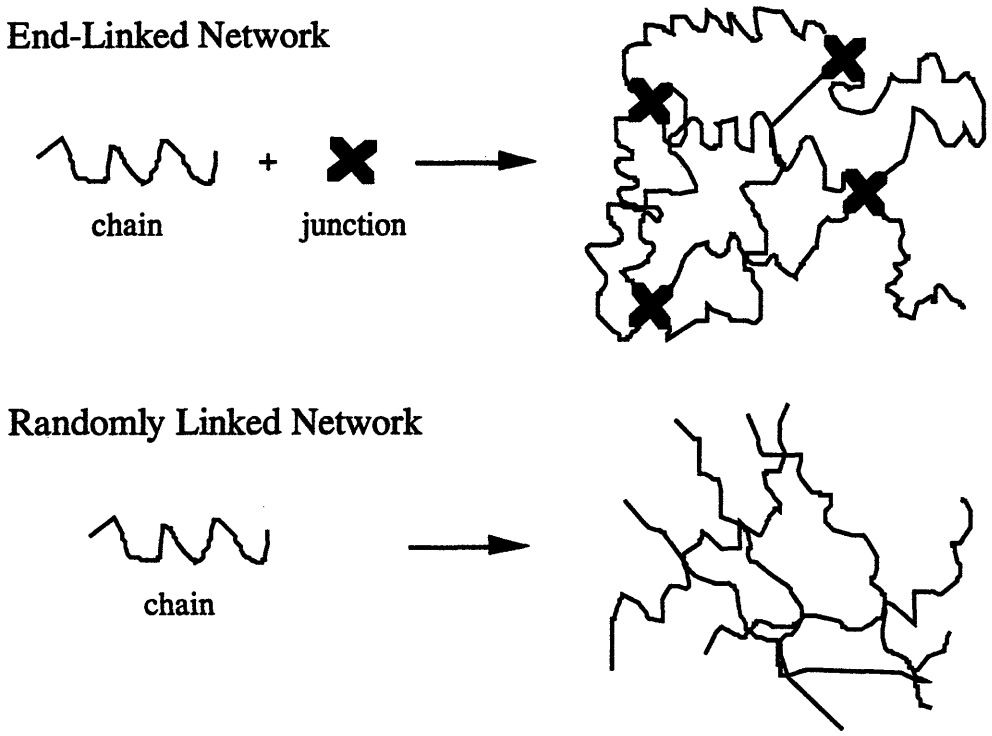

Figure 1-2. PEO Networks. End-linked networks have chemical crosslinking agents and few chain ends available for ligand derivatization. Randomly linked networks are crosslinked along the polymer backbone.

1.4. Cell Receptors

One of the ways cells interact with their environment is through receptors, proteins on the surface of cells which have binding sites with high affinity for particular substances, referred to as "ligands". Receptors fall into several classes, depending on their primary functions. Some receptors serve to transduce signals which control cell growth, govern protein synthesis and secretion, and regulate the composition of intracellular fluids. Selective binding of ligands such as hormones, pheromones or neurotransmitters initiates a sequence of reactions that changes the cell function. Other receptors are involved in the selective uptake of extracellular proteins, growth factors and hormones via receptor-mediated endocytosis. Two examples include the low-density lipoprotein (LDL) receptor which removes LDL cholesterol from the blood stream and the asialoglycoprotein receptor (ASGP-R) which removes abnormal serum glycoproteins to be destroyed in the cell lysosomes. Receptors also play a role in cell adhesion, both cell-cell adhesion (*e.g.* cadherins) and cell-matrix adhesion (*e.g.* integrins). Molecular biologists have been

making great strides towards increasing the understanding of molecular-level events involved in receptor-mediated cell interactions. Thus, there is an emerging rational basis for design of biomaterials with immobilized ligands which control cell behavior via receptor-mediated events. To create a transplantation scaffold for the treatment of liver disease, the polymer matrix should interact in a highly selective manner with hepatocytes while remaining bland to other cells.

1.4.1. Integrins and Cell Adhesion

Integrins form a major class of cell receptors which interact with proteins of the extracellular matrix (ECM) leading to cell adhesion. Integrins are transmembrane heterodimeric glycoproteins composed of noncovalently associated α and ß subunits with a single ligand binding site (Figure 1-3). At least 14 α subunits and 8 ß subunits have been identified, but the $ß_1$ and $ß_3$ subfamilies are primarily involved in interactions with the ECM. Integrin subunit structure, binding characteristics, and function have been described in detail in several reviews (Ruoslahti, 1987; Buck, 1990; Kühn, 1994). Once the integrin binds ligand, conformational changes lead to an association between the cytoskeletal portion of the receptor and the attachment proteins vinculin, talin, and α-actinin forming focal adhesion patches (Stamatoglou, 1990; Massia, 1991; Wang, 1993). These attachment proteins then bind to actin and microtubules in the cytoskeleton to physically link actin-associated proteins with the extracellular matrix (Beckerle, 1990; Otey, 1990; Turner, 1990). Through this direct link, bound integrins are able to transmit mechanical forces from the extracellular matrix to the cytoskeleton, affecting cell adhesion, shape and function (Ingber, 1991, Wang, 1993; 1994).

Cell adhesion to foreign surfaces in the body is typically mediated by proteins adsorbed from extracellular fluids. Specific amino acid sequences found in extracellular matrix proteins form the ligands which bind to integrins. The RGD sequence (found in fibrinogen, fibronectin, vitronectin, collagen, thrombospondin, and von Willebrand factor) was one of the first to be identified as an integrin-recognition motif; its binding to various integrins has been well documented (Buck, 1990; Orlando, 1991; Kühn, 1994). Surfaces which present immobilized RGD become cell adhesive as the peptide is bound by the integrins, transferring forces to the cell cytoskeleton (Massia, 1991a,b; Lin, 1992). Other amino acid sequences have been found to have similar effects, including arginine-glutamic acid-aspartic acid-valine (REDV) found in fibronectin (Hubbell, 1991) and tyrosine-isoleucine-glycine-serine-arginine (YIGSR) found in laminin (Hubbel, 1991; Massia, 1991b). Nonspecific adhesion occurs when proteins adsorb onto a surface,

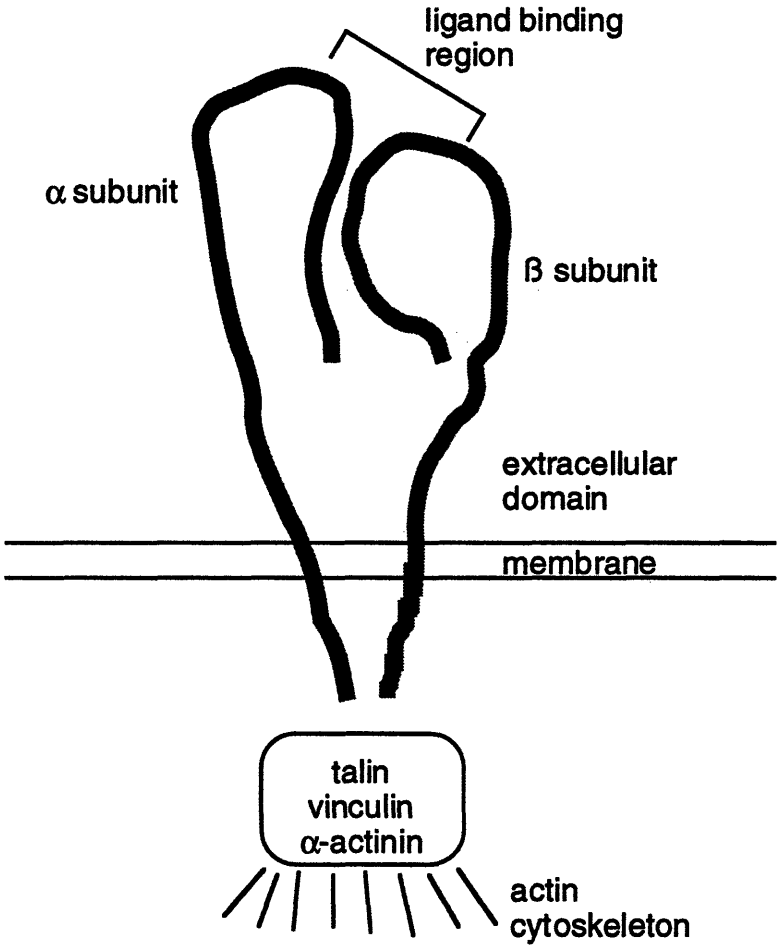

Figure 1-3. The integrin receptor is composed of an α and ß subunit with a single ligand binding site. Ligand-bound integrins interact with the cytoskeleton through attachment proteins talin, vinculin and α-actinin. (Redrawn from Buck, 1990.)

thereby presenting these and other cell adhesion moieties to cell adhesion receptors (van Wachem, 1987). One approach to promote cell adhesion to synthetic scaffolds is to incorporate these natural peptides into the polymer matrix. However many cells, including endothelial cells, fibroblasts and connective tissue, have receptors for these peptide sequences, limiting the usefulness of an inert base. The integrin receptor for REDV seems to be unique to endothelial cells since REDV modified surfaces do not support the adhesion of human foreskin fibroblasts, human vascular smooth muscle cells or platelets while promoting human umbilical vein endothelial cell adhesion (Hubbell, 1991). There may be other peptide/integrin pairs which are unique to particular cell

types, even hepatocytes, but they have yet to be identified. A material which will permit the adhesion of hepatocytes while remaining bland to the rest of the biological milieu would incorporate a ligand which interacts with a receptor unique to hepatocytes.

1.4.2. Hepatic Asialoglycoprotein Receptor

Hepatocytes have a unique receptor for asialoglycoproteins (ASGP) which may be exploited for development of a cell transplantation device. Unlike integrins, the ASGP receptor is not known to be attached to the cytoskeleton, but it may still provide a mechanism for hepatocyte adhesion. The ASGP receptor has been studied extensively both in the solubilized form (Sarkar, 1979; Baenziger, 1980; Lee, 1987; Drickamer, 1988) and intact within the hepatocyte membrane (Hubbard, 1979; Connolly, 1982; Lee, 1983; Townsend, 1986) and the results have been summarized in several excellent reviews (Schwartz, 1984; Spiess, 1990; Lodish, 1991; Geffen, 1992). Long researched as a model for receptor-mediated endocytosis, the ASGP-R binds asialoglycoproteins – proteins which have lost sialic acid endgroups exposing a terminal galactose residue which is bound by a ß-bond to the next residue. The ASGP-R has specific affinity for galactose residues, functioning to clear these damaged proteins from the circulation. Ligand-bound receptors migrate to clathrin-coated pits which are endocytosed, forming vesicles which transport the damaged proteins to lysosomes for degradation (Wall, 1981; Drikamer, 1988; Fuhrer, 1991). Once the ligand has separated from the receptor, the receptor is recycled to the cell surface with a cycle time of 60-150 minutes (Bridges, 1982; Schwartz, 1982; Weigel, 1984). (Figure 1-4)

The hepatic ASGP-R is a member of the class of mammalian lectins designated C-type lectins, which exhibit an absolute requirement for Ca^{++} to bind carbohydrate ligands (Tolleshaug, 1980). Affinity studies indicate that while mono-, bi-, and triantennary galactose-terminated oligosaccharides are all taken up by the ASGP-R, receptor binding affinity in intact hepatocytes increases by five orders of magnitude as the ligand valency increases from a single galactose to a tri-branched form (Connolly, 1982; Rice, 1993). Binding affinity for the isolated receptor does not vary with ligand valency, suggesting an organizational or structural difference between the isolated receptor and the intact receptor in the cell membrane. The human ASGP-R is a hetero-oligomer composed of two related polypeptide chains designated HHL-1 and HHL-2 (HHL for Human Hepatic Lectin) (Lodish, 1991), each with its own galactose binding site (Figure 1-5). The rat ASGP-R is composed of three subunits, RHL-1, RHL-2 and RHL-3. The only difference

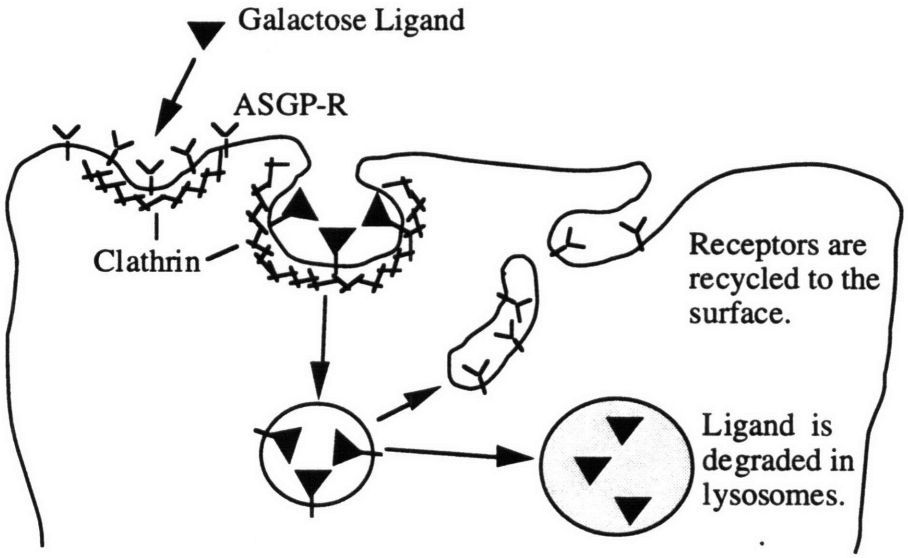

Figure 1-4. Asialoglycoprotein receptor endocytosis and recycling.

between RHL-2 and RHL-3 is the glycosylation pattern, which does not affect ligand binding or receptor oligomerization (Sawyer, 1988; Rice, 1993). These two receptor subunits can be considered as one, RHL-2/3, equivalent to the HHL-2. Both HHL-1 and HHL-2 receptor subunits have been cloned and expressed in fibroblasts and hepatoma cells; from these studies it has been demonstrated that the subunits HL-1 and HL-2 cooperate to enable high-affinity binding of triantennary ligands. HL-1 by itself is unable to bind and internalize triantennary ligands, while HL-2 functions to enable high affinity binding of triantennary ligands without affecting endocytosis of bound ligand-receptor complexes (Shia, 1989). Evidence points to a structure of the fully functional ASGP-R as comprising at least one HL-2 chain and at least three HL-1 chains (Lodish, 1991, Rice 1993). The optimal spacing of sugar moieties in tri-branched ligands (*i.e.*, the spacing giving the highest affinity binding) is consistent with the spacing between the binding sites of a [$(HL\text{-}1)_3$(HL-2)] receptor structure as described by Lodish (Lodish, 1991) and shown in Figure 1-5. Molecular dynamics simulations provides a carbohydrate conformational theoretical basis for the observed relationship between galactose spacing and binding affinity (Balaji, 1993). The great affinity of binding triantennary ligands suggests a conformational change on triantennary binding which induces cytoskeletal interactions (Baenziger, 1980; Connolly, 1982).

The ASGP receptor appears an attractive candidate for hepatocyte adhesion to the polymer scaffold. It is unique to the hepatocyte and exhibits selective binding to galactose-terminated oligosaccharides, which can be immobilized on PEO tethers. The binding affinity for di- and triantennary ligands are greater than the binding affinity between integrins and ECM proteins (Table 1-3). The long flexible PEO tethers may allow multifunctional receptor binding, even with monoantennary ligands. Achieving trivalent binding may induce a conformational change which leads to cytoskeletal interactions (Baenziger, 1980; Connolly, 1982) and cell spreading.

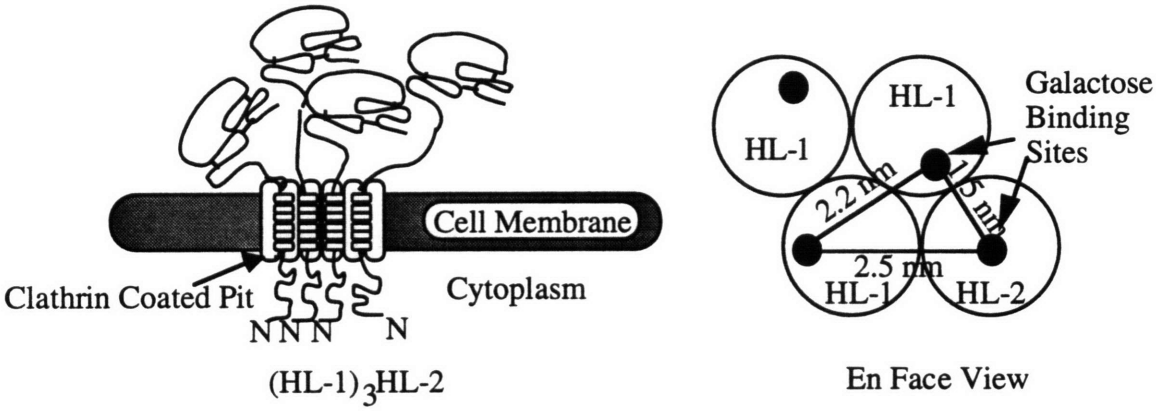

Figure 1-5. Asialoglycoprotein Receptor

1.5. Hepatocyte Adhesion to Materials with Bound Glycosides

Hepatocyte adhesion to bound glycosides was first investigated to study the role carbohydrates may play in cell-cell adhesion (Weigel, 1978; 1979; Guarnaccia, 1982a,b). Flat synthetic polyacrylamide gels which had been derivatized with various carbohydrates were used as a model system. Researchers found a specificity of rat hepatocyte adhesion to immobilized galactose-terminated ligands, matching observations made with soluble ligands. Adhesion was found to be a threshold phenomena with a critical ligand concentration of 3 mM (mmoles ligand per liter of gel) (Weigel, 1979). Immobilization of a cluster glycoside which contains three glycosidically linked sugars (Figure 1-6) did not alter the critical ligand concentration (Weigel, 1979). This result may be expected as the cluster glycoside used does not have the galactose spacing which soluble ligand affinity studies have shown to be critical for high affinity binding (YC Lee, 1984;1989;

Table 1-3. Ligand dissociation constants.

Receptor	Ligand	K_d (nM)	Ref.
Integrin	fibronectin	1500-3000	Hubbell, 1991
	fibrinogen	2200-2300	Altieri, 1991
	vitronectin	900-1000	Orlando, 1991
ASGP-R	Gal(ß1-4)GlcNAc(ß1-2)Man	283,000	YC Lee, 1984; 1989
	Gal(ß1-4)GlcNAc(ß1-2)Man(α1-6)\ Man Gal(ß1-4)GlcNAc(ß1-2)Man(α1-3)/	13,200	YC Lee, 1984; 1989
	Gal(ß1-4)GlcNAc(ß1-6)\ Man Gal(ß1-4)GlcNAc(ß1-2)/	1,750	YC Lee, 1984; 1989
	Gal(ß1-4)GlcNAc(ß1-6)\ Gal(ß1-4)GlcNAc(ß1-2)Man(α1-6)\ Man Gal(ß1-4)GlcNAc(ß1-2)Man(α1-3)/	81.3	YC Lee, 1984; 1989
	Gal(ß1-4)GlcNAc(ß1-2)Man(α1-6)\ Man Gal(ß1-4)GlcNAc(ß1-2)Man(α1-3)/ Gal(ß1-4)GlcNAc(ß1-4)/	1.85	YC Lee, 1984; 1989

Gal - galactose
GlcNAc - N-acetylglucosamine
Man - mannose

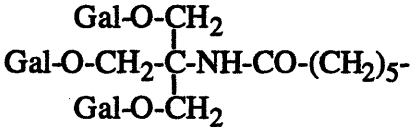

Figure 1-6. Polyacrylamide gel-bound cluster glycoside.

Rice, 1993). A distinct and separable critical concentration of 30-70 mM is required for adherent hepatocytes to spread, 10 fold greater than that required for hepatocyte adhesion (Oka, 1986). One theory put forward to account for the difference is that the force generated between the substratum and the cell surface must attain a minimum value per unit surface area of contact in order for spreading to occur (Oka, 1986). This force could be increased by increasing the total number of hepatocyte-substratum interactions (increasing the ligand concentration) or by increasing the association constant of a constant number of interactions (using high affinity ligands).

Polyacrylamide surfaces containing covalently bound carbohydrates were used further to study ASGP-R function intact within the cell membrane. Because the hepatic ASGP-R is a C-type lectin, Ca^{++} is required to achieve ligand binding (Geffen, 1992). Asialoglycoproteins bound to the ASGP-R from the solution state are rapidly released from the receptor in the presence of a divalent cation-free buffer containing a chelating agent (Tolleshaug, 1980; Weigel, 1984; Schwartz, 1984). Similar behavior might be expected of hepatocytes adherent to surfaces through the ASGP-R. However, hepatocytes are difficult to remove from galactose-modified polyacrylamide gels using a chelating agent (Schnaar, 1978; Weisz, 1991a). This inability to remove adherent cells depends on the time of incubation on the substrate; for incubation times less than about 30 minutes cells can be released readily by a chelating agent but they become progressively more difficult to remove as the incubation time is increased (Schnaar, 1978; Weigel, 1978). Receptor-ligand binding is a noncovalent, reversible phenomena. While free ligand was successful in blocking hepatocyte adhesion, once bound the cells exhibited sugar-resistant adhesion on the same time scale as resistance to chelating agents (Guarnaccia, 1982b). Concomitant with increasing difficulty of disrupting the bonds between the ASGP-R and immobilized ligands using chelating agents or competitive ligand, the strength of adhesion between the cells and the substrate, as assayed by centrifugal detachment, also increases over the first 45 minutes (Guarnaccia, 1982a; Weisz, 1991b). Adhesion-strengthening requires the concerted interactions of cytoskeletal components, actin and microtubules, and clathrin, a major component of coated pits. All of these elements had to be disrupted to counteract the time dependent adhesion strengthening (Weisz, 1991b). Based on these observations, Weisz and Schnaar proposed an interaction between the ligand-bound receptor and the cytoskeleton which required the participation of coated pit proteins (Weisz, 1991b) but did not describe a mechanism.

1.5. Hepatocyte Adhesion to Materials with Bound Glycosides

Oligosaccharide-substituted styrene-type macromers and their polymerizates have been produced as a coating agent to enhance hepatocyte adhesion and viability on polystyrene culture dishes (Kobayashi, 1988). Galactose-specific adhesion with a critical threshold concentration required for adhesion was observed, similar to the behavior of hepatocytes seeded onto galactose-modified polyacrylamide gel. Hepatocytes adherent to polystyrene culture dishes which had been precoated with polystyrene-co-lactose were better able to maintain differentiated function over seven days in culture as compared to hepatocytes cultured on standard collagen-coated tissue culture dishes (Gutsche, 1993).

In the context of biomaterials design, the ultimate goal of understanding a particular receptor-ligand interaction is an ability to control cell and tissue behavior *in vivo*. Ideally, an *in vitro* assay should mimic the *in vivo* situation as closely as possible. Thus, the material used to present ligands in the *in vitro* assay should also be suitable for physiological implant. Polyacrylamide exhibits unsatisfactory biocompatibility *in vivo* (Gin, 1990) and is thus not an ideal material for such applications. Any adsorbed modifications, such as the polystyrene-co-lactose, will wear away *in vitro*, proving unsuitable over time.

The ideal biomaterial, as described by Ratner and Hoffman (Ratner, 1976) "does not cause thrombosis, destruction of cellular elements, alteration of plasma proteins, destruction of enzymes, depletion of electrolytes, adverse immune responses, damage to adjacent tissue, cancer and/or toxic or allergic reactions." PEO meets these criteria: it has been shown to minimize protein and platelet adsorption and activation, has been approved by the FDA, and can be made into hydrogels with the desired mechanical properties to mimic soft tissue. Derivatization with galactose ligands should produce a hepatocyte specific material, and the long flexible PEO arms may permit multi-valent ligand binding on the ASGP-R.

2. Materials Development and Characterization

The polymer scaffolds produced for this thesis are based on poly(ethylene oxide), a biomaterial which is generally recognized as exhibiting minimal nonspecific protein adsorption. The majority of the work focuses on PEO hydrogels, which present a pure PEO surface to cells in culture. A complementary system of PEO chains grafted to glass was also considered.

2.1. PEO Characteristics

Poly(ethylene oxide) stars produced by living anionic polymerization from divinyl benzene (DVB) cores were provided by P. Rempp and B. Schmidtt of Strasbourg, France. Star PEO was obtained in the form of a powder which contained traces of the initiator, naphthalene, and other impurities. Analysis of a 5% (w/v) solution of the polymer in deuterated chloroform by proton NMR revealed, in addition to the expected peaks at δ = 3.7 (ether hydrogens) and δ = 7.3 (aromatic hydrogens), several broad peaks in the range δ = 0.9 - 2.6. Impurities were removed by adsorption on activated charcoal from a 5% (w/v) solution of the polymer in MilliQ-purified water. The charcoal was precipitated from the solution by repeated centrifugation at 1200xg and the resulting clear polymer solution was dried by rotary evaporation. NMR analysis of the purified polymer revealed only the ether hydrogens and a peak at δ = 7.3 arising from the hydrogens on the DVB core of the stars. A peak due to hydrogens in the terminal hydroxyl position was not detected above the noise; this peak would be < 50% of the area of the aromatic hydrogens. The unassigned peaks which had been observed prior to purification were completely removed. Star characteristics have been studied by light scattering (Allgor, unpublished). While the polydispersity of star arm molecular weight (M_a) is very narrow, the number of arms attached per star (f) is quite broad leading to a large range of star sizes in a give batch.

Linear PEO (nominal MW 100K) obtained from Polysciences as a powder containing approximately 1% silica added as a flowing agent was purified in a similar fashion. The molecular weight and polydispersity of linear PEO was determined by GPC in chloroform using a 3-column sequence (PL-gel guard, linear, and 1000-Å) with RI detection. Data were analyzed with Perkin Elmer Turbochrome 3 software. Values of Mn = 29,750 and Mw/Mn = 4.3 were obtained. Characteristics of the polymer precursors used in forming the gels are shown in Table 2-1.

Table 2-1. Polymer Characteristics

Linear Polymer		
Polymer Designation	Molecular Weight	Polydispersity
PEO	29,750	4.3
Oligomer		
Polymer Designation	Molecular Weight	
PEG	1000	
TEG	200	
Star Polymer		
Polymer Designation	Number of Arms	Arm Molecular Weight
S3210	40	3,460
S3498	36	10,000
S3509	55	10,473
S3510	70	5,200
BS10.4	186	10,000

2.2. PEO Hydrogel Formation

PEO hydrogels present a pure PEO surface to the cells, eliminating any chance of interaction with an underlying surface which may be present in a grafted system. Irradiation crosslinking provides two advantages over chemical crosslinking: (1) Crosslinks formed via irradiation occur along the polymer backbone, preserving the hydroxyl endgroups for derivatization and ligand attachment. (2) Irradiation crosslinking does not incorporate reagents such as those needed for chemical crosslinking which may produce undesired functionalization, affecting the cell response.

Many of the technologically important properties of gels, such as the permeability to solutes, elastic modulus, and the average length of dangling chain ends which can be functionalized with specialized chemical groups, are functions of the network structure. The structure of a gel network formed by radiation-induced crosslinking of star molecules will fall between two extremes depicted in Figure 2-1. At one extreme, crosslinks are formed primarily between arms of the same star molecule, with few star-star crosslinks. This behavior is expected if the stars essentially repel each other in solution. At the other extreme, the dominant mode of crosslinking is star-star, resulting from free

interpenetration of the arms of adjacent star molecules in solution. Assuming that chains of neighboring stars interpenetrate freely at concentrations above a critical concentration, it should be possible to obtain both extremes of network behavior by varying the weight concentration ω_p of a particular star molecule in the crosslinking solution or, alternatively, by varying the arm molecular weight, M_a, at constant star functionality, f, and ω_p. For identical crosslink concentrations, these two structures are expected to yield different properties. Dominance of star-star crosslinking should result in a higher elastic modulus and lower permeability to solutes.

Crosslinked star networks may have a fundamental application in helping elucidate the solution properties of star polymers. Free-radical mediated crosslinking of polymer chains in solution serves to "freeze" neighboring segments; the resulting network structure should reflect aspects of the relative proximity of interchain and intrachain segments. In solutions of star molecules, analysis of network structures formed by radiation crosslinking may allow corroboration of light- and neutron-scattering evidence which suggest that in the semi-dilute regime the arms of star polymers freely interpenetrate and behave essentially as solutions of linear molecules (Adam, 1991; Willner, 1994).

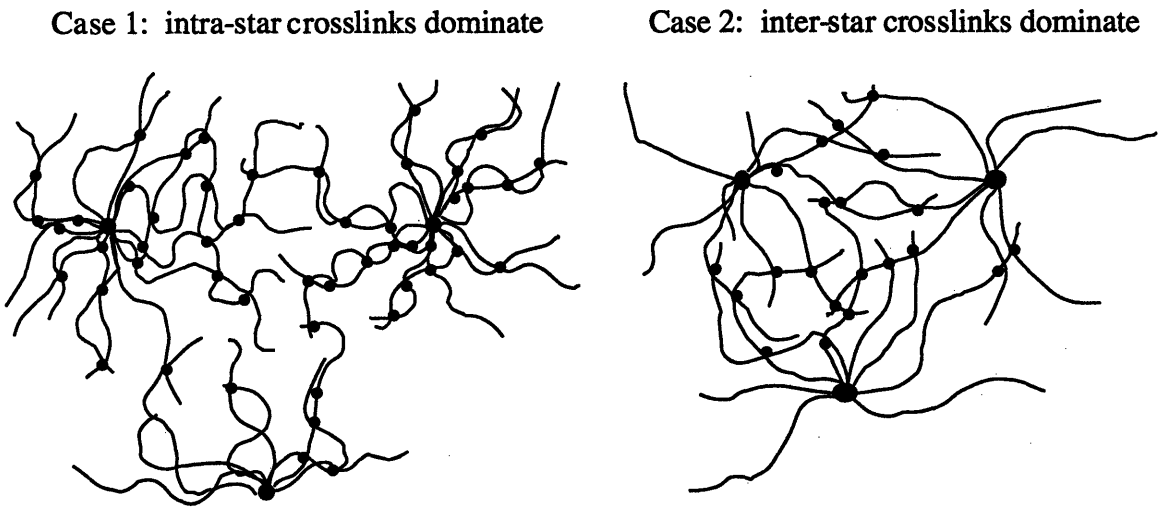

Figure 2-1. Radiation induced crosslinks in star PEO will fall between the extremes of intra-star and inter-star crosslink dominance.

2.2.1. Radiation Chemistry

Polymers will either crosslink or degrade when subjected to ionizing radiation. (Here ionizing radiation may be either high energy electron or gamma radiation.) While the distinction between which polymers will crosslink *vs.* degrade is not clear, some trends have been observed. Radiation effects can be considered a kinetic phenomena with crosslinking and chain scission (degradation) as competing reactions. Crosslinking is favored between polymers with an easily abstracted hydrogen or methyl group while large side groups off the polymer backbone lead to degradation (Peppas, 1986). Chapiro notes a correlation between the heat of polymerization and the tendency to crosslink, reporting that polymers with a heat of polymerization greater than 16 kcal/mol tend to crosslink (Chapiro, 1962).

Specifically considering poly(ethylene oxide), crosslinks are formed when hydrogens are abstracted from the polymer backbone creating macroradicals. These macroradicals diffusion terminate by coupling to each other, forming the covalent carbon-carbon crosslink. The competing reaction of main chain scission leaves a carbon or oxygen radical at the end of a polymer chain which will degrade to an inert chain end by various mechanisms. When crystalline PEO is irradiated in the bulk, chain scission dominates over crosslinking (King, 1967). Crosslinking is slightly favored when irradiation is carried out in the melt, likely due to the increased mobility of the polymer chains (Graham, 1960).

Increased chain mobility was the original objective when researchers started to irradiate polymers in solution (King, 1970). Indeed, crosslinking greatly dominates when PEO is irradiated in solution. However, the preference for crosslinking is not solely due to increased chain mobility, but rather to a change in the route towards the formation of crosslinks. PEO crosslinks in solution are formed by an indirect interaction with water radiolysis products as the mediator which increases the efficiency of formation of main chain carbon radicals and thus increases the efficiency of crosslinking (King, 1970). Chemical reactions involved in water radiolysis and PEO crosslinking are outlined in Table 2-2. Since PEO crosslink formation from macroradicals is a bimolecular reaction, the reaction rate should be proportional to the second power of macroradical concentration. Maximizing the radiation dose rate would maximize the concentration of macroradicals and favor crosslinking over degradation. Therefore, electron radiation, with a dose rate three orders of magnitude greater than gamma radiation, is the preferred radiation source to optimize radiation crosslinking of PEO solutions (Merrill, 1990).

The presence of oxygen during irradiation can adversely affect the crosslinking process, leading to polymer degradation, particularly at low dose rates (Peppas, 1986). Degradation may be initiated by the formation of weak peroxidic bonds in the polymer backbone which decompose causing oxidative degradation of the main chain (Table 2-2) (Dennison, 1986). The degradation creates carbonyls in the network, an undesirable functionality for "inert" biomaterials. The strong polarity of carbonyl groups imparts a charge to the polymer, which increases nonspecific protein adsorption and cell adhesion (Andrade, 1992; van Wachem, 1987). The increased dose rate of electron beam irradiation reduces the oxygen effect (Peppas, 1986).

2.2.2. Van de Graaf Electron Generator

PEO crosslinking was achieved using high energy electrons produced from a 3 MeV van de Graaf electron generator at the MIT High Voltage Research Laboratory. Mr. Kenneth Wright operated the generator at all times. The generator can provide up to 10 Mrad/s to a sample up to 7.5 cm wide, with a uniform penetration depth of about 1 cm in aqueous PEO solutions. Samples pass through the beam on a conveyer belt, with the dose rate delivered varying with electron beam current and belt speed. The total dose received depends on the dose rate and number of passes through the beam.

Radiation was delivered to samples at a rate of 250,000 rad/s with total dose delivered ranging from 2 to 25 Mrad. In a few instances, samples were packed in ice, but in general no attempt was made to dissipate the heat generated during irradiation. Hydrogen gas produced during radical recombination (Table 2-2) may become trapped and form bubbles in the finished gel. Bubble formation was prevented by staging the irradiation in 2 Mrad doses separated by a minimum of 20 hours, allowing the hydrogen to diffuse from the gel.

2.2.3. Sample Preparation

After purification, PEO was dissolved in sterile MilliQ water to the desired concentration (2-20 wt%). All linear/oligomer hydrogels were formed from solutions containing a 4:1 weight ratio of linear PEO to oligomer. Radiation-induced chain scission and formation of side products (carbonyls, unsaturation) was minimized by degassing the polymer solutions to remove oxygen. Solutions were deaerated under vacuum for approximately 1 hour and then backflushed with nitrogen. Samples were irradiated in 2-g aliquots weighed into clean 60-mm glass petri dishes, keeping the depth of PEO solution exposed to the beam below 3 mm to insure that the dose received

Table 2-2. Radiation Chemistry

water radiolysis

(1)

hydrogen abstraction

(2)

PEO crosslinking

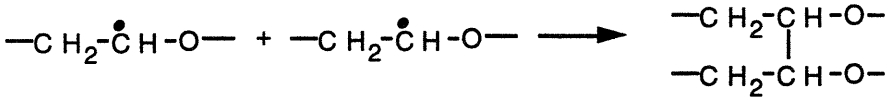

(3)

radical recombination

(4)

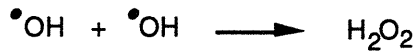

(5)

chain scission

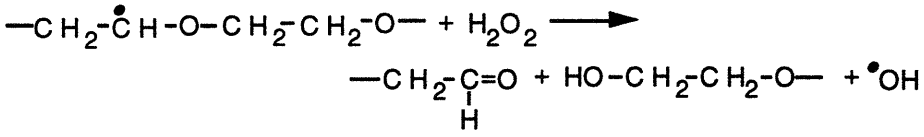

(6)

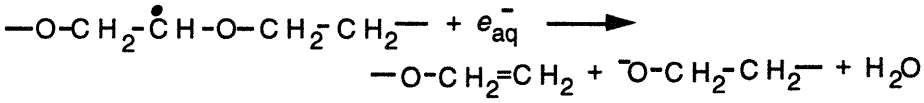

(7)

oxygen reactions

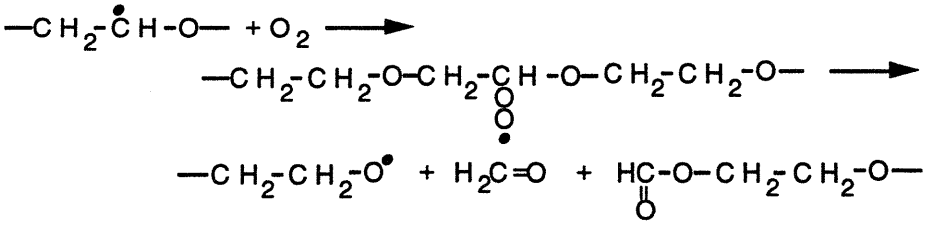

(8)

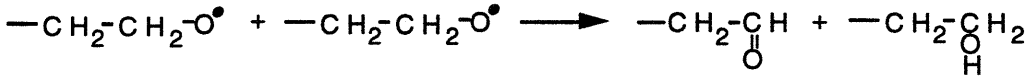

(9)

remained uniform throughout the material. The dishes were covered with standard glass petri dish covers and the edges were sealed with parafilm. The high radiation dose effectively sterilizes the gels and they were handled as sterile after crosslinking. Samples were stored in a 4°C refrigerator between staged irradiation doses and after the final irradiation.

2.2.4. Hydrogel Functionalization

The main reaction incurred during radiation crosslinking is recombination of main chain carbon radicals to form crosslinks. However, other minor reactions can occur which lead to formation of carbonyl groups and unsaturated linkages, which are undesirable because these groups are often reactive in a biological environment (Table 2-2). FTIR spectroscopy analysis was used to verify that the crosslinking conditions used in these experiments did not result in formation of undesired reactive groups. The FTIR spectrum of purified PEO in Figure 2-2a shows the canonical C-H stretch at 2950 cm^{-1}, the C-O-C ether band at 1125 cm^{-1}, and various C-H modes between 600 and 1500 cm^{-1}. There is a small peak at 2000 cm^{-1} which is traceable to residual bound water present in the polymer. This bound water is notoriously difficult to remove entirely from the polymer (Pedley, 1979). The spectrum of the crosslinked polymer shown in Figure 2-2b is substantially similar to that of the parent material, which indicates that there is no gross alteration in the chemistry of the base material from irradiation, either by oxidation, conjugated π-bond formation or other degradation pathways. There is a notable absence of any peaks in the 1500-1900 cm^{-1} region, which clearly indicates the lack of any carbonyl functionalities in the gel. There are also no unsaturated bonds in the gels, judging by the absence of any significant peaks in the 2000-2600 cm^{-1} region. Finally, the absence of conjugated linkages is also borne out by the colorlessness of the gels. Irradiation of PEO to form hydrogels does not appear to alter the properties important for inert characteristics.

2.3. Molecular Weight Between Crosslinks

The network structure of PEO hydrogels produced by electron beam irradiation influences the accessibility of the gel-linked ligand to cell surface receptors and governs the permeability of the gel to nutrients and to molecules (such as extracellular matrix proteins) secreted by the cells. The average molecular weight between crosslinks, M_c, is a significant measure of the hydrogel network structure. The average molecular weight between crosslinks is also the average molecular weight between a terminal crosslink and

A

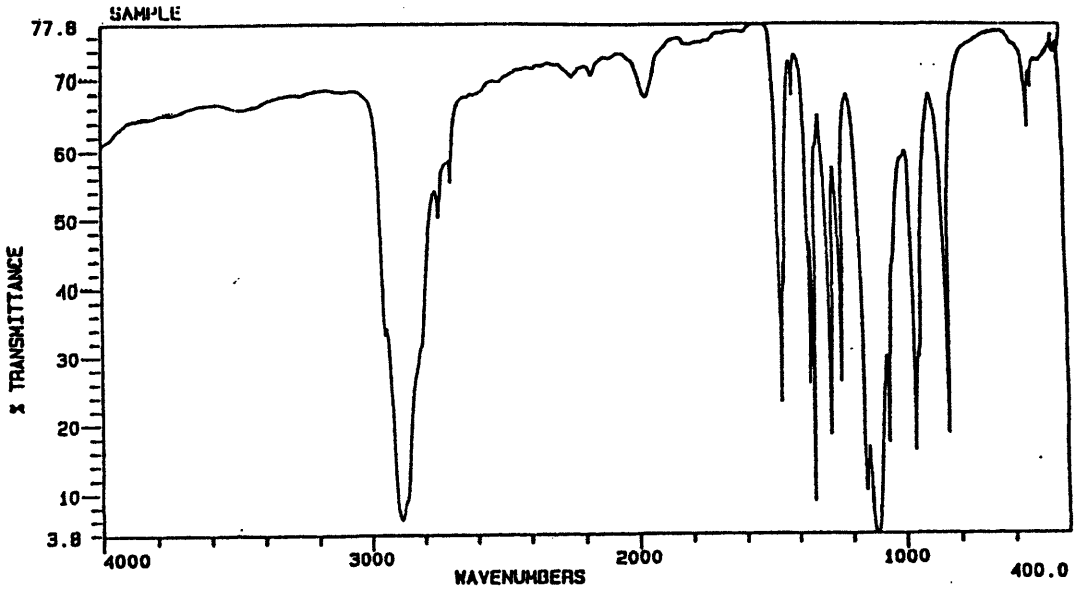

B

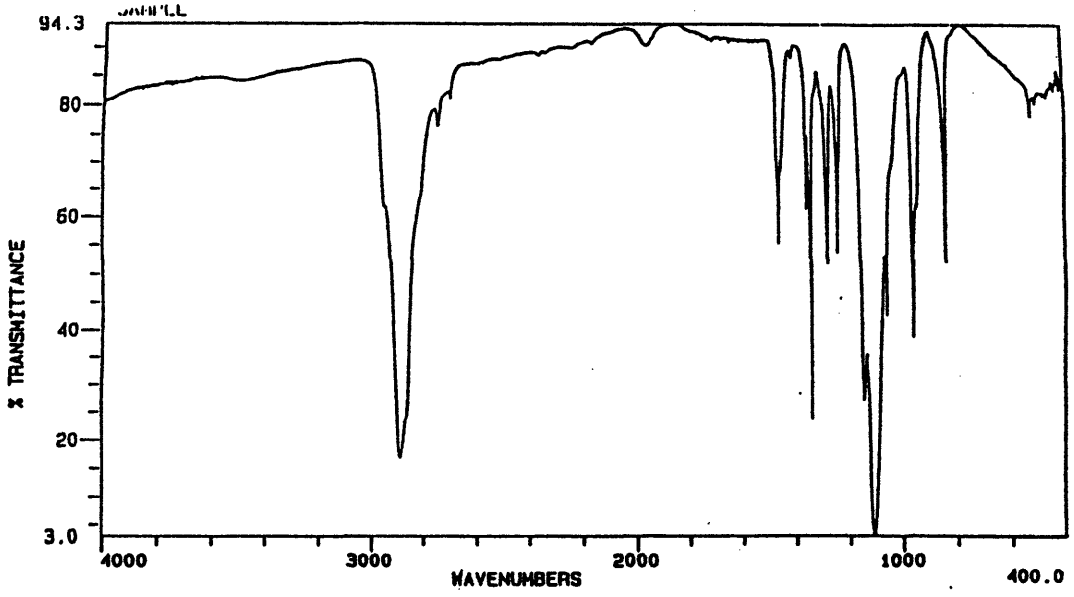

Figure 2-2. FTIR spectra of (a) pure 100,000 MW PEO and (b) dried PEO gel formed by crosslinking a 20% solution with a radiation dose of 8 Mrad.

the chain end, therefore, for linear and star gels, M_c is also the average ligand tether length. For linear/oligomer gels, 70-90% of ligand is linked to the ends of the oligomers, and thus the tether length for these gels is closer to 0.5 $MW_{oligomer}$. M_c can be determined from rubber elasticity theory using either equilibrium swelling measurements or stress-strain curves obtained from uniaxial deformation.

2.3.1. Equilibrium Swelling

Once irradiated, a hydrogel will swell in solvent to an equilibrium swollen volume (or deswell in the case of syneresis). This swelling behavior of hydrogel networks has been investigated for many years. Theoretical and experimental investigations support the use of Flory's theory based on Gaussian chain statistics for predicting the crosslink density in networks which possess a low volume fraction of polymer, homogeneous F-functional junctions, and low or moderate degrees of crosslinking (Flory, 1950; Gnanou, 1987). Bray, Peppas and Merrill modified the original swelling equation to account for networks formed in the presence of solvent (Bray, 1973; Peppas, 1976).

The theoretical development is based on the balance of elastic forces of the chains holding the network together and the mixing forces trying to pull the chains apart as solvent enters the hydrogel. Mathematically, equilibrium is reached when the chemical potential of the solvent in the network is equal to the chemical potential of the solvent in the bulk.

$$\mu_1 - \mu_1^0 = 0 = \frac{\partial \Delta G}{\partial n_1} \tag{2-1}$$

where μ_1 and μ_1^0 are the chemical potentials of solvent in the network and in the bulk, respectively, ΔG is the change in free energy, and n_1 is the number of moles of solvent. As noted above, the change in free energy includes a mixing term and an elastic term:

$$\Delta G = \Delta G_{mix} + \Delta G_{el} \tag{2-2}$$

The standard Flory-Huggins relationship is used to determine the free energy of mixing polymer and solvent, yielding:

$$\frac{\partial \Delta G_{mix}}{\partial n_1} = kT\left[\ln(1-\upsilon_{2s}) + \upsilon_{2s} + \chi_1 \upsilon_{2s}^2\right] \tag{2-3}$$

where k is the Boltzmann constant, T the absolute temperature, χ_1 the polymer-solvent interaction parameter (referred to as "chi parameter"), and υ_{2s} the polymer volume fraction of the fully swollen gel.

The elongation term was developed from a statistical mechanical treatment of the entropic change with network swelling (Flory, 1950). The theory takes into account the number of elastically effective chains and the degree of stretching. An elastically effective chain extends between two crosslinks in the network, and therefore does not include loops or free chain ends (Figure 2-3). Including the modification developed by Bray and Peppas for networks formed in solution where the relaxed network is partially swollen (Bray, 1973; Peppas, 1976), the elongation term is expressed:

$$\frac{\partial \Delta G_{el}}{\partial n_1} = \frac{kTV_1}{v_p^*}\left(\frac{1}{M_c} - \frac{2}{M_n}\right)\upsilon_{2r}\left[\left(\frac{\upsilon_{2s}}{\upsilon_{2r}}\right)^{1/3} - \frac{1}{2}\left(\frac{\upsilon_{2s}}{\upsilon_{2r}}\right)\right] \tag{2-4}$$

where V_1 is the solvent molar volume, v_p^* the polymer specific volume, M_n the number average molecular weight of the uncrosslinked polymer, and υ_{2r} the polymer volume fraction of the relaxed, unswollen gel. The $(2/M_n)$ term takes into account free chain ends which are a necessary result of radiation crosslinking. The (1/2) in the final term

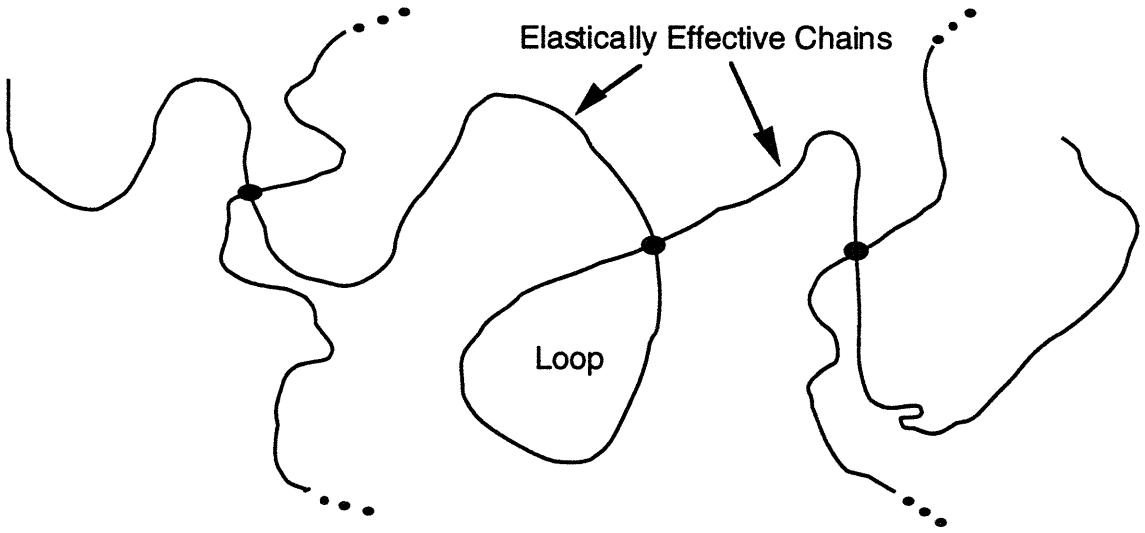

Figure 2-3. Elastically Effective Chains.

assumes tetrafunctional crosslinks – four polymer chains emanating from a crosslink junction – which is valid for radiation-induced crosslinks formed along the polymer backbone.

Combining equations (2-1) through (2-4) and solving for the quantity of interest, M_c, yields the swelling equation:

$$\frac{1}{M_c} = \frac{2}{M_n} - \frac{\frac{v_p^*}{V_1}\left[\ln(1-\upsilon_{2s}) + \upsilon_{2s} + \chi_1 \upsilon_{2s}^2\right]}{\upsilon_{2r}\left[\left(\frac{\upsilon_{2s}}{\upsilon_{2r}}\right)^{1/3} - \frac{1}{2}\left(\frac{\upsilon_{2s}}{\upsilon_{2r}}\right)\right]} \tag{2-5}$$

2.3.1.1. Swelling Measurements

Immediately after irradiation, hydrogels were weighed, transferred to sterile 100 mm tissue culture dishes and swollen in sterile MilliQ water. The gels were allowed to swell for 5-15 days, exchanging swelling media daily. Fully swollen hydrogels, free of any sol fraction, were carefully reweighed and stored in 70% ethanol to maintain sterility and minimize possible polymer degradation from free radicals (McGary, 1960). Equations (2-6) and (2-7) were used to calculate polymer volume fractions from experimental measurements.

$$\upsilon_{2,r} = \frac{w_p}{w_p + \left(w_r - w_p\right)\left(\frac{\rho_p}{\rho_s}\right)} \tag{2-6}$$

$$\upsilon_{2,s} = \frac{w_p}{w_p + \left(w_s - w_p\right)\left(\frac{\rho_p}{\rho_s}\right)} \tag{2-7}$$

where ρ_p and ρ_s are the polymer and solvent density, respectively (1.2 g/cm^3 for PEO, 1.0 g/cm^3 for water), w_r the weight of the relaxed hydrogel, w_s the weight of the fully swollen gel and w_p the dried polymer weight in the gel. To obtain the dried polymer

weight, portions of swollen hydrogel were weighed into glass petri dishes which had been dried in a 50°C oven for a minimum of 24 hours to remove any moisture. Dishes with swollen hydrogel were placed in a 40°C vacuum oven with desiccant until a constant volume was obtained (2-5 days). Dried polymer and dish were reweighed, with the dish weight subtracted out to obtain the final dried polymer weight.

2.3.1.2 Linear Hydrogels

The endgroup concentration (and therefore potential ligand concentration) of a hydrogel made strictly from linear PEO chains is relatively low, making them less adaptable for a bioactive scaffold. The primary aim in crosslinking linear PEO in this work was to provide a reference for analyzing the crosslinking results for the more complex star solutions or linear/oligomer mixed solutions formed under identical conditions. Crosslinking of linear PEO by irradiation in aqueous solutions has been studied extensively (Dennison, 1986; Minkova, 1989) and the general relationships between dose, initial polymer concentration, and resulting crosslink density have been described. The Flory-Huggins χ_1 interaction parameter for linear, uncrosslinked PEO (M_n = 35,000) has a constant value of 0.426 in the volume fraction range 0.04-0.15; increasing linearly with volume fraction at higher polymer concentrations (Dennison, 1986). The volume fractions of PEO in the linear gels produced for this thesis are all within the range where χ_1 is constant.

In radiation-induced crosslinking, the number of macroradicals formed is proportional to the dose received. As expected, for a constant initial volume fraction of polymer, υ_{2r}, M_c decreases with increasing radiation dose but a limit is reached where M_c is small and chains are constrained from further crosslinking; this limit for PEO in water is $M_c \approx 1500$ (Dennison, 1986). Increasing the dose above this limit switches the kinetics from favoring crosslinking to favoring degradation, so chain scission dominates. The total number of radicals formed at a given dose is constant. The initial polymer volume fraction affects the molecular weight between crosslinks at a given dose: a lower concentration of polymer would receive more radiation per chain, leading to a decreased M_c.

A quantity which can be derived from linear crosslinking experiments is the concentration of radiation-induced crosslinks (number of crosslinks per volume of relaxed hydrogel, μ_r) formed as a function of dose and initial polymer concentration. This quantity is

$$\mu_r = \frac{\omega_p}{2M_n}\left(\frac{M_n}{M_c} - 1\right) \tag{2-8}$$

where ω_p is the weight concentration of polymer in the initial solution. As discussed above, the molecular weight between crosslinks is a function of both dose and polymer volume fraction in the irradiated solution. However, the concentration of crosslinks formed at a given dose is relatively insensitive to the concentration of polymer over the range of conditions used to make hydrogels (Figure 2-4).

Plotting the average crosslink concentration over all polymer volume fractions *vs.* dose shows a strong correlation and confirms the weak dependence on polymer volume fraction (Figure 2-5). The curve starts to decrease at a dose of 20 Mrad (Figure 2-5 A), which corresponds to the M_c plateau described in Dennison's work (Dennison, 1986). At high doses, chain scission actively competes with crosslink formation decreasing the total number of crosslinks formed. Removing data points which include significant chain scission or syneresis, a linear relationship is found between dose and crosslink concentration ($r^2 = 0.992$, Figure 2-5 B):

$$\mu_r = 1.2232 \bullet D - 1.8308 \tag{2-9}$$

where μ_r is expressed in mM and D is Mrad irradiation dose. Although the data at 20 Mrad was not used to fit the curve, the large error bars at that point make the curve prediction a reasonable estimate of crosslink formation in the 2-20 Mrad dose range.

2.3.1.3. Star Hydrogels

2.3.1.3.1 Theoretical Development

The network structure obtained by radiation crosslinking of star PEO solutions will depend on the degree of interpenetration of adjoining stars, which calls for a quantitative relationship between the concentration of PEO stars in aqueous solution and the expected degree of arm overlap. The polymer chains are modeled as a string of blobs of diameter $\xi(r)$ where $\xi(r)$ increases with distance r from the star core (Figure 2-6) (Daoud, 1982; Birshtein, 1984). In dilute solutions, the behavior of stars deviates significantly from linear molecules – stars act as individual molecules with little interpenetration (Figure 2-6 A). In slightly more concentrated solutions, the Daoud-Cotton model describes a star in terms of three regions: an extended core of melt-like segments, an intermediate region

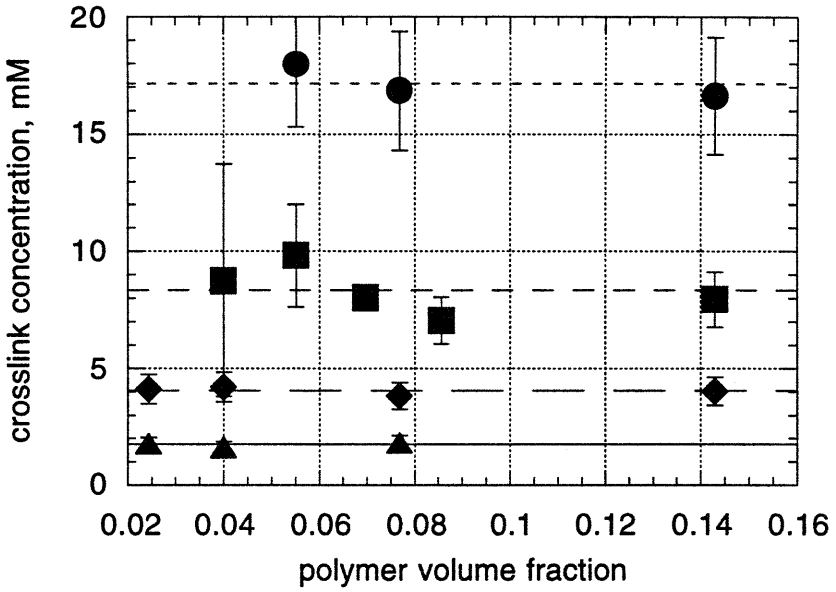

Figure 2-4. Crosslink concentration for four representative irradiation doses administered to PEO in aqueous solution over a range of initial polymer volume fractions: circles – 20 Mrad, squares – 8 Mrad, diamonds – 5 Mrad, triangles – 2.5 Mrad. Crosslink concentration is relatively insensitive to polymer concentration for a given irradiation dose. Error bars represent standard deviation of 2-10 measurements. Figure includes some data taken from Dennison (Dennison, 1986).

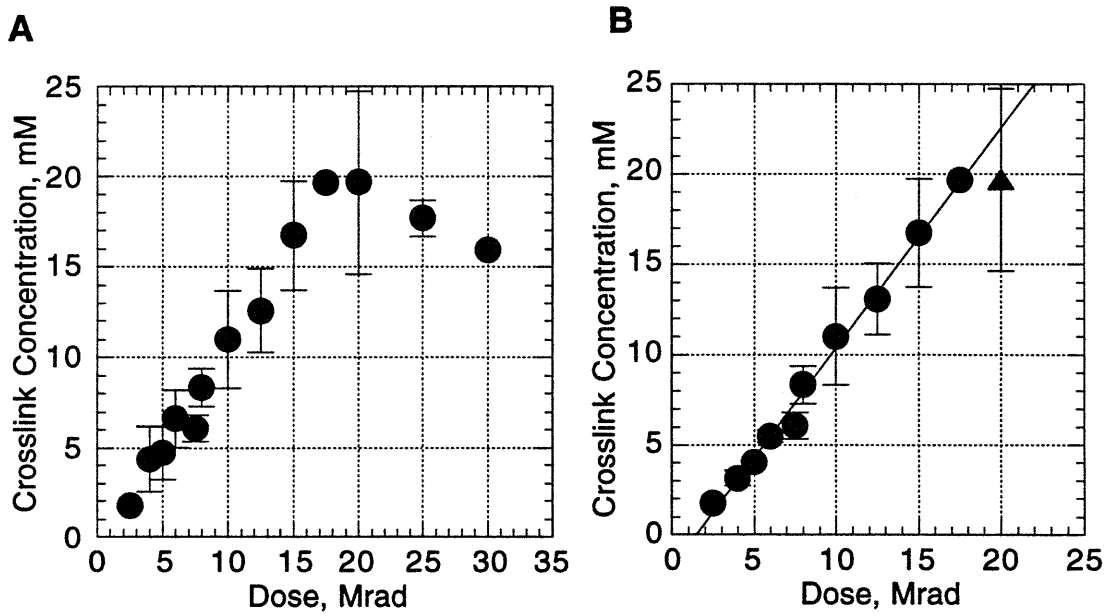

Figure 2-5. Crosslink concentration plotted as a function of radiation dose received (A) for all linear PEO data points or (B) excluding data points with significant chain scission or syneresis. Line is fit through crosslink concentration through 17.5 Mrad by least squares regression ($r^2 = 0.992$). Error bars represent standard deviation of 2-10 measurements. Figure includes some data taken from Dennison (Dennison, 1986).

where the chains are ideal and concentrated, and an outer region where the chains are semidilute (Daoud, 1982). Chain overlap occurs in this outer region (Figure 2-6 B).

Experimental and theoretical results (Birshtein, 1986; Grest, 1987; Vagberg, 1991; Roovers, 1993) support a model in which the outer semidilute regime dominates suggesting extensive chain overlap. An asymptotic scaling of the segment density ρ as a function of r for stars with $f > 30$ can be written:

$$\rho(r) \propto f^{(3\lambda-1)/2\lambda} r^{(1-3\lambda)/\lambda} \tag{2-10}$$

For a star of specified functionality f, this scaling law can be written

$$\rho(r) = A(r/a_s)^{1/\lambda} r^{-3} \tag{2-11}$$

where a_s is the statistical segment size. The exponent λ has the value 3/5 for a good solvent and thus applies for the PEO-water system. This same scaling dependence on r has been verified by self-consistent field analysis of polymer chains in a good solvent

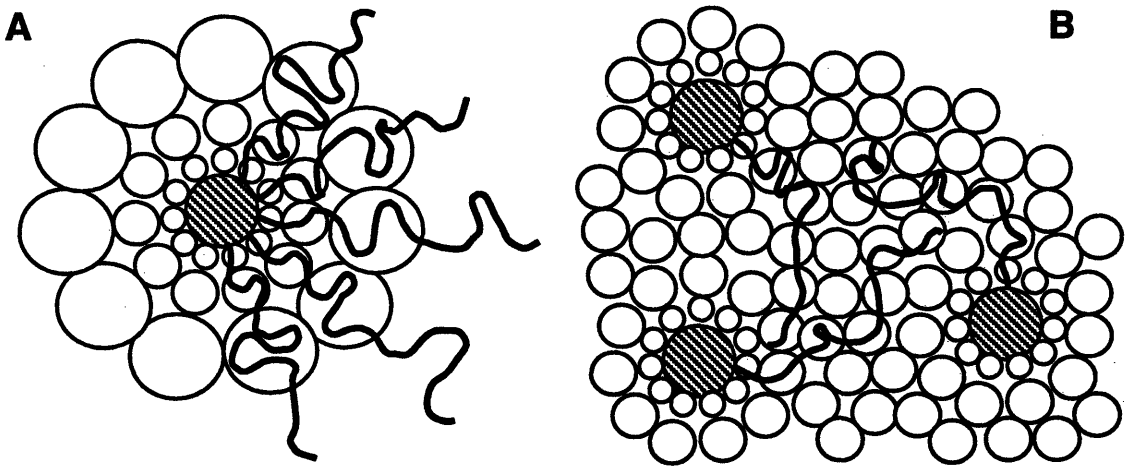

Figure 2-6. Star polymer conformation in solution. (A) In dilute solution stars act as individual molecules. (B) In semi-dilute solutions star arms overlap in the semi-dilute region (Region III). Region I, the extended core of melt-like segments, is represented with diagonal lines. (Redrawn from Birshtein, 1986.)

attached at high densities to spherical interfaces (Dan, 1992). Equating the segment density at the core-corona boundary leads to a quantitative value for the scaling prefactor:

$$A = \frac{3 \bullet 4^{1/\lambda} f^{(3\lambda-1)/2\lambda}}{32\pi} \tag{2-12}$$

Near the overlap regime, experimental evidence for star-star repulsion and liquid-like ordering has been reported (Adam, 1991). At higher concentrations, in the semidilute range, extensive overlap between stars is predicted (Daoud, 1982; Witten, 1986). This overlap has been demonstrated experimentally. Furthermore, light scattering and neutron scattering studies have shown that solutions of stars in the semi-dilute regime exhibit static and dynamic behavior similar to solutions of linear chains at the same concentration (Adam, 1991; Willner, 1994).

The extent to which the arms of adjacent stars interpenetrate can be estimated by equating the local segment density with the average concentration in solution (Daoud, 1982) and solving for the radius R_0 corresponding to the boundary between the more concentrated core region and the bulk. A schematic of the segment density as a function of the distance from the star core for overlapping stars is shown in Figure 2-7. For the case of extensive overlap, denser core regions are just small perturbations in bulk average concentration and the equality is simply

$$\frac{\omega_p N_a}{M_m \bullet 10^{21}} = \frac{A(R_0/a_s)^{1/\lambda}}{R_0^3} \tag{2-13}$$

where N_a is Avagadro's number, and M_m is the molecular weight of a single monomer unit (44 gm/mol) ω_p is in gm/ml, and r and a_s are in nm (a_s = 2.0 nm; EM Lee, 1990). This is the regime in which crosslinked structures should be formed in order to analyze the behavior by a modified swelling theory, because that theory pertains to networks with a homogeneous segment density. For a star with specified f and M_a, the appropriate ω_p to achieve essentially complete overlap of stars can be estimated by setting R_0 approximately equal to the size of the core. At lower concentrations (and thus less extensive overlap), contributions to the total concentration from the non-overlapping, excluded regions and the overlapping, bulk regions contributions must be considered separately. Thus the "bulk" concentration on the left-hand side of Equation (2-13) is corrected for the presence of denser cores and the equality becomes:

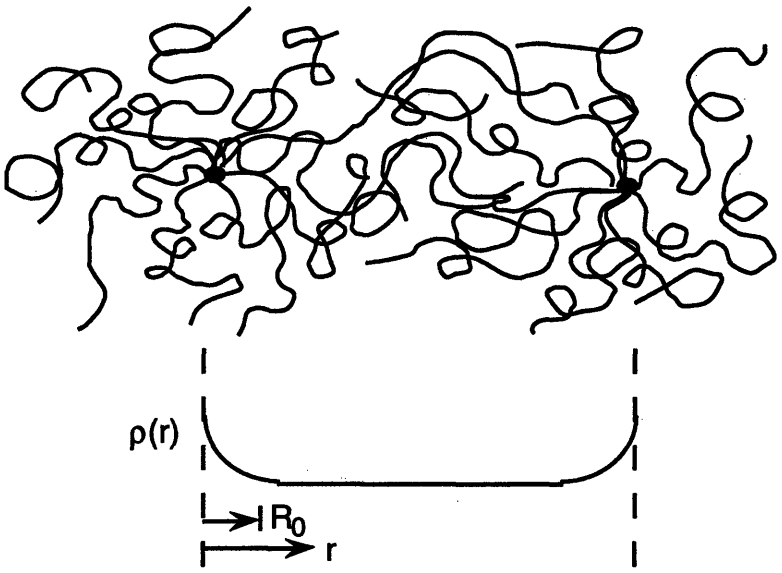

Figure 2-7. Local segment density as a function of distance r from the star center in semidilute solutions. At R_0, the local segment density is equal to the average bulk concentration and the stars interpenetrate up to this distance.

$$10^{-21}\frac{\frac{\omega_p}{M_m}-\frac{\omega_p N_a}{M_{star}}\int_0^{R_0}4\pi r^2\rho(r)dr}{1-\frac{\omega_p N_a}{M_{star}}\frac{4\pi R_0^3}{3}}=\rho(R_0). \qquad (2\text{-}14)$$

Properties of the star solutions used for crosslinking are shown in Table 2-3, along with the overlap radius, R_0. The average distance d_c between the cores of neighboring stars is also shown for comparison. The volume fraction corresponding to non-overlapping regions is < 2% in all cases. Thus, from the perspective of segment density, the solutions of stars can be treated as solutions of linear molecules and the resultant hydrogels can be analyzed with a modified swelling equation.

The swelling equation derived for linear polymers cannot be applied directly to radiation-crosslinked star hydrogels because star hydrogels contain a bimodal distribution of crosslink functionalities – tetrafunctional junctions induced by radiation and *f*-functional junctions at the star cores. Under the assumption that the arms of the star

Table 2-3. Star Solution Overlap Radius

Polymer	M_a	f	ω_p	d_c (nm)	R_0 (nm) (a_S = 2 nm)	R_0 (nm) (a_S = 1 nm)
S3210	3,460	40	0.0837	14	1.0	2.3
			0.0434	17	1.6	3.8
S3498	10,000	36	0.0923	19	0.9	2.0
			0.0750	20	1.0	2.6
			0.0387	25	1.6	3.9
S3509	10,473	55	0.0750	23	1.2	3.0
S3510	5,200	70	0.0387	25	2.3	5.5
BS10.4	10,000	186	0.0923	32	2.0	4.6

molecules behave as Gaussian chains, the Flory-Bray swelling equation can readily be modified to account for a bimodal crosslink distribution.

To account for bimodal crosslink functionalities, we follow Flory's original development (Flory, 1950) in which a network is formed from ν chains joined into $2\nu/F$ junctions, where F is the junction functionality (commonly, 4). Flory gives the probability that all ν chains will be joined into $2\nu/F$ groups as

$$\Omega = \left(\frac{F\Delta\tau}{V}\right)^{2\nu(F-1)/F}\left[\left(\frac{2\nu}{F}\right)!\right]^{F-1} \tag{2-15}$$

where $\Delta\tau$ is the volume increment and V is the total volume of the system containing all the ν chains.

For a bimodal distribution of crosslink functionalities, we assume that the network is formed in two steps: formation of star cores ($F_2=f$) followed by formation of tetra-functional radiation-induced crosslinks ($F_1=4$). The network ultimately consists of internal subchains which are joined to the network at both ends and subchains with free terminal ends. In the crosslinked star system the number of free terminal ends is assumed equal to the number of star arms, f, since the joining of two free arm ends by radiation is an unlikely event.

To describe the formation of the crosslinked star network, let ν_0 denote the total number of pairs of ends linked to junctions and $\nu_s/2$ the pairs of free chain ends. The total number of chains in the fully developed network is thus $\nu_0 + \nu_s/2$. The first step is formation of ν_s/F_2 star cores from a subset of all available ends, $2\nu_0 + \nu_s$. The tetrafunctional links (designated by F_1 for generality) are then formed from a subset of the remaining ends. The total probability thus becomes:

$$\Omega = \frac{\left[\left(\frac{2(\nu_0+\nu_s/2)}{F_2}\right)!\right]^{F_2-1}\left[\left(\frac{2\nu_0}{F_1}\right)!\right]^{F_1-1}}{\left[\left(\frac{2\nu_0}{F_2}\right)!\right]^{F_2-1}\left[\left(\frac{\nu_s}{F_1}\right)!\right]^{F_1-1}}\left(\frac{F_2\Delta\tau}{V}\right)^{\nu_s(F_2-1)/F_2}\left(\frac{F_1\Delta\tau}{V}\right)^{2(\nu_0-\nu_s/2)(F_1-1)/F_1} \tag{2-16}$$

Derivation of the entropy and enthalpy of network formation and swelling then follows directly from the development of Flory (Flory, 1950). The resulting expression for the change in free energy of the network ΔG with respect to change in the number of solvent molecules n_1 during swelling becomes:

$$\frac{1}{kT}\frac{\partial\Delta G}{\partial n_1} = \chi_1 \upsilon_{2s}^2 + \ln(1-\upsilon_{2s}) + \upsilon_{2s} + (\nu_0 - \nu_s/2)\frac{V_1}{V_r}\left[\left(\frac{\upsilon_{2s}}{\upsilon_{2r}}\right)^{1/3} - \left(\frac{2}{F_1} + \frac{\nu_s}{(\nu_0-\nu_s/2)F_2}\right)\frac{\upsilon_{2s}}{\upsilon_{2r}}\right] \tag{2-17}$$

where V_r is the total volume of the solution which undergoes irradiation. This reduces to Flory's equation when $F_1 = F_2$ or $\nu_s = 0$ (all chains are in F_1-functional linkages). The effect of the bimodal crosslinking distribution is seen in the coefficient of the last term in brackets in Equation (2-17),

$$\frac{2}{F_1} + \frac{\nu_s}{(\nu_0-\nu_s/2)F_2} \tag{2-17a}$$

which represents the sum of the relative numbers of F_1 and F_2 -type crosslinks in the gel. For a gel with a single crosslink functionality F, the value of this term falls from 0.5 to 0

as F increases from 4 to infinity. For gels with bimodal crosslink functionalities, the value is increased from the unimodal situation. For crosslinked gels of highly functional stars ($f > 20$), the value of this coefficient will be dominated by the F_1 term. Equation (2-17) can be cast in terms of the molecular weight between crosslinks, M_c, by recognizing that

$$\left(\nu_o - \frac{\nu_s}{2}\right) = \left(\nu_o + \frac{\nu_s}{2}\right)\left(1 - \frac{M_c}{M_a}\right) \tag{2-18}$$

and

$$\nu = \nu_0 + \frac{\nu_s}{2} = \frac{V_p}{\nu_p^* M_c} \tag{2-19}$$

where V_p is the total volume of polymer added to the crosslinking solution. The derivative in equation (2-17) is zero at equilibrium. The final result is implicit in M_c due to the effects of the bimodal crosslink distribution:

$$\frac{1}{M_c} = \frac{1}{M_a} - \frac{\nu_p^*}{\upsilon_{2r} V_1}\left[\left(\frac{\upsilon_{2s}}{\upsilon_{2r}}\right)^{1/3} - \left(\frac{2}{F_1} + \frac{1}{(M_a / M_c - 1)F_2}\right)\frac{\upsilon_{2s}}{\upsilon_{2r}}\right] \frac{\chi_1 \upsilon_{2s}^2 + \ln(1-\upsilon_{2s}) + \upsilon_{2s}}{} \tag{2-20}$$

2.3.1.3.2 Swelling Analysis

Star PEO hydrogels were produced to cover a range of hydroxyl endgroup concentrations and PEO tether lengths, assumed to be equal to M_c (Table 2-4). In all cases, the star PEO concentration was within the semidilute range (Bieze, 1994) where chain overlap dominates, approximating solutions of linear PEO. The swelling equations calculate M_c from the measurable volume fraction of polymer in the relaxed and swollen hydrogel states, υ_{2r} and υ_{2s}, respectively. The results obtained from swelling experiments are compared to linear gels crosslinked under identical conditions (*i.e.*, same polymer concentration and same radiation dose). The comparison is valid provided the solutions of star polymers behave as solutions of linear polymers at similar concentrations with respect to the crosslinking reaction. Radiation crosslinking of star

PEO may be less effective than radiation crosslinking of linear PEO if the chain mobility of the stars is reduced compared to linear, thus decreasing the probability that an active main-chain radical will find another main chain. The observations that the dynamic properties of star chains are similar to those of linear chains when the concentration of stars is in the overlap regime (Adam, 1991) suggest that the crosslinking behavior of linear and star PEO will be similar in the overlap regime.

Both the star cores and irradiation induced crosslinks contribute to elastically effective chains measured with the modified swelling equation. The crosslink/dose relationship developed for linear PEO hydrogels (Equation (2-8)) does not count star cores as crosslinks. The number of radiation crosslinks formed per star arm, X_a, is a useful measure of the crosslink density which allows facile comparison of crosslinks calculated from swelling measurements and those expected from the dose relationship.

$$X_a = \frac{M_a}{M_c} - 1 = 2M_a \frac{\mu_r}{\omega_p} \tag{2-21}$$

The modified swelling equation can be recast in terms of X_a.

$$X_a = \frac{\frac{M_a v_p^*}{V_1}\left[\ln(1-\upsilon_{2s}) + \upsilon_{2s} + \chi_1 \upsilon_{2s}^2\right]}{\upsilon_{2r}\left[\left(\frac{\upsilon_{2s}}{\upsilon_{2r}}\right)^{1/3} - \left(\frac{1}{2} + \frac{1}{X_a f}\right)\left(\frac{\upsilon_{2s}}{\upsilon_{2r}}\right)\right]} \tag{2-22}$$

In their study of water-swollen PEO gels formed by end-linking PEO chains (M_w = 1000-10,000) with pluriisocyanates (f = 2-9), Gnanou and coworkers calculated χ_1 in star-like PEO hydrogels, reporting values in the range 0.45-0.58 (Gnanou, 1987). The lower bound, which is close to the reported literature value, was obtained for gels with long chains and low polymer volume fractions. The authors reasoned that the hydrophobic urethane linkages served to increase the value of χ_1 for stars with short chains. The authors found χ_1 to increase with PEO star polymer volume fraction, as is observed in linear polymer systems (Malcom, 1957; Dennison, 1986). The hydrophobic DVB cores of the stars may act in a similar fashion to the urethane linkages, slightly elevating the value of χ_1 for stars relative to that for linear PEO. A low polymer volume fraction was used in all cases, so χ_1 was limited to the lower end of the range determined

by Gnanou (Gnanou, 1987). In calculating X_a for star PEO, χ_1 was increased 12.5% over the value used for linear PEO to 0.48.

Table 2-4 and Figure 2-8 summarize the results of the swelling experiments for star gels. The values of M_c and X_a "from swelling" are calculated from Equation (2-22) using a value of v_p^* identical to that for linear PEO. The values of M_c and X_a "from dose" are calculated using Equation (2-8) to predict μ_r. No significant differences are observed between gels which exhibited syneresis during crosslinking and those which did not. The results for X_a shown in Table 2-4 are depicted graphically in Figure 2-8 to illustrate the agreement between the modified swelling equation and predictions from linear hydrogel formation. Each of the different types of PEO stars appear to fall on the line, except for star 3510 where the X_a measured in the swelling equations using $\chi_1 = 0.48$ exceeds the predicted value from dose. Star 3510 has a large number (70) of relatively short (5200 MW) arms. A high segment density on curved surfaces, such as the star core, leads to an extended core region observed in Table 2-3 and a resultant increase in χ_1. The modified swelling equation predicts an X_a comparable to that predicted by dose for star 3510 when $\chi_1 = 0.50$ (Table 2-4; Figure 2-8, solid diamonds). The effect is not observed for the BS10.4 stars, even though they have a high functionality (186) because the long arms (10,000 MW) more than compensate for the extended core – the cores make up only a small portion of the total solution. The correlation between $X_{a,dose}$ and $X_{a,swelling}$ extends through the range of X_a examined for all varieties of star PEO. These results corroborate light- and neutron-scattering evidence that in the semi-dilute regime, the arms of star polymers freely interpenetrate and behave essentially as solutions of linear molecules (Adam, 1991; Willner, 1994). The differences between solutions of star and linear PEO comes forth in the elevation of χ_1.

As with linear PEO, the molecular weight between crosslinks (and thus the ligand tether length) in star PEO hydrogels can be reduced by increasing the radiation dose received. An M_c range was sought from solutions of S3510 (5200 MW arms) and S3210 (3460 MW arms). Irradiation of a mixture of linear and star polymer provides ligand tethers with an average length approximately equal to the length of star arms, the hydrogel macrostructure is produced from the linear PEO component. S3210 was mixed with 29,750 MW linear PEO (3 wt% star, 5 wt% linear, 8 Mrad) to produce hydrogels with long tethers. Similar hydrogels were produced from a mixture of S3510 and 5×10^6 MW linear PEO (2 wt% star, 2 wt% linear, 2 Mrad – The high MW linear PEO becomes crosslinked at lower irradiation doses due to its highly entangled nature). Dose data suggests 5-10 arms per star would become crosslinked to the linear macrogel, leaving the

Table 2-4. Crosslink Density of Star PEO Hydrogels

Polymer	υ_{2r}	υ_{2s}	$M_{c,dose}$	$M_{c,swelling}$	$X_{a,dose}$	$X_{a,swelling}$
S3210	0.0698	0.0607	2087 ± 230	2113 ± 156	0.66 ± 0.07	0.65 ± 0.12
	0.0588	0.0498	2247 ± 247	2276 ± 341	0.54 ± 0.06	0.52 ± 0.08
	0.0400	0.0466	1929 ± 212	2001 ± 300	0.79 ± 0.09	0.73 ± 0.11
	0.0361	0.0511	1842 ± 203	1623 ± 153	0.88 ± 0.10	1.15 ± 0.21
	0.0324	0.0543	1429 ± 157	1271 ± 266	1.42 ± 0.16	1.80 ± 0.55
S3498	0.0769	0.0476	3672 ± 404	5150 ± 654	1.72 ± 0.19	0.97 ± 0.24
	0.0625	0.0471	3204 ± 352	4640 ± 362	2.12 ± 0.23	1.17 ± 0.18
	0.0400	0.0548	2318 ± 255	2405 ± 740	3.31 ± 0.36	3.47 ± 1.26
	0.0323	0.0370	3873 ± 426	4150 ± 707	1.58 ± 0.17	1.47 ± 0.49
S3509	0.0625	0.0606	2682 ± 295	3128 ± 343	2.90 ± 0.32	2.38 ± 0.35
	0.0588	0.0643	2563 ± 282	2594 ± 389	3.09 ± 0.34	3.04 ± 0.46
S3510	0.0323	0.0537	2853 ± 314	1524 ± 255[a]	0.82 ± 0.09	2.48 ± 0.57[a]
				2512 ± 354[b]		1.10 ± 0.29[b]
	0.0323	0.0614	1658 ± 182	1015 ± 101[a]	2.14 ± 0.24	4.16 ± 0.51[a]
				1755 ± 162[b]		1.98 ± 0.27[b]
BS10.4	0.0769	0.0319	8774 ± 790	7382 ± 707	0.14 ± 0.02	0.36 ± 0.05
	0.0769	0.0415	6427 ± 578	6031 ± 591	0.56 ± 0.06	0.66 ± 0.10
	0.0769	0.0502	4737 ± 426	4862 ± 485	1.11 ± 0.12	1.06 ± 0.16

a $\chi_1 = 0.48$

b $\chi_1 = 0.50$

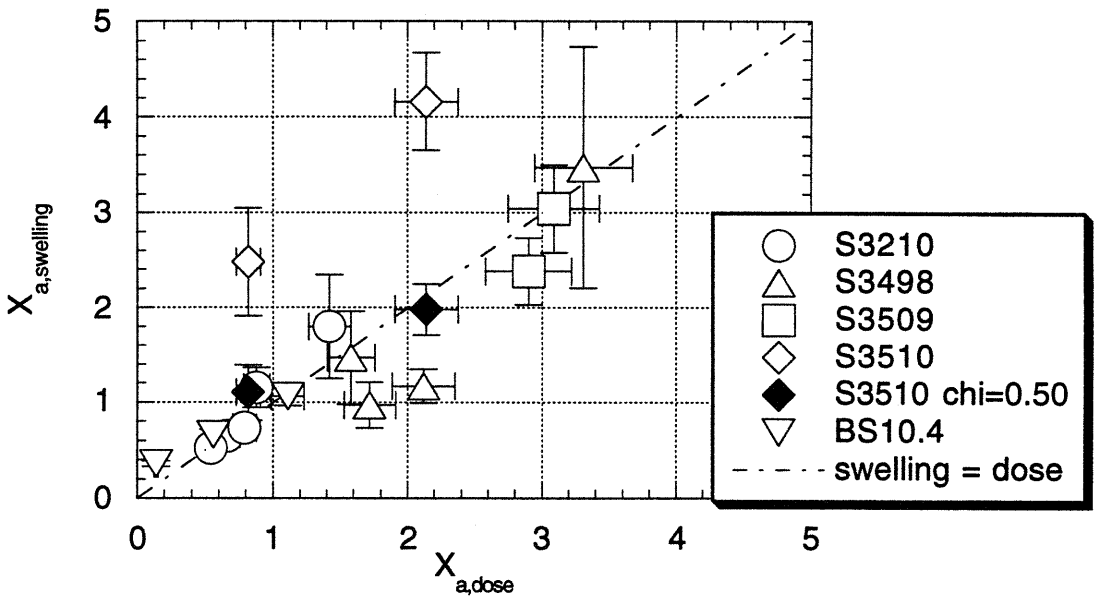

Figure 2-8. Crosslinks per star arm as predicted by the dose received ($X_{a,dose}$) or from the modified swelling equation ($X_{a,\ swelling}$) with $\chi_1 = 0.48$. S3510 data matches dose predictions if $\chi_1 = 0.50$ (solid diamonds).

remaining star arms at full length for ligand derivatization. The long tether limit was complemented with a range of lower M_c produced by irradiating 4 wt% polymer solutions with 4, 6, 8, or 12 Mrad doses (Table 2-5). In general, the approach achieves the objective of reduced M_c with increasing dose, but a limit is reached as M_c falls below 1500. As predicted from the behavior of linear PEO, extensive syneresis and chain scission was noted for both star hydrogels which surpassed this limit, those receiving 12 Mrad radiation. Although the dishes were sealed with parafilm, approximately 50% of the initial solution mass of these gels was lost to vaporization during the radiation procedure.

2.3.1.4. Linear/Oligomer Mixed Hydrogels

Linear/oligomer hydrogels were produced to increase the ligand loading capabilities of PEO hydrogels. The high MW PEO component provides hydrogel macrostructure while low MW PEO oligomers are added to increase the number of endgroups. All linear/oligomer hydrogels were formed from solutions containing a 4:1 weight ratio of linear PEO to oligomer. The average molecular weight between crosslinks is also the

Table 2-5. M_c variation with radiation dose for star polymer hydrogels.

Polymer	Radiation Dose (Mrad)	Initial Solution Weight (g)	Irradiated Gel[a] Weight (g)	M_c	Hydroxyl Concentration (mM)[b]
S3210 w/linear	8	2.20	2.03	3500[c]	7.2
S3210	6	2.24	2.24	1600	16.7
	8	2.20	2.06	1300	17.7
	12	2.28	0.99	1600	15.8
S3510 w/linear	2	2.18	2.14	5200[c]	3.1
S3510	4	2.35	2.30	2500	12.3
	8	2.19	2.14	1800	14.0
	12	2.30	1.37	1900	13.5

a Prior to equilibrium swelling.
b After equilibrium swelling.
c 5-10 arms per star become crosslinked, leaving the majority at full length.

average ligand tether length in star and linear PEO hydrogels, but for linear/oligomer gels, 70-90% of ligand is linked to the ends of the oligomers, and thus the tether length for these gels is closer to 0.5 $MW_{oligomer}$. Determination of the network structure of the linear/oligomer hydrogel is still an important step in the determination of the endgroup concentration.

The concentration of terminal hydroxyls in an equilibrium-swollen gel of the linear or star type can readily be determined based on the measured mass of the polymer, the volume of the gel, and MW of the polymer which underwent irradiation, provided the rate of chain scission during crosslinking is negligible. The assumption of minimal chain scission is supported by the studies of Dennison for the range of conditions studied here (Dennison, 1986). The hydroxyl concentration in linear/oligomer gels cannot be predicted or determined so readily because a significant amount of material present in the initial solution does not react to become part of the final gel. Thus, the amount of oligomer incorporated into the gel cannot be accurately determined by simple swelling or measurements of dried weights before and after crosslinking. Not all of the long-chain polymer initially present in the crosslinking solution is incorporated into the gel; thus the difference (if any) between the weight of the dried gel (after sol has been removed) and

the amount of long-chain polymer in the initial crosslinking solution does not represent the amount of oligomer incorporated into the gel. Likewise, the sol fraction includes a mixture of unreacted oligomer, unreacted polymer and partially reacted species of both, and thus its weight cannot be used to determine the amount of oligomer incorporated into the gel.

If monomers in the polymer chain are designated "A" and those in the oligomer chain "B", then three types of crosslinks can be formed by irradiation: A-A, A-B and B-B. The physical structure of the network is determined by the number of A-A crosslinks formed, assuming the number of individual oligomer molecules which participate in two A-B crosslinks (and are thus elastically effective) is negligibly small. Since the minimum average M_c for PEO gels formed by radiation crosslinking is about 1500, this assumption is reasonable for the 200-1000 MW oligomer used. Quantifying the three types of crosslinks will yield the desired information.

For the linear/oligomer gels, Mc (and thus the number of main chain crosslinks) cannot be determined exactly from swelling measurements but can be estimated with relatively small error if the weight fraction of oligomer in the final gel is small. A modified swelling equation which minimizes the error can be developed by considering the origin of the terms in the Flory-Bray equation for equilibrium swelling of a gel crosslinked while the chains are in solution. The change in free energy upon addition of solvent to the gel (i.e., swelling) arises from a mixing term and an elastic term (Equation 2-2) and equilibrium is reached when $\delta(\Delta G)/\delta n_1 = 0$ where n_1 refers to the number of solvent molecules. Oligomers in the gel contribute to the free energy of the system in the mixing term but not to the elastic free energy because they do not create effective elastic chains. In the derivation of Flory (Flory, 1950), the number of elastically effective subchains, ν_e, is related to the total number of subchains ν by

$$\nu_e = \nu\left(1 - \frac{2M_c}{M_n}\right) \tag{2-23}$$

In the linear/oligomer system, the total number of chains is the sum of the elastically effective chains (assumed to all derive from the high MW precursor), the free ends of the high MW chains, and the free ends of the oligomer chains:

$$\nu = \nu_e + \frac{2M_c}{M_n}\nu_p + \nu_o = \nu_p + \nu_o \tag{2-24}$$

where ν_p is the total number of chains deriving from the linear polymer and ν_o is the total number of chains deriving from the oligomer. Thus,

$$\nu_e = \nu_p\left(1-\frac{2M_c}{M_n}\right) \tag{2-25}$$

and the Flory-Bray swelling equation becomes

$$\frac{1}{M_c}=\frac{2}{M_n}-\frac{\frac{\nu_p^*}{V_1}\left[\ln(1-\upsilon_{2s})+\upsilon_{2s}+\chi_1\upsilon_{2s}^2\right]}{\upsilon_{2r}^*\left[\left(\frac{\upsilon_{2s}}{\upsilon_{2r}}\right)^{1/3}-\frac{1}{2}\left(\frac{\upsilon_{2s}}{\upsilon_{2r}}\right)\right]} \tag{2-26}$$

where υ^*_{2r} is the volume fraction of long chain *polymer* in the solution undergoing irradiation, and all other terms are volume fractions of *polymer* plus *oligomer*.

The statistics of the crosslinking process were modeled in order to predict *a priori* what crosslinking conditions would lead to gels with appropriate concentrations of oligomer. Assuming that the relative reactivities of the monomers in the polymer and oligomer chains with respect to both forming radicals and then combining to form carbon-carbon crosslinks are the same, the probabilities of forming A-A, A-B and B-B crosslinks are $p_{A\text{-}A} = x_A^2$, $p_{A\text{-}B} = 2x_Ax_B$, and $p_{B\text{-}B} = x_B^2$, respectively, where x_A is the mass or mole fraction of monomer contained in the polymer and x_B is the mass or mole fraction of monomer contained in the oligomer (mass and mole fractions are identical because the monomers are identical). In these studies $x_A = 0.8$ and $x_B = 0.2$, thus, the relative probabilities are $p_{A\text{-}A} = 0.64$, $p_{A\text{-}B} = 0.32$, and $p_{B\text{-}B} = 0.04$. Using this rationale, only 4% of the crosslinks formed will be "unproductive" B-B crosslinks. This does not mean that only 4% of the oligomer originally present will fail to crosslink to the gel, though, because only a small fraction of the total number of monomer units present (< 5%) undergo a crosslinking reaction. Much of the oligomer will remain unreacted in the sol fraction. We can estimate the concentration of A-B crosslinks which will be formed for a given set of irradiation conditions by

$$\mu_{A\text{-}B} = p_{A\text{-}B}\,\mu_R \tag{2-27}$$

Concentrations of A-A and B-B crosslinks can be estimated in a similar fashion. Equation (2-9) provides an estimate of μ_R for the linear-oligomer system, assuming that crosslinking proceeds in the linear-oligomer system in the same fashion as in the linear system. This approach was used to target irradiation conditions which would likely result in a reasonable amount of oligomer incorporation and a reasonable value of M_c. The equations were used again to compare predictions with the swelling results obtained after crosslinking.

A comparison of $\mu_{A\text{-}B}$ values derived from experimental results with $\mu_{A\text{-}B}$ values predicted using Equation (2-27) shows that monomers in the long-chain polymer and the oligomer do not follow the simple probabilities described above. Values for $\mu_{A\text{-}B}$ can be derived from the experimental results according to

$$\mu_{A\text{-}B,\,experimental} = \mu_R - \mu_{A\text{-}A} \tag{2-28}$$

where μ_R is predicted from Equation (2-9) and $\mu_{A\text{-}A}$ is calculated from the relationship

$$\mu_{A-A} = \frac{\omega_p}{2M_n}\left(\frac{M_n}{M_c} - 1\right) \tag{2-29}$$

where M_c is determined from swelling equilibrium measurements using Equation (2-26).

A comparison of $\mu_{A\text{-}B}$ values predicted *a priori* with those derived from the experimental results using Equation (2-28) is shown in Figure 2-9. The oligomer incorporation is 2-5 times higher than expected from probability theory. This discrepancy can be accounted for by recognizing that crosslinks are formed by diffusion termination of radicals on the polymer chains. Oligomers should diffuse more easily through the polymer network; thereby having a higher probability of finding a radical on the main chain or on another oligomer than expected based solely on weight fractions of the oligomer. The probabilities of crosslink formation should therefore be weighted to account for the greater mobility of the B units.

$$p_{A-A,weighted} = \frac{x_A^2}{\left(x_A + Kx_B\right)^2} \tag{2-30a}$$

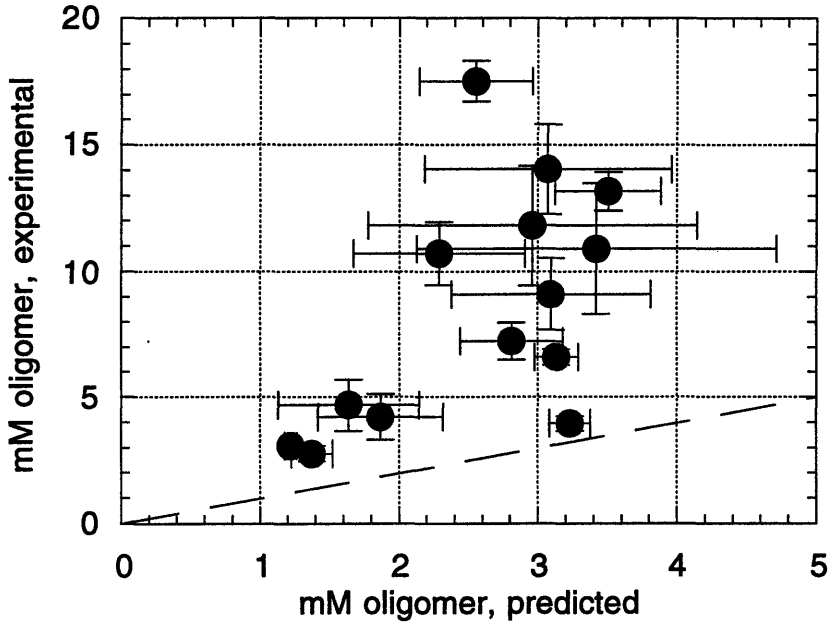

Figure 2-9. Comparison of oligomer/main chain crosslink concentration predicted *a priori* with those derived from experimental results. Line represents experimental results equal to predicted values.

$$p_{A-B,weighted} = \frac{2Kx_A x_B}{(x_A + Kx_B)^2} \tag{2-30b}$$

$$p_{B-B,weighted} = \frac{(Kx_B)^2}{(x_A + Kx_B)^2} \tag{2-30c}$$

The mobility factor, K, is determined by fitting data over a range of concentrations and differing amounts of radiation received for all linear/oligomer hydrogels produced. The relative mobility of main chains and oligomer chains will be affected by the solution concentration. PEO hydrogels are irradiated in staged 2 Mrad doses, therefore K may increase with dose received as the high MW PEO main chain becomes less mobile with increased crosslinking. Specifically, K is calculated from $\mu_{A\text{-}A}$ (determined from swelling measurements) and μ_R (determined from Equation (2-9)):

Table 2-6. Oligomer Mobility Factor

Main chain concentration[a]	Dose, Mrad	Mobility Factor, K[b]	
		PEG	TEG
6%	8		2.10 ± 0.86
7.5%	8	1.65 ± 0.74	
11.25%	6	2.13 ± 0.13	1.74 ± 0.36
	12	1.71 ± 0.40	
	14	1.96 ± 0.73	3.10 ± 1.18
	16	2.26 ± 1.28	2.80 ± 1.45
	18	2.29 ± 0.36	2.90 ± 1.03
	20		3.92 ± 0.70
20%	10	0.89 ± 0.12	
	12		1.50 ± 0.15

a Grams of main chain per 100 ml MilliQ water, 4:1 ratio main chain to oligomer.
b ± standard deviation of 2-5 samples

$$K = \frac{x_A}{x_B}\left(\sqrt{\frac{\mu_R}{\mu_{A-A}}} - 1\right) \tag{2-31}$$

Average K values are summarized in Table 2-6. In general, the mobility factor for the smaller TEG oligomer is higher than that for PEG, as expected. The dose effect can be seen in the 11.25 wt% oligomer systems, where K increases slowly with dose received.

As before, the concentration of main chain crosslinks is determined from the modified swelling equation. Then the concentration of oligomer/main chain crosslinks is calculated from the revised probability theory using Equation (2-32).

$$\mu_{A-B} = \left(\frac{2Kx_A x_B}{x_A^2}\right)\mu_{A-A} \tag{2-32}$$

A comparison of μ_{A-B} values predicted using the mobility factor with those derived from the experimental results using Equation (2-28) is shown in Figure 2-10. The oligomer incorporation derived from experimental results does not take oligomer-

oligomer crosslinks into account, and therefore is slightly higher than that determined by the revised probability theory. Figure 2-11 compares the total concentration of crosslinks calculated from probability theory ($\mu_{A\text{-}A}$ determined from swelling measurements added to $\mu_{A\text{-}B}$ and $\mu_{B\text{-}B}$ calculated from equation (2-32)) to that expected from the dose received. The agreement is quite good.

The concentration of endgroups in the swollen polymer can be calculated from $\mu_{A\text{-}B}$ and the volume ratio of swollen:irradiated hydrogel. Table 2-7 compares these results with the ADGal concentration measured in derivatized hydrogels. The endgroup concentration derived from experimental results is higher than that calculated by the weighted probability because the experimental calculation does not count oligomer-oligomer crosslinks which get washed from the system ($\mu_{B\text{-}B}$). Reasonable agreement is seen in both PEG and TEG based linear/oligomer systems. The weighted probability relationship provides an adequate means of predicting oligomer incorporation, and therefore ligand loading capabilities, in radiation crosslinked linear/oligomer hydrogels.

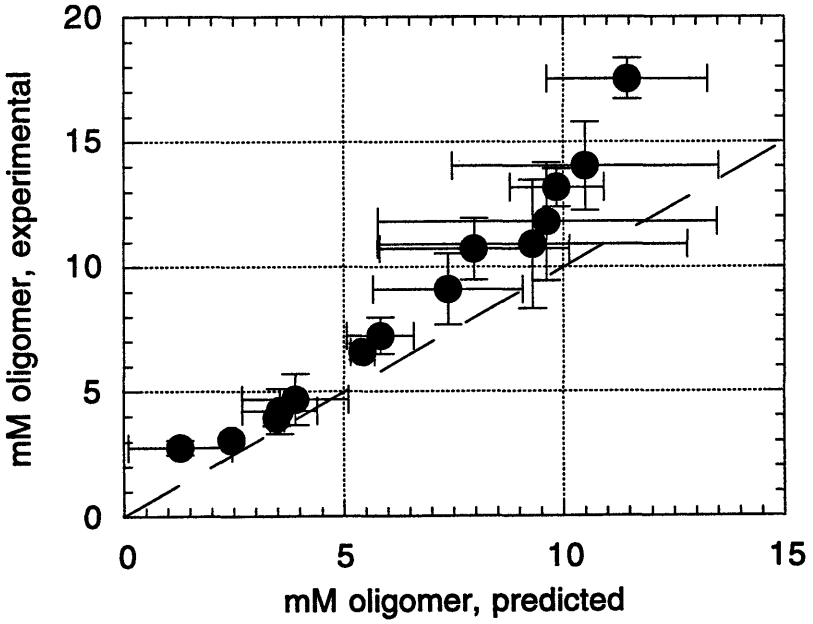

Figure 2-10. Comparison of oligomer/main chain crosslink concentration predicted using the mobility factor with that derived from experimental results. Line represents experimental results equal to predicted values.

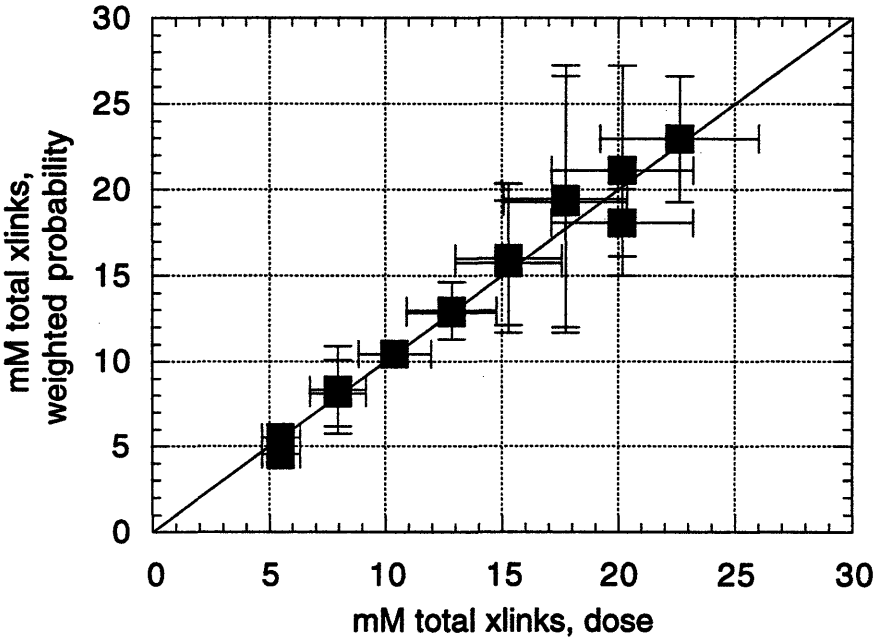

Figure 2-11. Comparison the total concentration of crosslinks predicted from the revised probability theory to that predicted from the dose received.

Table 2-7. Oligomer Endgroup Concentration

Polymer	Dose	Calculated Endgroup Concentration (mM)		Measured ADGal
		experimentally determined	weighted probability	(mM)
PEG	6	1.1 ± 0.1	0.9 ± 0.1	0.6 ± 0.1
	12	5.4 ± 0.5	4.4 ± 0.7	3.0 ± 0.3
	14	7.0 ± 1.1	5.9 ± 1.8	3.8 ± 0.3
	16	8.6 ± 2.0	7.5 ± 3.2	4.3 ± 0.4
	18	11.3 ± 0.7	8.4 ± 1.0	2.4 ± 0.5
TEG	6	1.0 ± 0.1	0.5 ± 0.4	0.4 ± 0.1
	14	8.3 ± 1.0	6.2 ± 1.8	3.8 ± 0.1
	16	9.3 ± 1.9	7.7 ± 3.2	4.7 ± 0.1
	20	16.8 ± 0.8	11.1 ± 1.9	9.9 ± 1.1

2.3.2. Uniaxial Deformation

Compression testing provides an independent method of determining M_c which can be compared to the swelling results. Elastic moduli of the linear, linear/oligomer and star PEO hydrogels listed in Table 2-8 were derived from stress/strain data obtained from compression experiments. Compression testing was performed on an Instron Mechanical Testing Machine equipped with a 200-g tension/compression load cell and aluminum compression platen. Gels were swollen in MilliQ water, then cut with a #5 cork borer to make 1 cm diameter disks. Gel thickness prior to compression was measured with a micrometer (1.20 ± 0.29 mm). A drop of water placed on the top of each gel maintained gel hydration throughout the test. Samples did not yield under the compressive forces engaged and no stress relaxation was observed.

Rubber elasticity theory (Treloar, 1975) provides a relationship between elongation (λ) and stress (σ) in terms of the elastic modulus (G):

$$\sigma = G\left(\lambda - \frac{1}{\lambda^2}\right) \tag{2-33}$$

Data plotted as stress vs. elongation were fit to Equation (2-33) as in Figure 2-12. Experimental data were reproducible with triplicate runs on the same type of material and agree well with the theory. The fitted parameter, G, is the material elastic modulus

Table 2-8. Hydrogel Samples Subjected to Uniaxial Deformation

	PEO volume fraction		Dose	Elastic Modulus
Polymer	υ_{2r}	υ_{2s}	(Mrad)	(N/m^2)
30K MW linear PEO	0.143	0.030	8	7019 ± 121
4:1 ratio PEO:PEG	0.172	0.027	10	5590 ± 299
4:1 ratio PEO:TEG	0.172	0.026	12	4056 ± 128
Star 3210	0.070	0.058	8	5999 ± 238
Star BS10.4	0.077	0.032	2	2876 ± 137
Star BS10.4	0.077	0.042	3.5	5778 ± 140
Star BS10.4	0.077	0.050	5.5	8748 ± 93

± standard deviation of three gels.

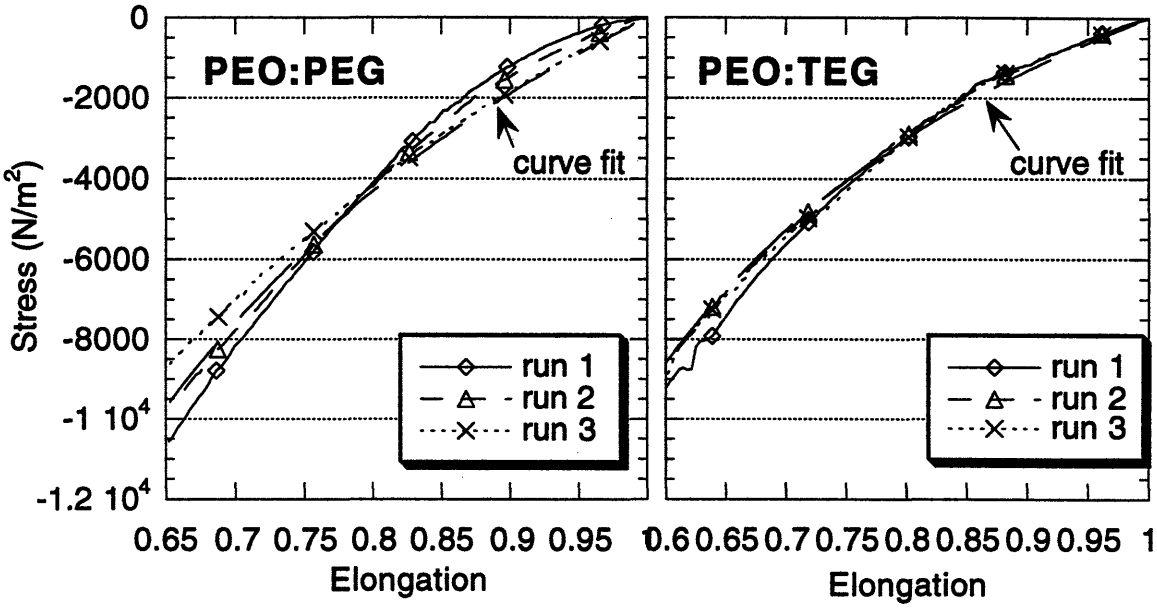

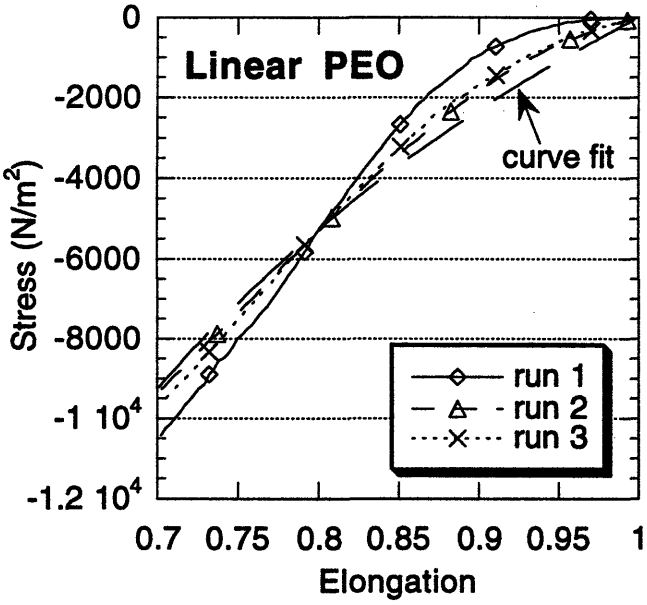

Figure 2-12. Hydrogel Stress-Strain Curves

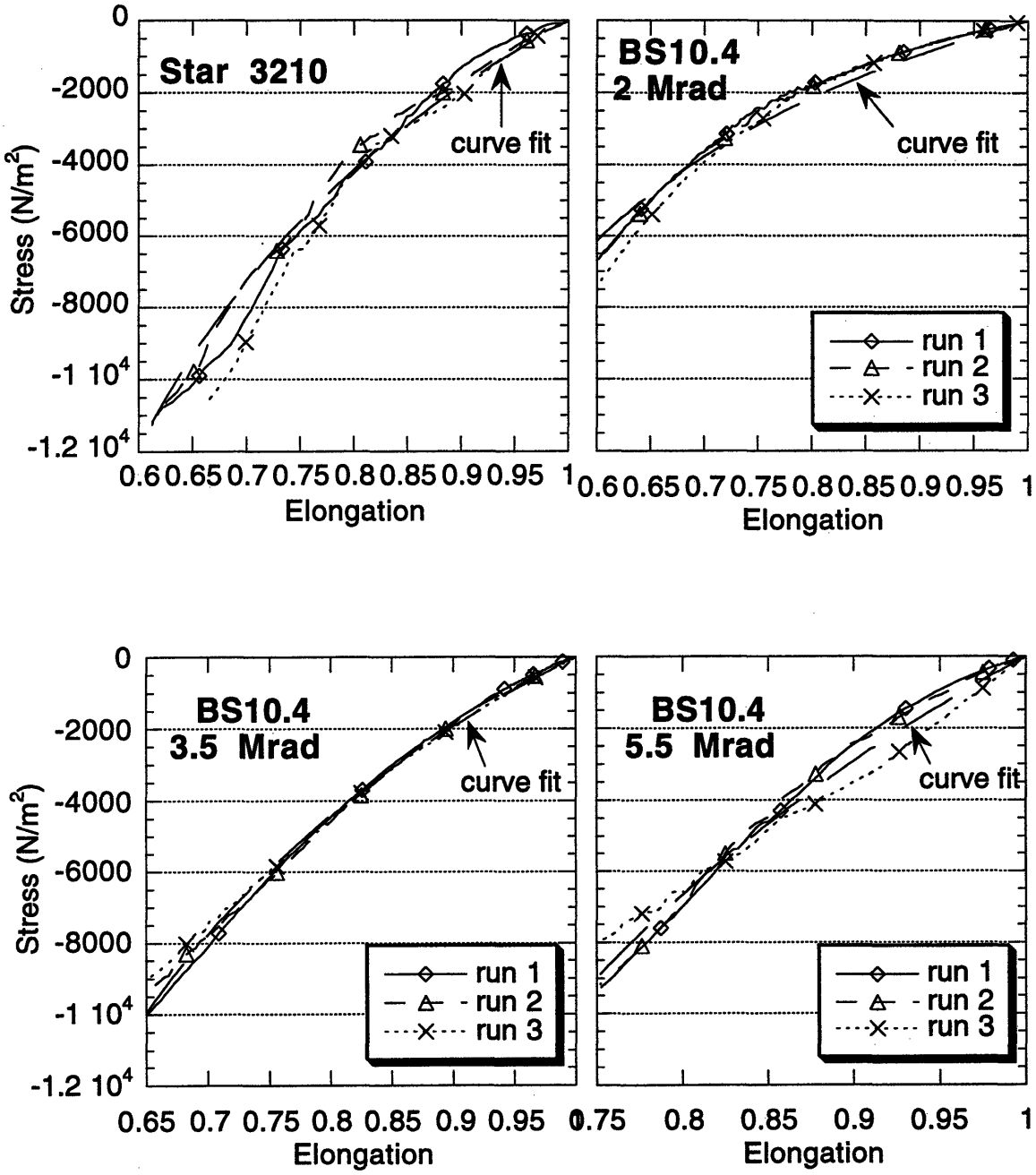

Figure 2-12. Hydrogel Stress-Strain Curves

(Table 2-8). The elastic modulus increases with increasing radiation dose received, as can be observed with the BS10.4 stars. This behavior is expected, as increased radiation increases the material crosslink density. A similar phenomena is observed with the linear hydrogels, as addition of PEG and TEG decreases the elastic modulus. The addition of PEG and TEG effectively reduces the main-chain crosslink concentration as radicals create polymer-oligomer and oligomer-oligomer crosslinks. More structurally unproductive crosslinks are created with the TEG oligomers due to the greater mobility of short chains in the network. While maintaining physical integrity, PEO hydrogels tested exhibit lower elastic moduli than other biomaterials such as cornea, which has an elastic modulus of around 1.3×10^6 N/m^2 (Tighe, 1976).

The elastic modulus can be related to the physical structure of the network, ultimately yielding a measure of the molecular weight between crosslinks (M_c). In Treloar's original development network junctions (crosslinks) were assumed to be affine with respect to macroscopic strain and fluctuations of the junctions are completely suppressed. This leads to an affine relationship between strain and chain end-to-end vectors. The total free energy of the network is the sum of the contributions of all individual strands. Derivation of the free energy equation over the reference volume V^0 gives the affine modulus:

$$G_{affine} = \frac{\nu_e RT}{V_r}\left(\frac{\upsilon_{2s}}{\upsilon_{2r}}\right)^{1/3} \tag{2-34}$$

The number of elastically effective chains, ν_e, is defined in Equation (2-23), with the total number of subchains, ν, defined in equation (2-19). Making the appropriate substitutions into Equation (2-34) and rearranging (noting that $V_p/V_r=\upsilon_{2r}$) gives an expression for M_c:

$$\frac{1}{M_{c,affine}} = \left(\frac{G_{affine} v_p^*}{RT\upsilon_{2r}}\right)\left(\frac{\upsilon_{2r}}{\upsilon_{2s}}\right)^{1/3} + \frac{2}{M_n} \tag{2-35}$$

In "phantom" networks (James, 1947; Flory, 1976) chains are modeled as immaterial giving them freedom to cross each other. The chains exert forces on the junctions, which are free of constraints and can thus move independently of the stress. This leads to a chain vector distribution which is the convolution of the mean chain vector distribution

with the fluctuation distribution. The phantom theory reduces the elastic free energy from the affine theory (Flory, 1976):

$$G_{phantom} = \frac{\xi RT}{V_r}\left(\frac{\upsilon_{2s}}{\upsilon_{2r}}\right)^{1/3} \tag{2-36}$$

where ξ is the network cycle rank or the number of independent circuits in the network. Flory (Flory, 1979; 1982) equates the cycle rank to the difference between the number of subchains and the number of "labeled points" where labeled points include crosslinks and free chain ends. For a network with one type of crosslink,

$$\xi = \nu_e\left(1-\frac{2}{F}\right) \tag{2-37a}$$

As F approaches infinity, the phantom model approaches the affine model. For the bimodal crosslink distributions obtained in radiation crosslinked star hydrogels,

$$\xi = \nu_e\left[1-\left(\frac{2}{F_1}+\frac{1}{(M_a/M_c-1)F_2}\right)\right] \tag{2-37b}$$

As with swelling behavior, the elastic behavior is dominated by the F_1 crosslinks for gels formed with highly functional stars. Substitution and rearrangement gives a second expression for M_c:

$$\frac{1}{M_{c,phantom}} = \left(\frac{2G_{phantom}v_p^*}{RT\upsilon_{2r}}\right)\left(\frac{\upsilon_{2r}}{\upsilon_{2s}}\right)^{1/3} + \frac{2}{M_n} \tag{2-38a}$$

or

$$\frac{1}{M_{c,phantom}} = \left(\frac{2G_{phantom}v_p^*}{RT\upsilon_{2r}}\right)\left(\frac{\upsilon_{2r}}{\upsilon_{2s}}\right)^{1/3} + \frac{2}{M_a}\left(\frac{1}{2}-\frac{1}{F_2}\right) \tag{2-38b}$$

for bimodal crosslinks.

2.3. Molecular Weight Between Crosslinks

The behavior of real networks falls between the affine and phantom limits, and can be described by including terms to reflect partial suppression of junction fluctuations and by the contribution of physical chain entanglements (Ferry, 1978; Dossin, 1979). A comprehensive study of model PEO networks synthesized by end-linking linear PEO chains with plurifunctional crosslinking reagents (f = 2-9) demonstrated that the elastic behavior of such networks very closely approached the phantom limit for networks with a high solvent content ($\upsilon_{2r} < 0.2$) or short chains ($M_c < 4000$) (Gnanou, 1987). Behavior close to the affine limit was exhibited by networks with long chains or high volume fractions of polymer. Ferry (Ferry, 1978) estimated the average M_{en} between physical entanglements in bulk linear PEO as 2200. One would expect on average 2.9 entanglements between each crosslinked chain in the linear gels described in Table 2-8 (M_C = 8500) if they behave like bulk linear PEO. However, fewer entanglements are expected at low polymer volume fractions. Indeed, the concentration of entanglements was reported as zero for PEO gels with M_c = 5600 and a polymer volume fraction of 0.043 (Gnanou, 1987), a volume fraction comparable to that of the PEO hydrogels described in Tables 2-8 and 2-9.

The M_c for linear and linear/oligomer hydrogels measured from swelling theory falls between the two extremes predicted from uniaxial compression, as expected (Figure 2-13, Table 2-9). The star gels behave differently than linear gels – the M_c measured from swelling theory is almost identical to that predicted for the phantom model for star BS10.4, similar to the behavior of the endlinked hydrogels of Gnanou (Gnanou, 1987). The swelling behavior of star 3210 hydrogels predicts a value of M_c which falls outside the range of both the affine and phantom models. The elastic behavior suggests fewer crosslinks are formed than would be predicted from swelling theory, leading to a larger M_c and lower X_a, as shown in Table 2-8. The value for M_c (2100) is still well above the plateau regime where chains are constrained from crosslinking.

In the semidilute regime, the dynamic properties (mutual diffusion coefficients) of linear and star molecules in a good solvent are independent of chain architecture and depend only on concentration (Adam, 1991). The probability that two main-chain radicals will encounter each other should be the same for solutions of linear and star molecules. There is no compelling reason that fewer crosslinks would form in star gels in comparison to linear gels formed under the same conditions. The elastic behavior suggests that a significant fraction of crosslinks (about 25%) occur between two adjacent star arms, leading to unproductive "loops" in the network and to an apparent lower number of crosslinks. This effect is more pronounced with the star 3210 which has short

arms (3460 MW as compared to 10,000 MW arms for BS10.4) so that the extended core regions comprises a larger portion of the solution volume during irradiation.

Table 2-9. Network Structures Derived from Elastic Moduli of Water-Swollen PEO Gels

Polymer	Molecular Weight Between Crosslinks (M_c)			
	dose	swelling	affine	phantom
30 K MW PEO		8,517 ± 610	10,526 ± 53	7,468 ± 64
4:1 ratio PEO:PEG		9,180 ± 290	11,083 ± 152	8,168 ± 199
4:1 ratio PEO:TEG		9,379 ± 320	11,891 ± 75	9,283 ± 110
Star 3210	2087 ± 230	2,113 ± 156	3,127 ± 12	2,870 ± 24
Star BS10.4, 2 Mrad	8,774 ± 790	7,382 ± 707	8,557 ± 59	7,174 ± 98
Star BS10.4, 3.5 Mrad	6,427 ± 578	6,031 ± 591	7,633 ± 44	5,767 ± 60
Star BS10.4, 5.5 Mrad	4,737 ± 426	4,862 ± 485	6,941 ± 23	4,885 ± 27

	Crosslinks per Star Arm (X_a)			
	dose	swelling	affine	phantom
Star 3210	0.65 ± 0.12	0.65 ± 0.12	0.11 ± 0.01	0.21 ± 0.01
Star BS10.4, 2 Mrad	0.14 ± 0.02	0.36 ± 0.05	0.17 ± 0.01	0.39 ± 0.02
Star BS10.4, 3.5 Mrad	0.56 ± 0.06	0.66 ± 0.10	0.31 ± 0.01	0.73 ± 0.02
Star BS10.4, 5.5 Mrad	1.11 ± 0.12	1.06 ± 0.16	0.44 ± 0.01	1.05 ± 0.01

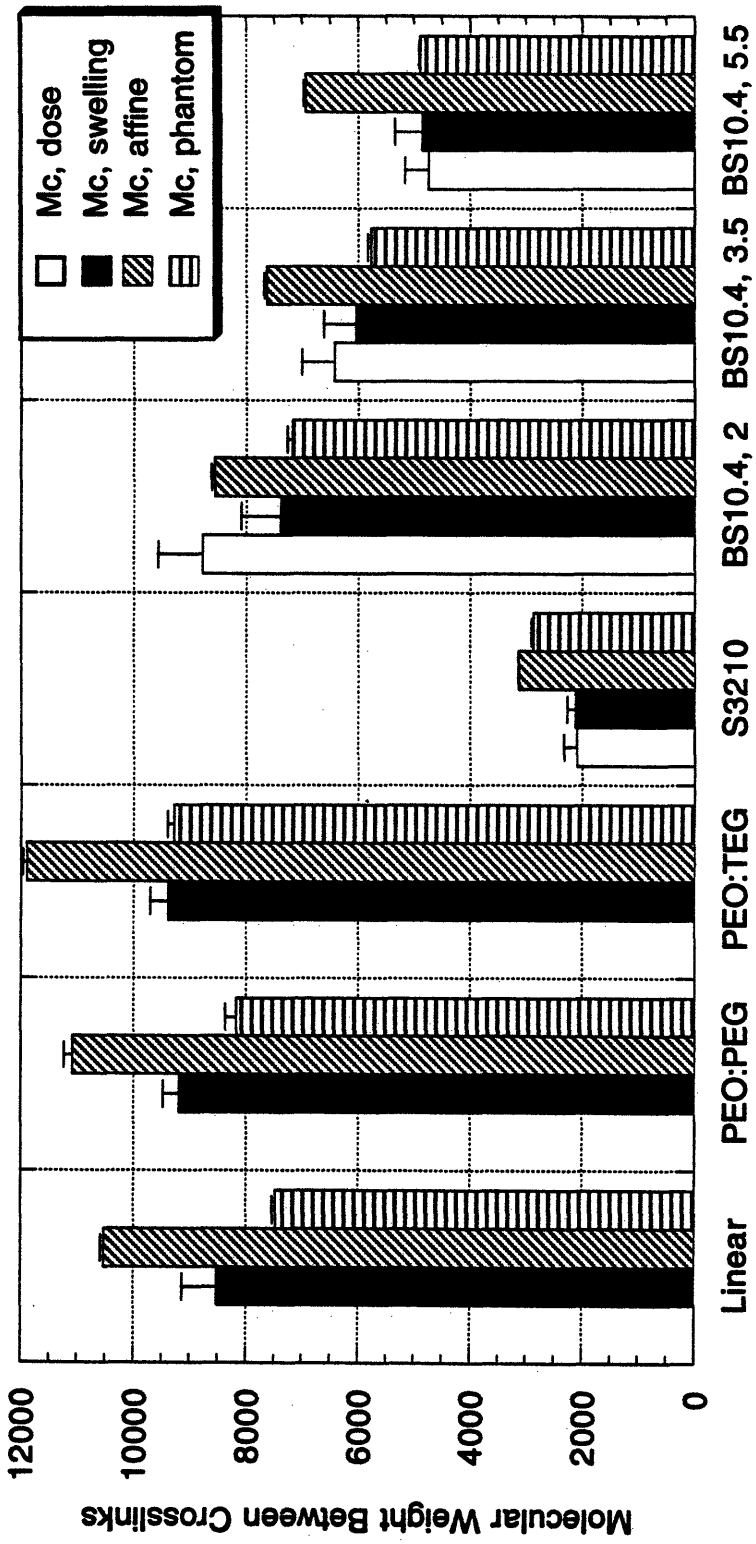

Figure 2-13. Molecular weight between crosslinks determined from radiation dose received (plain), swelling data (solid) or compression data and affine rubber elasticity theory (diagonal stripes) or phantom theory (horizontal stripes).

3. Substrate Derivatization and Characterization

Appropriate ligands were covalently coupled to poly(ethylene oxide) substrates producing materials which elicit a desired cellular response. The peptide arginine-glycine-aspartic acid (RGD) binds to integrins, cell adhesion proteins, creating a nonspecific cell adhesive material. Galactose ligands bind specifically to the hepatic asialoglycoprotein receptor (ASGP-R), creating a material which selectively permits hepatocyte adhesion. Immobilization of hormones or growth factors, such as EGF, may promote cell growth. Hydroxyl endgroups on the PEO chains provide the site for attaching ligands. The hydroxyls are first activated, providing a leaving group which will then couple to the desired ligand.

3.1. Derivatization Chemistry

Activated supports have long been used to immobilize antibodies for immunoaffinity chromatography (Shaltiel, 1976; Hjerten, 1981). Various activation agents have been used including N-hydroxysuccinimide (NHS) (Cuatrecasas, 1972), hydrazide (O'Shannessey, 1990), carbonyldiimidazole (CDI) (Bethel, 1979), 1,4-butanediol diglydicyl ether (BDGE) (Sundberg, 1974), divinyl sulphone (DVS) (Porath, 1975) cyanogen bromide (CNBr) (March, 1974), tosyl chloride (Nilsson, 1984) and tresyl chloride (Nilsson, 1981; Nilsson, 1984). Of the two sulfonates (tosyl chloride and tresyl chloride), tresyl chloride reactivity is two orders of magnitude greater, making it attractive for substrate activation (Crossland, 1971). Coupling instability is the most significant problem with immobilized proteins, leading to leakage of bound proteins from activated supports (Sato, 1987; Bessos, 1991). Several studies have addressed the leakage issue by comparing activation agents (Nilsson, 1981; Ubrich, 1992; van Sommeren, 1993). Tresyl chloride activation has been shown to be the most stable procedure, and therefore has been chosen for this work.

The tresyl chloride activation reaction is shown in Figure 3-1. Activation is performed in a water-free solvent to minimize hydrolysis of sulfonyl chloride. A strong base is added to neutralize liberated protons. In the Nilsson development, pyridine was the base of choice (Nilsson, 1981). In an earlier study, triethylamine, a stronger organic base, was shown to be more effective in creating tresylates (Truce, 1963). The work of Comfort confirmed that supports activated in the presence of triethylamine exhibited higher activity retention (Comfort, 1989). Most pertinent to this work, activation of PEO in the presence of pyridine led to extensive chain cleavage while cleavage was avoided by conducting the activation in triethylamine (Harris, 1984). Based on these results,

triethylamine was used in all activation procedures. The covalently bound tresylate is stable as long as the substrate is stored under acidic conditions (1 mM HCl) at 4°C (Nilsson, 1984).

The tresylate on the activated hydrogel provides a good leaving group which will react with strong nucleophiles to couple the desired ligand (Figure 3-1). Primary amino groups and thiols are the most effective reactive groups for coupling, but other nucleophiles may also be used (Nilsson, 1984). Neutral to basic conditions are required for efficient coupling. The coupling solution must have adequate buffering capability to prevent the pH from dropping during reaction.

Activation:

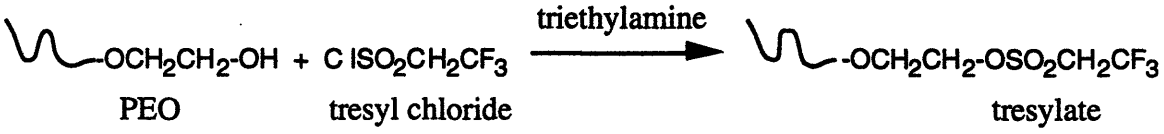

Coupling:

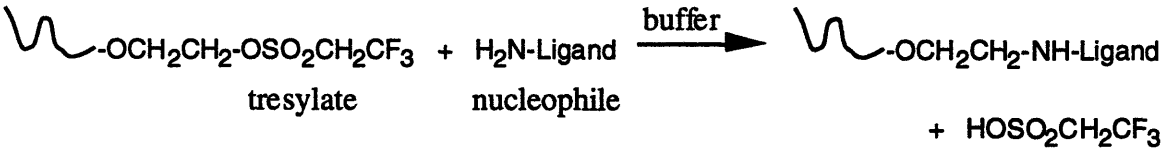

Figure 3-1. Derivatization Chemistry

3.2. Grafted PEO

A surface consisting of covalently bound PEO chains is conceptually attractive for systematic study of immobilized bioactive molecules. Grafting linear PEO with a narrow molecular weight distribution provides control of the ligand tether length. Other researchers have noted the difficulty in completely covering an underlying substrate with grafted PEO chains, which compromises the inert character of the underivatized PEO grafted system (Chaikof, 1986; Gombotz, 1989; JH Lee, 1989; Merrill, 1990; Desai, 1991a,b; Andrade, 1992; Prime, 1993; Drumheller, 1995). The dense PEO packing inherent in PEO stars may provide better coverage. When immobilizing bioactive

molecules such as hormones or growth factors, complete surface coverage may not be necessary or even desired; surface adsorbed proteins may be required for cell adhesion before the immobilized ligands can take affect. The activation and coupling chemistry described above was used to create PEO grafted glass materials.

3.2.1. PEO Activation

Linear and star PEO were activated with tresyl chloride according to the method of Nilsson (Nilsson, 1984), using triethylamine instead of pyridine. A detailed protocol can be found in Appendix B. Anhydrous conditions are required for high efficiency activation. Molecular sieve beads (4 Å) were added to a solution of PEO dissolved in methylene chloride, the mixture was allowed to dehydrate overnight at 4°C. Triethylamine was double distilled and stored over a KOH pellet for not more than one month to maintain dryness. Tresyl chloride was purchased from Sigma in small (1 g) sealed ampoules, using a fresh ampoule for each reaction. Reaction vessels and transfer pipettes were dried in a convection oven (80°C, 12-24 hours), sealed and refrigerated before use. The activation proceeds as follows: dehydrated PEO solution is decanted into a dried reaction vessel (flask). A volume of triethylamine equal to the volume of tresyl chloride to be used is slowly dripped into the flask, with stirring. Tresyl chloride is slowly dripped into the flask, with stirring, to create a 0.05 M solution, at least a 50% excess of the stoichiometric amount. This concentration was deemed to give optimal activation (Demiroglou, 1990). The reaction flask is sealed with parafilm, and the reaction is allowed to proceed for 105 minutes while continuing to stir. The methylene chloride is drawn from the activated polymer under vacuum (45 mm Hg) and captured in a trap for proper disposal. The product is then dissolved in acidic methanol (0.05 M HCl in methanol) and allowed to precipitate overnight in a -20°C freezer. The supernatant liquid is discarded after centrifugation, and the process is repeated 5 more times to remove all residual triethylamine. A final precipitation is done in pure methanol with no acid, and the final product is dried, lyophilized, and stored in a 0°C freezer.

Activation yield, the percent of available hydroxyl groups which become activated, was determined by elemental analysis of activated PEO. Linear methoxy-PEO with a narrow molecular weight distribution (Aldrich) was used as to analyze the activation yield (Table 3-1). Methoxy-PEO is terminated at one end with an hydroxyl and the other with a methyl group. The number average molecular weight and polydispersity index (ratio of weight average:number average MW) was determined by GPC analysis. Duplicate lyophilized samples from 4 activation runs were sent to Galbraith Laboratories

(Knoxville, TN) to analyze for fluorine, carbon, hydrogen, and oxygen content. The yield of 10-25% which was obtained on early samples (2 activation runs) was increased to a yield of 70-85% (2 activation runs) by strictly maintaining anhydrous conditions as outlined above. This compares favorably to the activation efficiency of 80% which has been reported for linear PEO using pyridine instead of triethylamine (Nilsson, 1984).

Table 3-1. Linear PEO Characteristics for Activation Analysis

Nominal MW	Measured MW	Polydispersity Index
2000	2060	1.09
5000	6272	1.07

3.2.2. PEO Coupling to Surfaces

The tresylate groups on the activated PEO will couple with amines immobilized on glass slides. Ms. Susan Sofia Allgor provided glass substrates with approximately 7 atom% primary amine coverage (as determined by XPS), following the method of Stenger (Stenger, 1992): after cleaning the glass surface with acid to free up the surface silanols (-SiOH), amino-trimethoxy silane is allowed to react. The methoxy groups on the silane first hydrolyze to form silanols which form silane oligomers through condensation reactions. The free silanols on the oligomers hydrogen-bond with the surface silanols. A heating step initiates a condensation reaction to form Si-O-Si bonds between the oligomers and surface silanols. This condensation is reversible and can be easily hydrolyzed at elevated pH, so care must be taken during coupling and reactivation steps to preserve the surface integrity.

Buffers, reaction times, and temperatures can be varied in the coupling procedure. Variables were systematically evaluated in an orthogonal (Taguchi) array to optimize the coupling of tresyl chloride-activated linear PEO to the aminated surface. Duplicate samples were coupled according to the array outlined in Table 3-2 to evaluate the following variables:

a) Temperature: The 4°C coupling temperature recommended in most references is likely suggested to preserve protein structure, not a concern when coupling PEO. Nakamura *et. al.* (Nakamura, 1989) show more rapid coupling at room temperature.

b) Buffer: Various buffers are recommended, depending on the author. Carbonate buffer (0.25 M) and phosphate buffer (1 M) are used most often. The pH was maintained at 7.4 to preserve aminated surface integrity.

c) PEO%: Ligand concentration may have an effect on coupling efficiency. The table lists PEO wt/vol % concentration in coupling buffer

d) K_2SO_4: Addition of K_2SO_4 (0.3 M) creates a salting out effect on PEO (Bailey, 1959). This could lead to greater coupling efficiency as the PEO is concentrated at the aminated surface (Nakamura, 1990).

e) Time: Most references suggest long coupling times, however shorter times may be effective.

f) BxK: Interaction effects between buffer and salt addition.

g) MW: The efficiency of coupling long vs. short PEO chains was examined. 1450 MW was chosen because that is the smallest chain which could give complete surface coverage, given the amine density measured and the polymer radius of gyration. 18,500 MW was chosen as the most effective chain length for minimizing protein adsorption as reported by Desai and Hubbell (Desai, 1991b).

Table 3-2. Coupling optimization.

Run	Design Variables							C-O/C-C
	Temp	Buffer	PEO %	K_2SO_4	Time	BxK	MW	
1	25°C	Phosphate	1	yes	4 hrs	1	1450	1.10
2	25°C	Phosphate	1	no	20 hrs	2	18,500	1.98
3	25°C	Carbonate	5	yes	4 hrs	2	18,500	4.46
4	25°C	Carbonate	5	no	20 hrs	1	1450	0.72
5	40°C	Phosphate	5	yes	20 hrs	1	18,500	5.81
6	40°C	Phosphate	5	no	4 hrs	2	1450	1.34
7	40°C	Carbonate	1	yes	20 hrs	2	1450	1.10
8	40°C	Carbonate	1	no	4 hrs	1	18,500	2.46

Coupling efficiency was extrapolated from analysis of the C-O/C-C ratio determined by X-ray photoelectron spectroscopy (XPS). XPS is a powerful technique for quantifying surface chemistry. The elements present on the top 50 Å of a surface are identified by bombardment of the surface with low energy X-rays which release core

electrons whose energy is characteristic of the element from which they were released. These electrons are detected and analyzed to yield valuable data. The resolution is such that ether carbons (C-O) can be distinguished from alkyl carbons (C-C). PEO consists solely of ether carbons, so surface grafting efficiency can be compared by examining the ratio of CO to C-C peaks, a larger ratio indicating greater PEO grafting (Table 3-2).

ANOVA statistical analysis of the results confirmed Desai's finding that coupling with 18,500 MW PEO yielded more ether groups on the surface than coupling with the shorter PEO chains (Desai 1991b). Coupling efficiency also increased with increasing PEO concentration in the coupling buffer. The buffer itself made little difference, but addition of K_2SO_4 to the PBS buffer did increase coupling efficiency (the effect was not seen with carbonate buffer). Increasing the coupling temperature marginally increased the efficiency, while length of reaction had no effect.

Based on these results, coupling of star PEO to aminated surfaces was carried out at room temperature in 1 M PBS with 0.3 M K_2SO_4 (pH 7.4). PEO concentration in the coupling buffer was maintained at 5 wt/vol%. The coupling reaction was allowed to proceed overnight. In order to minimize reagent use while maximizing concentration and to provide a convenient geometry for dry sequential chemistry, slides with a Teflon mask were used (Cel-Line Associates, Newfield NJ). The 5 mm diameter unmasked portions were aminated as described above; tresyl-activated PEO was coupled to the exposed surface. A 20 µl drop beads nicely on the unmasked portion. Slides were kept in a humidified box during coupling to prevent the drop from drying out. XPS analysis of star 3510 (70 arms, 5200 MW) -coupled slides show a prominent ether carbon peak (C-O/C-C ratio of 1.51), indicative of significant grafting. XPS analysis is carried out under a vacuum of at least 10^{-8} Torr, so polymer strands which will be extended out under solvated conditions are flattened during analysis. Star PEO, with its dense configuration, does not vary as much through this transition (Figure 3-2); a given C-O/C-C ratio indicates a higher PEO surface density in the solvated state for star PEO-coupled surfaces compared to linear PEO-coupled surfaces.

3.2.3. Grafted PEO Reactivation

Hydrolysis competes with coupling in the neutral buffer, so the immobilized PEO must be retresylated before ligand coupling can occur. The PEO-coupled surface was dried with successive washes of ethanol/water mixtures finishing with 100% ethanol. A 20 µl drop of reaction solution (methylene chloride, triethylamine and tresyl chloride) was placed onto the unmasked area and the reaction was allowed to proceed for 60

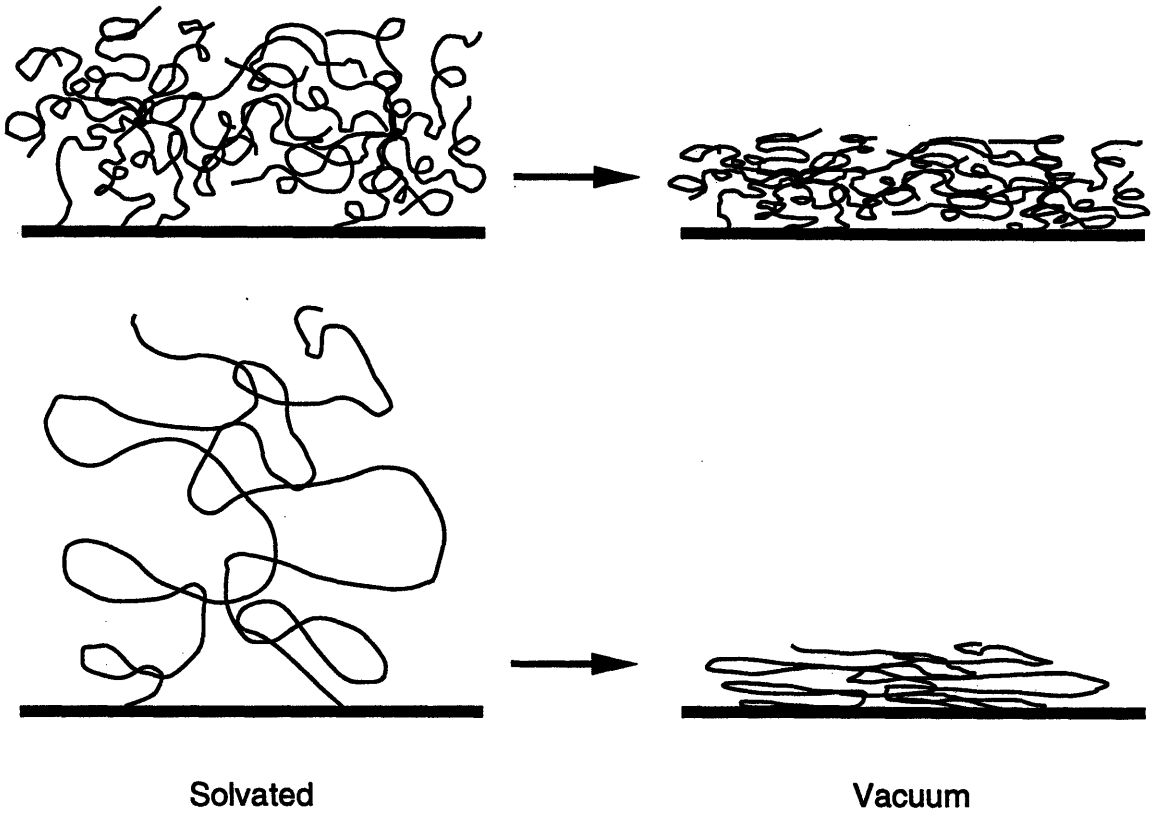

Figure 3-2. Grafted PEO flattens onto the surface when subjected to vacuum. The effect is less pronounced with star PEO (top) because the stars take on a dense configuration in the solvated state.

minutes. The activated surface was washed with acidic methanol, dried, lyophilized, and stored under nitrogen.

3.2.4. Ligand Coupling

The hepatic asialoglycoprotein receptor is unique to hepatocytes, thus targeting this receptor may create a hepatocyte specific surface. The ligand 1-amino-1-deoxy-ßD-galactose (ADGal) has a galactose moiety which binds to the ASGP-R and an amino group which will couple to the activated PEO. The amino substitution at the 1 carbon of the galactose assures the ligand will couple in the appropriate conformation to maintain ligand-receptor binding specificity.

Ligand coupling to reactivated grafted PEO follows a similar procedure as the original coupling of activated PEO to the aminated slide. A 25 mM solution of ADGal is

prepared in a 1 M phosphate buffer (pH 7.4). After a 20 µl drop is carefully placed on the retresylated surface the slide is placed in a humidified box to keep the drop from drying out. A 20 µl drop contains a large excess of ligand. Coupling is allowed to proceed overnight at room temperature, after which the slide is rinsed and then stored in sterile PBS (pH 7.4). XPS analysis of ADGal coupled to grafted star 3510 shows almost no loss of surface PEO as the C-O/C-C ratio remains at 1.39 as compared to 1.51 on the underivatized slide.

3.3. PEO Hydrogels

PEO hydrogels provide a pure poly(ethylene oxide) surface for derivatization, offering the most biologically inert scaffold possible. Through radiation crosslinking of star PEO and linear/oligomer mixtures, PEO hydrogels with a range of ligand tether lengths and hydroxyl concentrations are possible. The three dimensional nature of hydrogels lead to added complexities which must be addressed during activation and coupling.

3.3.1. Activation of PEO Hydrogels

Tresyl chloride activation of the terminal hydroxyl groups in PEO hydrogels was carried out in an anhydrous acetone solution. Anhydrous acetone is the solvent suggested in Nilsson's derivatization of sepharose gels (Nilsson, 1981). Gels are dried in successive washes of water/acetone mixtures (70/30, 40/60, 20/80), acetone, and dry acetone (dried over 4 Å molecular sieve beads). The effective diffusion coefficient for small solutes through PEO hydrogels is approximately $3x10^{-6}$ cm^2/s (Merrill, 1993). For hydrogels of 1 mm thickness, this corresponds to a characteristic diffusion time of one hour. To assure complete dehydration of the gels, washes were completed in triplicate on a roto-stir table, with a minimum of 30 minutes per wash. Dehydrated gels were placed in dried flasks (prepared as described above) and covered with dry acetone. A volume of doubly distilled dry triethylamine equal to the volume of tresyl chloride to be used is slowly dripped into the flask, with stirring. Tresyl chloride is slowly dripped into the flask, with stirring, to create a 0.05 M solution, at least a 50% excess of the stoichiometric amount. The reaction flask is sealed with parafilm, and the reaction is allowed to proceed for 105 minutes while continuing to stir. The gels are rehydrated with successive stirred washes of 1mM HCl/acetone mixtures (0/100, 30/70, 50/50, 70/30, 85/15, 100/0). Again, washes were continued for a minimum of 30 minutes, in triplicate. Gels were stored in 1mM HCl until coupled with desired ligand.

Elemental analyses of carbon, hydrogen, and fluorine content (Galbraith Laboratories, Knoxville, TN) in duplicate samples of linear PEO hydrogel were used to determine the amount of tresyl chloride linked per gram of polymer and this was converted to an efficiency of end group modification using the known molecular weight. The activation procedure is extremely sensitive to trace amounts of water. Initial attempts to activate gels resulted in efficiencies of ~25% (2 activation runs analyzed); this was improved to >70% (2 activation runs analyzed) by increasing the number and duration of drying steps and the length of the activation to obtain the final procedure described above.

3.3.2. Ligand Coupling

The terminal hydroxyl groups of gels were modified with 1-amino-1-deoxy sugars (glucose or galactose) or the RGD adhesion peptide. ADGal coupling produces a hepatocyte-specific scaffold. ADGlu coupling is a negative control for the ADGal-PEO. Amino-glucose coupling would invoke an almost identical physico-chemical change to the hydrogel, but there is no receptor for glucose on hepatocytes so no adhesion would be expected. The tri-peptide RGD is a sequence located within many cell adhesive proteins which is recognized as a ligand for integrin cell-surface adhesion receptors (Orlando, 1991; Kühn, 1994). In addition to the N-terminus amino group which is the desired coupling site, there are two amino groups on the arginine amino acid which might couple to the activated hydrogel (Figure 3-3). Coupling through these groups is likely to inactivate the RGD, but the RGD density required for endothelial cell spreading is very low (1 fmole/cm^2) (Massia, 1991a), so loss of some ligand activity may not adversely affect the material performance. RGD-PEO hydrogels should promote endothelial cell adhesion.

3.3.2.1. Coupling Procedure

Activated hydrogels are coupled with a 100% excess of ADGal, ADGlu or RGD peptide in phosphate buffered saline solution (PBS, pH 8.5) or 0.25 M sodium bicarbonate solution (pH 9.4). Coupling efficiency is optimal in the 7.5-9.5 pH range, peaking around pH 9 (Nilsson, 1981; Nakamura, 1989). The concern of surface integrity on the PEO-grafted materials does not apply to PEO hydrogels, so solutions with a higher pH can be used. Bicarbonate buffer is preferred for coupling carbohydrates to hydrogels as the ligand dissolves more efficiently in this buffer. Ligands are allowed to couple while stirring at room temperature (4°C for peptide ligands) for 20 hr. Upon completion of the coupling reaction, the hydrogel is washed in coupling buffer for 36 hours, with 5

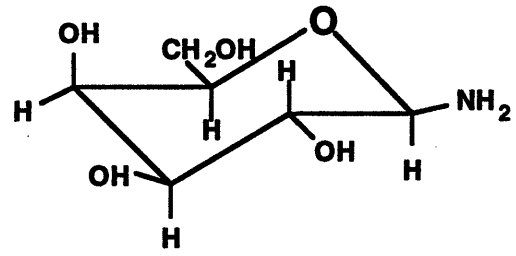

amino-deoxy-galactose

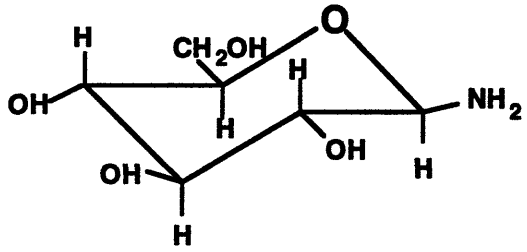

amino-deoxy-glucose

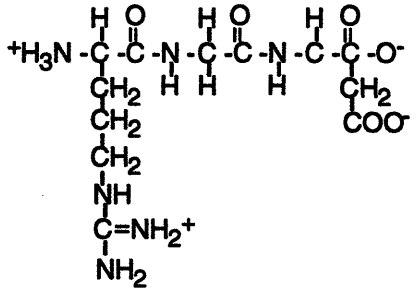

arginine-glycine-aspartic acid

Figure 3-3. Bioactive Ligands

solvent exchanges, to remove unreacted reagents. The solvent washes are retained for analysis of uncoupled ligand.

Coupling yield (moles ADGal/moles TC) was measured by elemental analyses of carbon, hydrogen, and nitrogen content (Galbraith Laboratories, Knoxville, TN). Duplicate ADGal-derivatized linear PEO hydrogels from two separate activation and coupling runs were analyzed by elemental analysis to validate procedures (Table 3-3). Elemental analysis for fluorine performed on the ligand-modified materials was negative, indicating an absence of tresyl chloride as expected. The yield on coupling (moles ADGal per mole tresyl chloride) was >98%. The overall yield on activation and coupling was thus 70-85% for ADGal-derivatized hydrogels. A similar activation and coupling yield was assumed for ADGlu- and RGD-derivatized hydrogels. Ligand concentration of RGD coupled to linear/oligomer hydrogels was not measured directly, but inferred based on the activation and coupling yield measured for ADGal-derivatized gels (Table 3-4).

Table 3-3. Coupling Yield

Run	Activated PEO		Coupled PEO		
	F, theoretical[a]	F, measured	N, theoretical[b]	N, measured	F, measured
1	569 ppm	425 ± 91 ppm	106 ± 23 ppm	104 ± 21 ppm	N.D.[c]
2	569 ppm	470 ± 85 ppm	118 ± 16 ppm	124 ± 17 ppm	N.D.[c]

a Theoretical ppm fluorine assuming 100% activation of available hydroxyl groups.
b Theoretical ppm nitrogen assuming 100% coupling of measured activated sites.
c Fluorine content below the level of detection (10 ppm).

Table 3-4. RGD Derivatized Linear/Oligomer PEO Hydrogel Characteristics

Polymer	Polymer Conc.[a] (gm/L)	Radiation Dose (Mrad)	Hydroxyl Conc. (mM)	RGD Conc.[b] (mM)
PEO:PEG	14.2 ± 1.0	6	0.91 ± 0.03	0.6
PEO:TEG	17.1 ± 2.8	6	0.48 ± 0.05	0.3

a After equilibrium swelling.
b Assuming 70% yield on coupling and activation.

3.3.2.2. Fluorescent Lectin Binding Analysis

Because the overall efficiency of modifying terminal hydroxyls with ligands is <1, diffusion limitations during the activation and coupling process might result in a non-uniform distribution of ligand within the gel. The ADGal distribution throughout the gel can be visualized by staining with a fluorescent affinity label specific for galactose. Lectins are noted for their specificity of binding to carbohydrate residues (Goldstein, 1986). *Ricinus communis* I (RCA-120, Vector Labs), a fluorescein-labeled lectin specific for N-acetyl-galactosamine and galactose, was used to examine ADGal-derivatized hydrogels and uncoupled controls. Samples listed in Table 3-5 (approximately 0.4 cm^2 by 1 mm thick) were incubated with the fluorescein-labeled lectin for 12-24 hours, washed extensively to remove unbound lectin (see Appendix B), and examined with fluorescent microscopy. Underivatized samples did not fluoresce

Table 3-5. Hydrogels used in fluorescent lectin binding analysis.

Polymer	Dose (Mrad)	υ_{2s}
S3210	8	0.0582
S3498	8	0.0517
30K PEO	8	0.0399
PEO:PEG[a]	18	0.0341
PEO:TEG[a]	20	0.0270

a 4:1 ratio 30K linear PEO:oligomer (PEG or TEG)

while ADGal-derivatized samples showed dim fluorescence, indicating galactose coupling.

Thin transverse sections of ADGal derivatized star 3210 hydrogels (14 mM ADGal) were labeled with RCA-120 and then examined using confocal microscopy to determine if ADGal coupling was uniform throughout the gel. The Confocal Laser Scanning Microscope, located at the Boston University School of Medicine, is a Leica Diaplan light microscope equipped with an argon ion laser light source for fluorescence emission and excitation in the rhodamine and fluorescein wavelengths. A computer-controlled scanning mechanism moves the focused laser light source across the object in the focal plane of the microscope and the resulting fluorescence emissions are detected by photomultiplier tubes. The images detected by the photomultiplier tubes are stored on a powerful computer system that can perform complex image processing functions. The stained cross-sections were scanned across their width generating a fluorescent intensity profile representing the relative concentration of ligand from one edge to the center to the other edge of the gel. Profiles generated in this way for three replicates of stained gel were flat, indicating a uniform distribution of ligand throughout the gel.

3.3.2.3. Colorimetric Analysis of Carbohydrate Concentration

Routine determination of carbohydrate ligand concentration in the gels was performed by measuring the residual ligand remaining in the coupling buffer and hydrogel washes and calculating the bound ligand by difference. The value obtained by this method was checked by assay of ligand released from thermally degraded gels. Thermally degraded gels were analyzed for sugar content every 2-4 coupling runs to validate analysis from supernatant. ADGal or ADGlu concentration can be determined by a colorimetric assay

in which a furfural derivative obtained by acid hydrolysis of the sugar reacts with acidic anthrone to create a colored (green) product whose absorbance can be measured at 625 nm (Zipf, 1952; Ashwell, 1957). A calibration curve is generated from dilutions of the original coupling buffer. The protocol is detailed in Appendix B. As expected, ADGal and ADGlu couple to tresyl chloride activated gels with identical affinity, yielding the same ligand concentration regardless of sugar coupled (Table 3-8).

PEO hydrogels thermally degrade at 80°C over 48-72 hours. The degraded polymer can be dissolved in phosphate buffered saline (PBS) and analyzed for sugar content as above. Approximately 0.01 g PEO would be present in the thermally degraded hydrogels used in the assay. Samples of underivatized PEO were degraded to check for background absorbance due to the polymer present in solution. Such background absorbance is negligible, as shown in Figure 3-4. Calibration curves created from stock ADGal , ADGal which has been thermally degraded in the same manner as the samples, and ADGal thermally degraded in the presence of PEO and water are interchangeable (Figure 3-5; 4 runs), so there is no concern that the PEO degradation procedure has altered the carbohydrates. The sum of sugar measured in the degraded gels and the coupling supernatant (with washes) equaled the total amount of sugar originally put in the coupling buffer (on a gel volume basis), mass balance closure was obtained with each degradation run (see Table 3-6 for representative results).

Table 3-6. Mass Balance Closure

Polymer	μmole ADGal/ml gel		
	degraded sample	supernatant	initial coupling buffer
30K PEO	0.9 ± 0.1	1.0 ± 0.2	2.0
PEO:TEG	10.3 ± 0.4	24.2 ± 0.5	35.0
S3210	14.1 ± 0.5	25.8 ± 0.7	40.0

± standard deviation from 3-4 samples

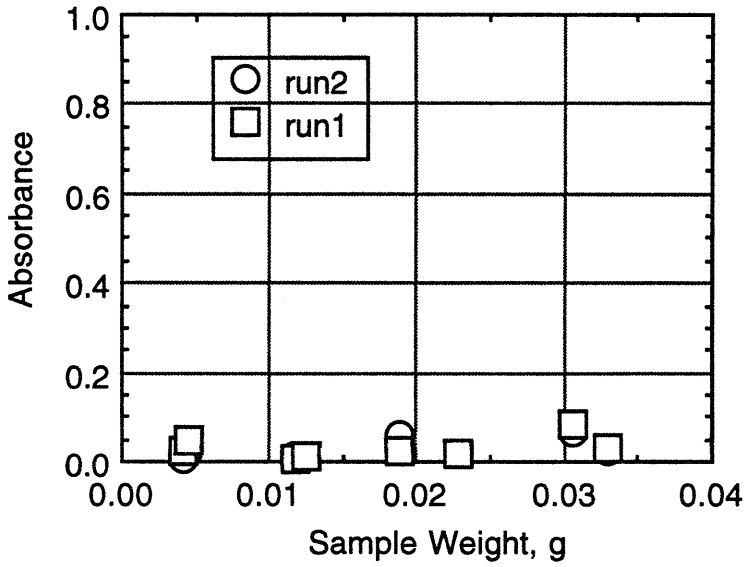

Figure 3-4. Background absorbance of thermally degraded PEO.

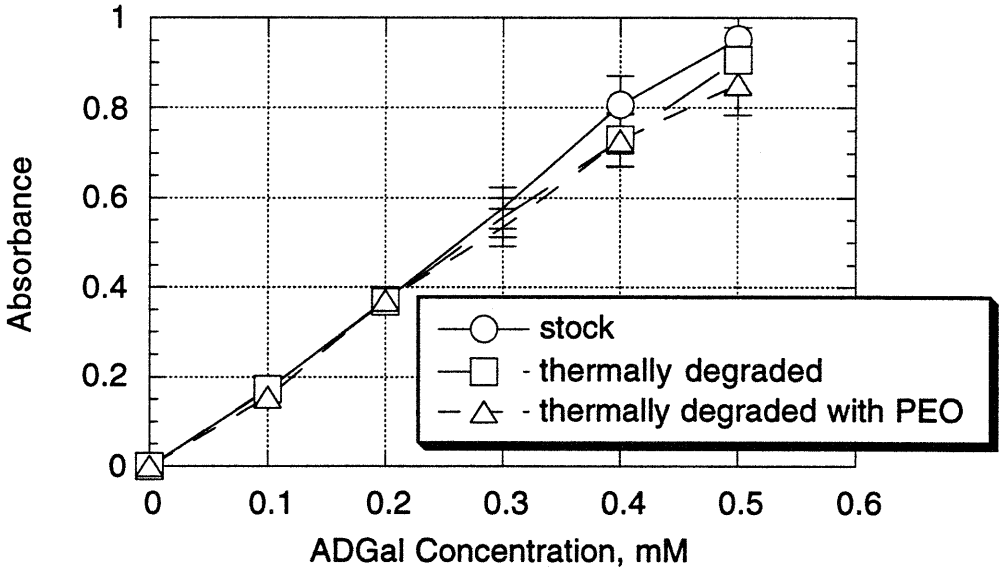

Figure 3-5. Calibration curve comparison.
Error bars represent standard deviation of 4 runs.

To achieve a range of ligand concentrations, it is desirable to couple less than the maximum amount of ligand to hydrogels. Uniform distribution of ligand cannot be assured when coupling gels at a substoichiometric ratio, as the ligand may react with the tresyl groups first encountered at the gel surface, only reaching the gel interior after surface groups have reacted. One would expect a gradient of higher ligand concentration at the gel surface, diminishing towards the gel center. Such a ligand distribution would be difficult to quantitatively characterize for accurate determination of ligand available to cells which will be seeded on the material. Two approaches for uniformly reducing ligand concentrations in the gel were investigated: (1) precoupling ligand to stars in solution followed by crosslinking; (2) coupling a mixture of active ligand (ADGal) and inactive ligand (ADGlu).

(1) Diffusion limitations present when coupling ligand in gels are not present when activating and coupling the ligand to stars in solution before crosslinking. Aqueous solutions of star PEO already coupled with a substoichiometric amount of ligand may be irradiated to form hydrogels with a low but uniform ligand distribution. Following the procedures outlined in Section 3.2. and Appendix B, S3510 was activated and then coupled with ADGal in substoichiometric amounts (10, 50 and 100% stoichiometric ligand amount). Uncoupled ligand must be removed from the coupled stars to get an accurate measure of coupled ligand concentration. Star and ligand were dissolved in various solvents including methanol, benzene and chloroform to find an appropriate solvent which would facilitate separation and preserve ligand for further analysis. Methanol was found to be the best choice: dissolution is rapid, the polymer precipitates at low temperatures (-20°C), the ligand remains in solution and can be retrieved for analysis after solvent evaporation, and ligand reactivity to acidic anthrone was unchanged by the separation procedure. Uncoupled ligand was removed from the coupled stars by repeated dissolution and precipitation of the polymer from methanol, as in the activation procedure (Appendix B). ADGal coupling yield determined with the acidic anthrone assay is shown in Table 3-7. The high yield observed with the 10% coupled material emphasizes that limitations occur in the activation step rather than the coupling step (all polymers were activated for high yield). Hydrogels were produced from 4 wt% solutions of ligand-coupled S3510 subjected to a 4 Mrad radiation dose. In stark contrast to identical gels produced from uncoupled S3510 (same concentration, same dose), the pre-coupled star hydrogels were fragile and difficult to remove from the petri dishes in which they were irradiated; they appeared stuck to the dish bottom and did not lift off with sterile MilliQ water as do other irradiated gels. Pre-coupled star hydrogels were allowed

to swell in MilliQ water for 5 days, reserving the water which was replaced daily. Carbohydrate analysis of the reserved solvent fraction revealed that nearly all ligand leached from the hydrogels (Table 3-7). The addition of ligand appears to have altered the irradiation chemistry to shift the equilibrium to chain scission, yielding fragile gels. Radicals may react more readily with the ligand or ligand/tether union releasing ligand from the gels. Pre-coupling star PEO was not an effective means of producing hydrogels with uniform but low ligand concentrations.

(2) Coupling star PEO hydrogels with a mixture of active (*i.e.* recognized by the ASGP-R) and inactive (*i.e.* not recognized) ligands may achieve the desired result of a low ligand concentration uniformly distributed throughout the gel if coupling activity is equivalent for both the active and inactive ligands. Nonspecific binding experiments have shown that hepatocytes do not adhere to ADGlu derivatized surfaces, yet ADGal and ADGlu couple to tresyl chloride activated gels with identical affinity, yielding the same ligand concentration regardless of sugar coupled (Table 3-8). The carbohydrate concentration can be determined with the acidic anthrone assay whether ADGal or ADGlu or a mixture of the two is coupled because these sugars show equal reactivity in the assay. Four star hydrogels were coupled with a 15-25:1 ratio of ADGlu:ADGal to achieve a uniform distribution of active ligand (ADGal) in the desired concentration range (Table 3-8).

Table 3-7. Ligand-coupled star 3510.

Stars in Solution		Pre-coupled Hydrogels	
Target Yield (%)[a]	Coupling Yield (%)[b]	Total Ligand (μmoles)[c]	Ligand in Supernatant (μmoles)[d]
100	49.1 ± 12.9	9.9	8.5 ± 0.9
50	29.3 ± 3.6	5.2	4.9 ± 0.4
10	9.2 ± 0.6	1.6	1.4 ± 0.2

a Percent of stoichiometric ligand amount added to coupling solution.
b Percent of stoichiometric ligand amount measured on coupled stars ± standard deviation of 4 samples.
c Amount of pre-coupled ligand on stars irradiated to produce hydrogels.
d Amount of ligand measured in supernatant collected from pre-coupled hydrogel swelling media (5 days) ± standard deviation of 3 samples.

Table 3-8. Hydrogel Ligand Concentration

Polymer	Polymer Conc. (gm/L)[c]	Radiation Dose (Mrad)	Hydroxyl Conc. (mM)	ADGal Conc. (mM)	ADGlu Conc. (mM)	ADGal + ADGlu Conc.
S3210 w/linear[a]	58.4 ± 6.3	8	7.2 ± 0.8	3.8 ± 0.4		
	58.4 ± 6.3	8	7.2 ± 0.8	0.08[d]		3.2 ± 0.8
S3210	69.0 ± 5.0	8	19.0 ± 1.4	14.1 ± 0.9		
	69.0 ± 5.0	8	19.0 ± 1.4	[e]4.1 ± 1.1		
	69.0 ± 5.0	8	19.0 ± 1.4		15.4 ± 1.0	
	69.0 ± 5.0	8	19.0 ± 1.4	0.53[d]		13.3 ± 1.3
	60.7 ± 3.4	6	16.7 ± 0.9	12.4 ± 0.8		
	64.5 ± 5.7	8	17.7 ± 1.6	12.3 ± 0.1		
S3498	56.6 ± 5.9	8	5.7 ± 0.6	3.7 ± 0.5		
	56.6 ± 5.9	8	5.7 ± 0.6	0.17[d]		3.4 ± 0.9
	56.0 ± 3.2	8	5.6 ± 0.3	4.0 ± 0.5		
	44.1 ± 4.8	4	4.4 ± 0.4	2.6 ± 0.1		
S3509	72.8 ± 3.8	10	7.0 ± 0.4	5.5 ± 0.3		
S3510 w/linear[b]	31.8 ± 4.1	2	3.1 ± 0.4	2.6 ± 0.2		
	31.8 ± 4.1	2	3.1 ± 0.4	0.11[d]		2.2 ± 0.7
S3510	63.8 ± 4.0	4	12.3 ± 0.8	8.6 ± 0.1		
	72.7 ± 2.0	8	14.0 ± 0.4	9.3 ± 0.7		
PEO:PEG	28.7 ± 5.2	6	0.9 ± 0.1	0.6 ± 0.1		
	38.5 ± 3.3	12	4.4 ± 0.7	3.0 ± 0.3		
	37.0 ± 6.0	14	5.9 ± 1.8	3.8 ± 0.3		
	38.9 ± 9.2	16	7.5 ± 3.2	4.3 ± 0.4		
	40.6 ± 2.9	18	8.4 ± 1.0	2.4 ± 0.5		
	40.6 ± 2.9	18	8.4 ± 1.0		2.9 ± 0.5	
PEO:TEG	27.4 ± 5.6	6	0.5 ± 0.4	0.4 ± 0.1		
	29.1 ± 7.2	14	6.2 ± 1.8	3.8 ± 0.1		
	35.0 ± 9.4	16	7.7 ± 3.2	4.7 ± 0.1		
	32.3 ± 4.1	20	11.1 ± 1.9	9.9 ± 1.1		
	32.3 ± 4.1	20	11.1 ± 1.9		11.0 ± 1.2	

a Star 3210 and 29,750 MW linear PEO were mixed (3 wt% star, 5 wt% linear) prior to irradiation to produce long ligand tethers, approximately equal to the star arm MW.
b Star 3510 and $5x10^6$ MW linear PEO were mixed (2 wt% each) prior to irradiation to produce long ligand tethers, approximately equal to the star arm MW.
c After equilibrium swelling.
d ADGal concentration calculated from the ratio of ADGal:ADGlu in the original coupling buffer, assuming equal coupling affinity for both ligands.
e A substoichiometric amount of ADGal added during the coupling stage reduced the final concentration.

3.3.2.4. Galactose Partitioning into Hydrogels

PEO derives its biologically inert character in part from its ability to sweep out a large excluded volume (Atha, 1981). Uniform ligand coupling to PEO hydrogels requires that the carbohydrate is able to diffuse throughout the gel. The partition coefficient of ADGal into linear PEO hydrogels was measured to assure sufficient ligand is accessible to the inner binding sites. Partitioning also plays a role when calculating the amount of ligand attached to the gel by measuring the amount retained in the supernatant. The partition coefficient can be defined as the ratio of the concentration of ligand in the hydrogel to the concentration of ligand in the bulk. The effective diffusion coefficient for small solutes through PEO hydrogels is approximately $3x10^{-6}$ cm^2/s (Merrill, 1993) which corresponds to a characteristic diffusion time of one hour per mm hydrogel thickness. A 1 mM solution of ADGal in PBS was allowed to diffuse into unactivated linear PEO gels (4 gels, 8 Mrad dose, 38.7 g polymer per swollen L gel) for 20 hours at room temperature, the same conditions used for carbohydrate coupling and time an order of magnitude greater than the estimate for diffusion limitations. The volume ratio of bulk solution to gel was 3:1. Residual ADGal concentration in the supernatant was then measured with the standard acidic anthrone assay; ADGal which had diffused into the gel was measured after thermally degrading the polymer. Mass balance closure was obtained as the initial 3 g ADGal/cm^3 gel was reconciled with the sum of sugar found in the degraded polymer and supernatant (0.61 ± 0.05 and 2.35 ± 0.07 ADGal/cm^3 gel, respectively). The ratio of ADGal concentration in the hydrogel (0.61 mM) to that in the supernatant (0.78 mM) gives a partition coefficient of 0.78 ± 0.08. A value close to unity suggests minimal interaction between solute and polymer in the hydrogel. Proteins (cyanocobalamin, lysozyme, chymotripsinogen, and albumin) in PEO hydrogels also display partition coefficients near unity (Merrill, 1993). Perez measured the partition coefficient for glucose in PEO hydrogels, obtaining a value close to 2 (Perez, 1994). Similar partition

coefficients were found for tricyclic antidepressants (protriptyline, desipramine, imiprine, amitriptyline and trimipramine), but the presence of nitrogen in the compound dropped the average partition coefficient from 2.55 to 1.8 (Merrill, 1993). Perhaps the amino group on the ADGal acts in a similar manner to drop the partition coefficient for the amino-sugar as compared to glucose.

3.3.3. Nonspecific Protein Adsorption

A critical property of the hepatocyte scaffold is its relative inertness. PEO has been shown to be resistant to protein and platelet adsorption, but irradiation and addition of ligands may compromise the inert character of PEO, permitting nonspecific protein adsorption.. FTIR results showed that no chemical functionalization of the hydrogels occurs through irradiation. Direct measurement of protein adsorption was completed to demonstrate that PEO hydrogels embody the inert character sought.

Polymer hydrogel mesh size was considered when selecting the model protein for adsorption experiments. An estimated mesh size can be calculated from Equation (3-1)

$$\zeta = \alpha_s \sqrt{2nl^2} \qquad (3\text{-}1)$$

where n is the number of bonds between crosslinks, l is the bond length, and α_s is the linear deformation of the end-to-end distance between two crosslinks (de Gennes, 1979). In polymer hydrogels where the chains extend beyond the end-to-end distance of freely rotating chains, $\alpha_s \approx 2$ (Korsmeyer, 1981). Table 3-9 outlines the polymer hydrogels examined for protein adsorption along with the molecular weight between crosslinks and approximate mesh size. Reinhart and Peppas show that a critical mesh size of 6.3 nm will allow diffusion of albumin (a globular protein of 4 x 14 nm) (Reinhart, 1984). The size and shape of fibronectin, a highly flexible protein approximately 6 x 60 nm (Williams, 1982), suggests it would not diffuse into the hydrogels examined during the adsorption experiments.

Fibronectin's role in hepatocyte function and spreading also makes it an attractive model protein for this study. Fibronectin will be present even in serum-free media since it is secreted by cultured hepatocytes within the first 2-3 hours post seeding. Fibrillar structures of fibronectin and fibrinogen which support cell adhesion and spreading are formed within 30 hours of culture (Stamatoglou, 1987). Large amounts of fibronectin adsorbed onto the modified PEO hydrogels may mask the interaction between the ASGP receptor and immobilized ligand.

Table 3-9. Hydrogel Mesh Size

Polymer	M_c	Average mesh size (nm)
PEO	5,300	8.1
PEO:PEG	5,800	8.4
PEO:TEG	6,300	8.8
Star 3210	2,100	5.1
Star 3498	5,100	7.9

Radiolabeled ^{125}I-fibronectin was diluted 8:1 with unlabeled fibronectin, giving a final specific activity of 0.329 μCi per μg. PEO hydrogels listed in Table 3-9 (derivatized and underivatized, 4 repeats of each gel) were incubated with protein in a 2 μg/ml solution of PBS at room temperature for 20 hours. The gels were drained of excess liquid on blotting paper, rinsed once, rinsed twice, and washed with protein-free PBS for 20 hours. Radioactivity associated with the hydrogels was measured after each step using a Searle Analytic Inc. Model 1185 automatic gamma counter.

Less than 150 ng protein adsorbs per cm^2 underivatized hydrogel (approximately 2% of the total protein available); less than 50 ng remains adsorbed after a 20 hour rinse (Figure 3-6). Even after the material has been coupled with ADGal, less than 100 ng protein adsorbs per cm^2 hydrogel (Figure 3-7). Monolayer adsorption of fibronectin would yield approximately 2,500 ng/cm^2 (DiMilla, 1992), more than 10 times that observed on PEO hydrogels. Ingber reports fibronectin adsorption onto tissue culture polystyrene in the range 1000-2000 ng/cm^2 (Ingber, 1990, Desai, 1991). Mooney examined the relationship between the amount of adsorbed protein on nonadhesive plastic dishes and the adhesion and spreading of rat hepatocytes (Mooney, 1992). He found that while adhesion was observed even at low fibronectin coating densities, a high fibronectin density (around 1000 ng/cm^2) was needed to support cell spreading. The small amount of protein adsorption measured is insufficient to support any hepatocyte spreading observed.

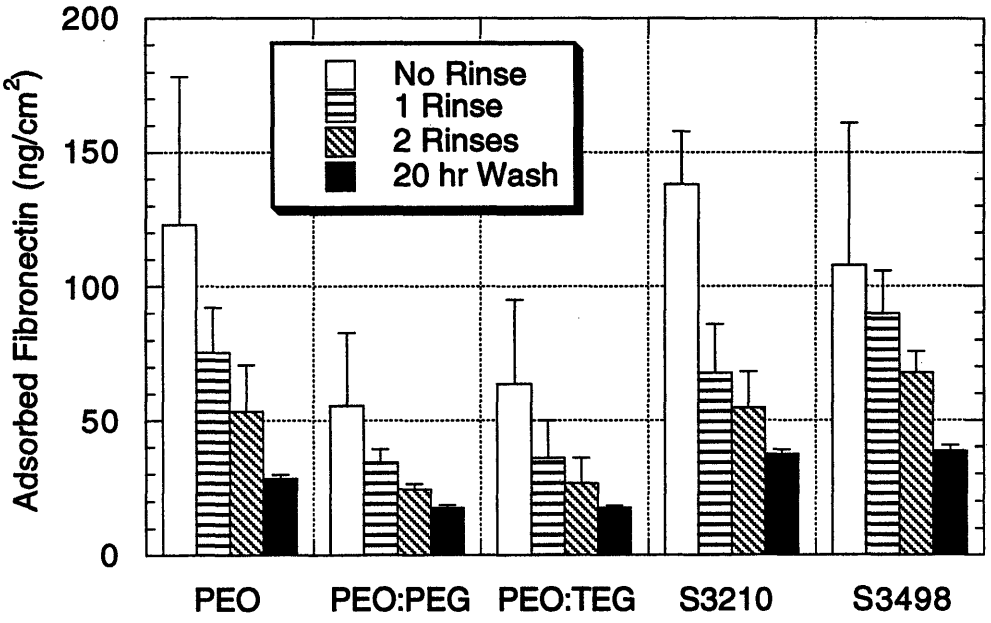

Figure 3-6. Fibronectin adsorption onto underivatized PEO hydrogels.

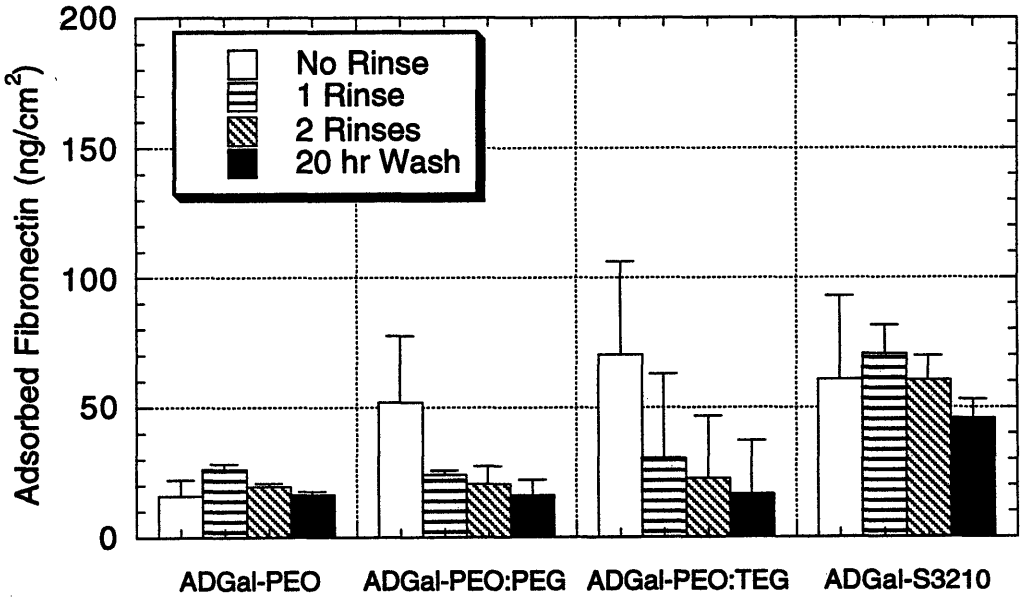

Figure 3-7. Fibronectin adsorption onto ADGal-PEO hydrogels.

3.4. Derivatization Induced Polymer Degradation

Activation and coupling reactions involving gels require extended reaction times due to the inherent diffusion limitations on reaction rates. Extended exposure of PEO to basic solutions may degrade the polymer. To evaluate this hypothesis, mock tresylation and coupling experiments were carried out on 10^5 MW linear PEO, taking samples at various time points to measure degradation. Polymer was extracted from reaction solutions with chloroform, then run through a GPC to measure molecular weight and polydispersity. No degradation was observed (Figure 3-8).

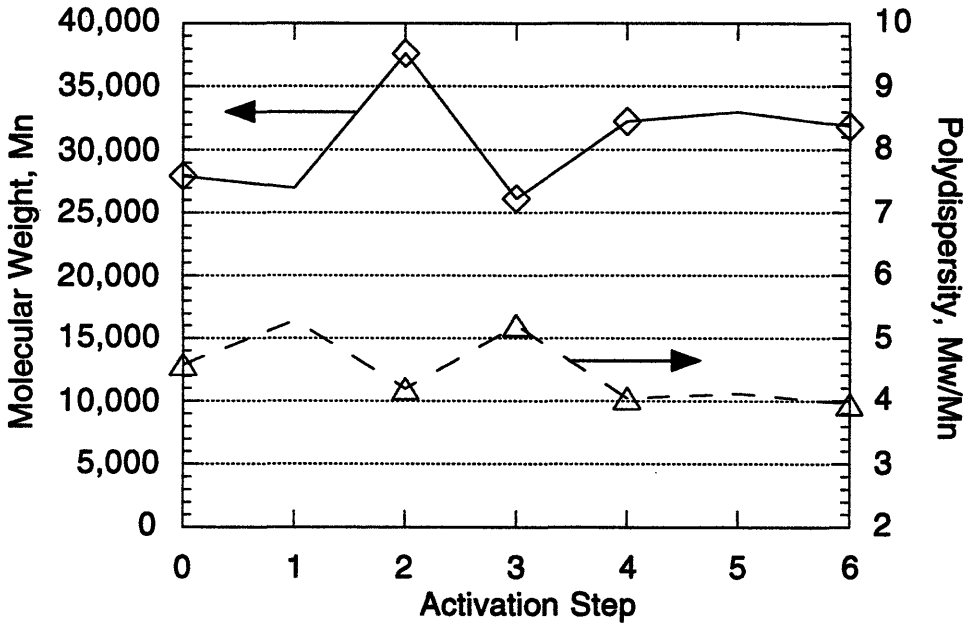

Figure 3-8. Effects of activation and coupling procedures on molecular weight and polydispersity of linear PEO. Activation steps correspond to: (0) Storage in MilliQ water, 3 days; (1) Drying/tresyl chloride reaction with 0.2% (v/v) dry triethylamine, 24 hours; (2) Rehydration and storage in 1mM HCl, 3 days; (3) Coupling reaction, 0.25M $NaHCO_3$, 1 day; (4) Storage in MilliQ water, 1 day.; (5) Wash unreacted solutes in MilliQ water, 5 additional days; (6) Storage in 70% ethanol, 3 days.

4. Hepatocyte Interactions

A series of radiation-crosslinked PEO hydrogels which spans a range of free chain end concentrations were synthesized, characterized and modified with bioactive ligands to create a scaffold for hepatocyte adhesion. Primary rat hepatocytes were seeded onto derivatized and underivatized PEO hydrogels and the ensuing cell response monitored.

4.1. Cell Culture Materials and Methods

4.1.1. Control Substrata

Hepatocytes do not adhere well to standard, unmodified polystyrene tissue culture dishes. Type I collagen is the extracellular matrix (ECM) protein most commonly used to precoat tissue culture dishes because most normal epithelial cells will attach more efficiently to collagen than to other cell culture substrates (Cailleau, 1975). Adsorption of Type I collagen provides a surface suitable for hepatocyte culture (Gjessing, 1980) which has been shown to substantially lengthen the survival of liver cells in culture (Michalopoulos, 1975) and to allow culture in serum-free chemically defined medium (Jauregi, 1983). Type I collagen coated polystyrene is the standard cell culture substrate in literature, so it was used as a control substrate for comparison of each hepatocyte isolation relative to other isolations. Tissue culture plates were coated with 10 μg Type I collagen (Vitrogen, Collagen Corp./Celltrix) per square centimeter cell culture area precipitated from a pH 9 sterile carbonate buffer solution overnight at 4°C. Dishes were washed twice with sterile phosphate buffered saline (PBS) and twice with cell culture medium prior to seeding with hepatocytes.

Cells are known to respond differently to Type I collagen when it is presented in the form of a gel; in particular, hepatocytes cultured on collagen gels maintain a cuboidal shape reminiscent of hepatocyte morphology *in vivo* while hepatocytes cultured on collagen coated dishes become elongated with ruffled contours, appearing almost "fibroblastic" within a few days of culture (Michalopoulos, 1975; DiPersio, 1991). Morphological differences are not limited to collagen gels, they are also observed on gels derived from the Englelbreth-Holm-Swarm (EHS) mouse tumor and matrigel, suggesting differences may be due to the ability of cells to deform gel substratum (Michalopoulos, 1975; DiPersio, 1991; Streuli, 1990; Mochitate, 1991). Collagen gels were prepared as control substratum for comparison to cell behavior on (deformable) PEO hydrogels. Type I collagen gels (3 mg/ml protein) were formed per the manufacturers directions by mixing over ice 8 mls Vitrogen (Collagen Corp./Celltrix), 1 ml 10x PBS (no divalent

ions) and 1 ml 0.1 M NaOH to bring the pH to 7.2 ± 0.3. Gelation is initiated by warming the neutralized Vitrogen solution to 37°C. The elevated temperature is maintained 4-18 hours to assure a stable gel.

4.1.2. Fibroblast 3T3 Cells

Fibroblast 3T3 cells were seeded in addition to hepatocytes as a test of adhesion specificity. 3T3 cells do not have an ASGP receptor and do not interact specifically with carbohydrates, yet 3T3 fibroblasts are tenacious in their ability to adhere nonspecifically to various materials (Sato, 1960). 3T3 fibroblasts used for non-specific adhesion studies were obtained from the American Type Culture Collection (ATCC) and were maintained in Dulbecco's Modified Eagles Medium (DMEM) supplemented with 10% fetal bovine serum (FBS) and 100 U/ml penicillin/streptomycin (Gibco). Cells were subcultured weekly using 0.05% trypsin and maintained sub-confluent. 3T3 cells used in experiments were between their 10th and 80th passage.

4.1.3. Hepatocyte Isolation

Primary rat hepatocytes were isolated from 180-250 g inbred male Fisher rats using a modification (Cima, 1991) of the two-step collagenase perfusion procedure of Seglen (Seglen, 1976). Briefly, the animal was anesthetized and then secured to the operating table. The inferior vena cava (IVC) at the level of the renal veins was exposed and cannulated with a #20 IV catheter. The portal vein was cut and the IVC clamped above the liver. The liver was perfused in the retrograde direction with calcium-free perfusion buffer (143 mM NaCl, 7 mM KCl, 10 mM HEPES, pH 7.4) at 30 ml/min. for 7 minutes, followed by the same perfusion buffer containing 5 mM calcium chloride and 0.5 mg/ml collagenase (Worthington) at 30 ml/min. until the liver became soft. Cells were dispersed in chemically defined serum-free culture medium shown to maintain hepatocyte viability and function in culture (Bucher, 1977) (William's E with 10 ng/ml epidermal growth factor (EGF) (Collaborative Research, Bedford, MA), 20 mU/ml insulin (Gibco, Grand Island, NY), 5 nmol/L dexamethasone (Sigma, St. Louis, MO), 20 mmol/L pyruvate (Gibco), and 100 U/ml penicillin/streptomycin (Gibco)) (Cima, 1991). This medium shall be referred to as "complete medium" and was used in all subsequent isolation and culture steps. Viable hepatocytes were separated from the liver mass and cellular debris through centrifugation in an isodensity Percoll solution. The hepatocyte pellet was resuspended in serum-free medium. Final cell viability was 70-95%, as determined by

trypan blue exclusion. The preparation of liver by this technique results in a cell population which is >95% pure hepatocytes (Kreamer, 1986; Mooney, 1993).

4.1.4. Hepatocyte Seeding

PEO hydrogels are sterilely cut and placed into tissue culture dishes. The hydrogel solvent fraction is exchanged with serum-free medium over a period of 24-48 hours prior to cell seeding. Primary rat hepatocytes are suspended in medium at a concentration of 10^6 cells/ml and seeded onto the gels to provide a surface density of approximately 30,000 viable cells/cm^2. Following an attachment period of 18-24 hours the medium is changed to remove unattached cells; cells are maintained in complete medium with daily medium changes. The ratio of medium volume/gel volume is approximately 4:1.

4.1.4.1. Harsh vs. Gentle Seeding

Hepatocytes seeded onto gels covered with medium could roll off before adhering to the hydrogel. Maintenance of hepatocyte-specific function is determined by measuring albumin secretion rates from the albumin found in the medium. If many hepatocytes roll off the gel and adhere to the culture dish, it would be impossible to measure albumin secretion of hepatocytes on the hydrogels. One way to minimize the loss of hepatocytes to the dish bottom is to seed cells directly onto the hydrogels in the absence of medium, trying not to break the surface tension and keeping the cell suspension drop on top of the hydrogel. After 60-90 minutes incubation, warmed medium is carefully added to the dish. Plating cells in the absence of medium is termed "harsh seeding" as opposed to "gentle seeding" where hepatocytes are seeded in the presence of medium (onto a hydrogel submerged in medium).

While harsh seeding is effective in keeping hepatocytes on the test substrate, it may affect cell viability and function. Measuring lactate dehydrogenase (LDH) activity in the medium gives an indication of cell viability (Berg, 1972; Schnaar, 1978; Jauregui, 1981). LDH is an enzyme found inside cells which functions in the last step of glycolysis, catalyzing the reversible reduction of pyruvate to lactate (Equation 4-1). Any LDH found in cell culture medium must come from cells which have lost their membrane integrity, indicative of cell mortality. Electrophoresis experiments conducted by Jauregui, et. al. show that LDH which has leaked into the medium is stable, and therefore its activity can be measured by monitoring the reaction with a UV spectrophotometer (Jauregui, 1981). The oxidation of NADH (reduced nicotinamide adenine dinucleotide) results in a

decrease in absorbance at 340 nm; the rate of absorbance decrease is directly proportional to LDH activity.

$$\text{pyruvate} + \text{NADH} + \text{H}^+ \xrightarrow{\text{LDH}} \text{lactate} + \text{NAD}^+ \qquad (4\text{-}1)$$

The effect of harsh seeding was determined in a controlled experiment where hepatocytes were seeded onto collagen-coated petri dishes (no hydrogel) at 30,000 viable cells/cm^2 under either "harsh" (in the absence of medium) or "gentle" (in the presence of medium) seeding conditions. Medium samples were taken daily to analyze for extracellular LDH activity (Figure 4-1). Two dishes seeded under each condition were sacrificed each day to count adherent cells (Figure 4-2). The large LDH activity in the sample taken after 24 hours is not indicative of the seeding technique, but rather comes from nonviable cells seeded at the start. On days 2-4, extracellular LDH activity of "harsh" seeding always exceeds that of "gentle" seeding indicating significant cell mortality, although the difference diminishes over the duration of the experiment as cells recover. A similar trend is observed with the cell counts (Figure 4-2). While it appears hepatocytes recover from "harsh" seeding, it is clear the method harms the cells at the start and should be avoided if possible.

4.1.4.2. Materials Transfer

Another way in which the metabolism of hepatocytes adherent to the materials could be analyzed without being obscured by activity from cells which had attached to the bottom of the dish during the seeding operation is to carefully transfer test samples to new tissue culture dishes 24 hours post seeding. The effect of transferring substrates was examined using collagen-coated Millipore filters as transfer substrates. Substrates prepared in the same manner but left untransferred and collagen-coated tissue culture dishes were used as controls. Medium samples were taken daily to analyze for extracellular LDH activity (Figure 4-3). Two dishes seeded under each condition were sacrificed each day to count adherent cells (Figure 4-4). The jump in LDH activity on day 2 in the extracellular medium of transferred cells (24 hours after transfer), but not of untransferred controls, suggests that many cells die upon transfer. The large loss of hepatocytes is apparent in the daily cell counts. Transferring substrates may be even more detrimental to hepatocyte viability than harsh seeding conditions.

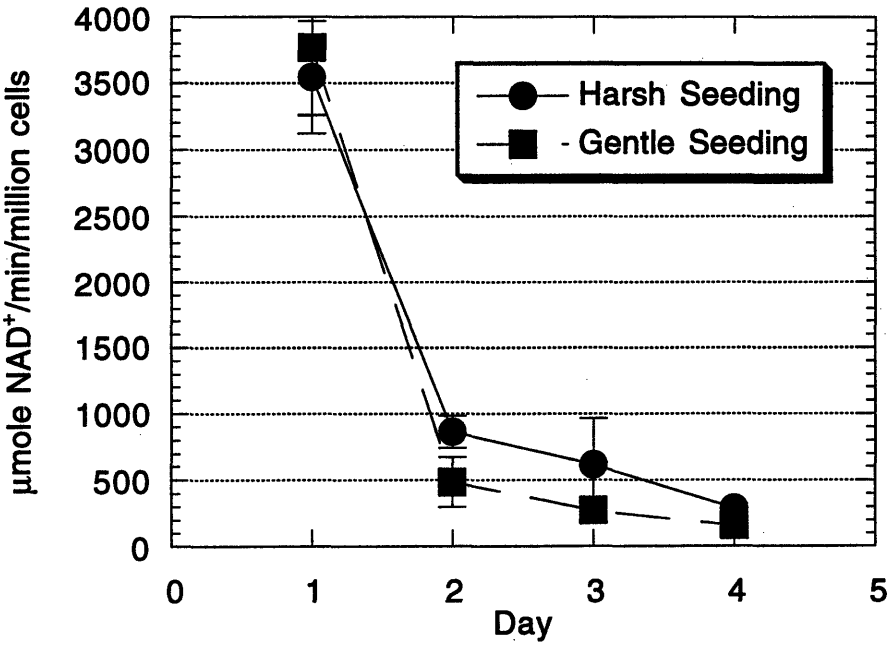

Figure 4-1. Lactate dehydrogenase activity of hepatocytes seeded under "harsh" or "gentle" conditions. Activity reported per million cells adhering to dishes.

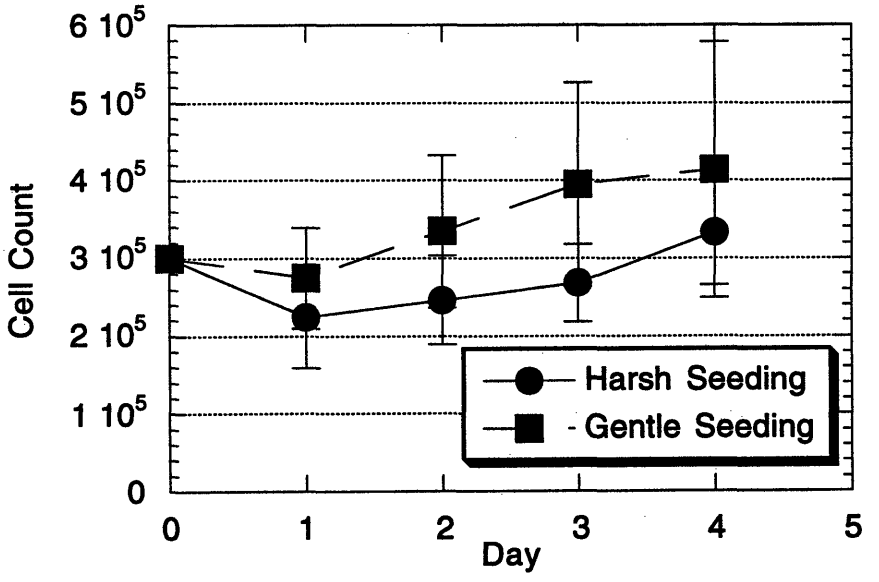

Figure 4-2. Daily cell count of hepatocytes seeded under "harsh" or "gentle" conditions.

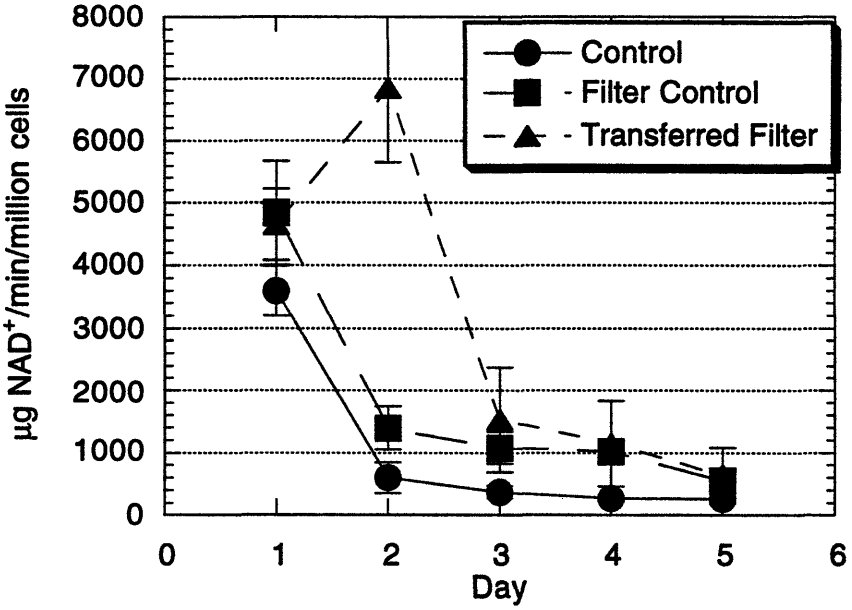

Figure 4-3. Lactate dehydrogenase activity of hepatocytes seeded onto collagen coated substrates. Control substrate is a standard tissue culture dish, filter control is an untransferred Millipore filter, and transferred filter is a Millipore filter which is transferred to a new dish 24 hours post seeding. Activity reported per million cells adhering to substrates.

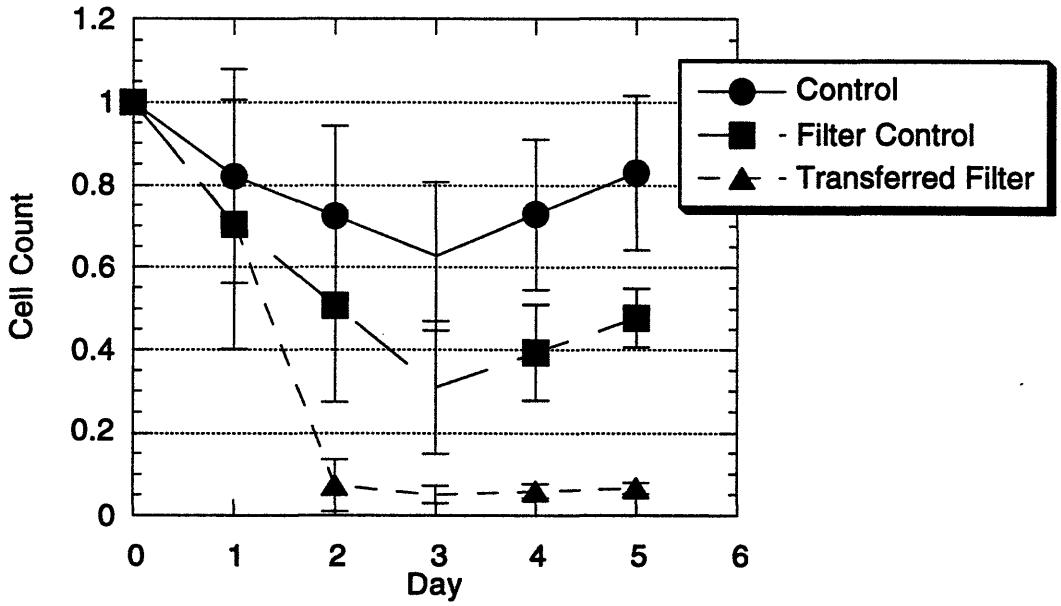

Figure 4-4. Daily cell count of hepatocytes seeded onto collagen coated substrates. Control substrate is a standard tissue culture dish, filter control is an untransferred Millipore filter, and transferred filter is a Millipore filter which is transferred to a new dish 24 hours post seeding. Cell count plotted as fraction of the number of hepatocytes originally seeded.

4.1.4.3. Tight Fit Wells

A method was devised to provide flat and uniform culture surfaces which ensured that all the cells seeded stayed on the gels, permitting a "gentle" seeding technique. Hydrogels were sterilely cut with a 6.0 mm trefaine blade to tight fit Costar 96-well culture dishes (6.5 mm ID). Gels were secured into the well with silicone rubber rings carefully cut from a 1.5 mm thick sheet (6.5 mm OD, 5.5 mm ID; Green Rubber Co.) and sterilized in 70% ethanol. The ± 0.5 mm difference between the hydrogel and ring dimensions allow the hydrogel to swell and deswell with changing temperature without compromising the tight fit nature of the setup, thus preventing hepatocytes from slipping beneath an intact gel. Precision cutting of hydrogels and test rings are required for the setup to function as intended. Hydrogels thus secured are washed extensively with sterile water and equilibrated with complete medium prior to cell seeding. The only surface available to cell attachment is the test substrate. The tight fit well method is the preferred setup for obtaining quantifiable hepatocyte metabolism data.

4.2. Hepatocyte Adhesion and Spreading

Cells seeded onto test and control substratum were examined visually with a Diaphot-TMD inverted phase contrast light microscope equipped with a Nikon 35 mm camera. Fibroblast 3T3 cells were seeded in addition to hepatocytes as a test of adhesion specificity. Typically, signs of adhesion are observed within 3 hr for both hepatocytes and 3T3 cells on control collagen substrates (Jauregui, 1986) although hepatocyte spreading may take up to 12 hours (Rotem, 1992), so cells were examined four hours after seeding and daily for the duration of the experiment.

4.2.1. PEO Grafted Surfaces

PEO Star 3510 (70 arms per star, 5200 MW arms) was grafted onto aminated glass surfaces as described in Chapter 3. Low adsorption of adhesion molecules to star grafted glass suggests that stars are dense enough to approximate complete surface coverage (Kuhl, unpublished). XPS analysis confirms significant PEO grafting onto aminated glass (Chapter 3). Hepatocytes were seeded onto derivatized and underivatized PEO grafted slides. The slides were submerged in complete medium, and hepatocytes were seeded through the medium onto the grafted area at 30,000 viable cells/cm^2. With complete PEO coverage, it is expected that no hepatocytes would adhere to the

underivatized slide. Hepatocytes should adhere and spread on ADGal-derivatized slides. Hepatocyte spreading was quantified at 24 and 48 hours post-seeding with a Hitachi CCD video camera hookup to the phase contrast microscope which allowed images to be digitized and captured on a Macintosh Centris 650 computer. LabVIEW (National Instruments, Austin, TX) based image analysis software utilizing Concept Vi operational software (Graftek Imaging, Mystic, CT) calculated the spread area of adherent hepatocytes.

Some cells did adhere to the underivatized PEO grafted slides, likely due to protein adsorption onto patches of underlying glass which were left ungrafted. However the number of adherent cells was 3-4 times greater on the derivatized PEO (Table 4-1). Spread cell area was measured on three sections each on duplicate slides, totaling 20-130 cells per slide. The average spread area on derivatized PEO was statistically greater than on underivatized slides (Table 4-1, $P < 0.01$, day 1; $P < 0.10$, day 2, student T-test). These results indicate that ADGal derivatization increases the material affinity for hepatocyte adhesion and spreading. The problem with incomplete coverage of the substrate is also evident as some cells adhere and spread on bare patches of the underivatized slide. Hepatocytes cultured on collagen coated dishes achieve a spread area of 1200-2000 μm^2 over the same time period.

Table 4-1. Hepatocyte cell count and area on PEO grafted slides.

Hours Post-Seeding	Underivatized PEO Graft		ADGal-PEO Graft	
	Cell Count[a]	Spread Area (μm^2)	Cell Count[a]	Spread Area (μm^2)
24	50	465±173[b]	148	614±246[b]
48	65	830±544[c]	265	991±512[c]

± standard deviation of counted cells
a Total number of cells counted on the 6 regions (3 regions on 2 slides)
b Statistically different by student t-test, $P < 0.01$
c Statistically different by student t-test, $P < 0.10$

4.2.2. PEO Hydrogels

PEO hydrogels provide a pure PEO system without complications from the underlying substrate observed in the grafted system. By using either star PEO or a combination of relatively high MW linear PEO with shorter oligomers and varying irradiation conditions, a range of ligand concentrations can be achieved. To provide flat and uniform culture surfaces which ensured that all the cells seeded stayed on the gels, hydrogels were prepared via the tight fit well method. Cells were plated in complete medium at a concentration of 30,000 viable cells/cm^2 culture surface area. Following an attachment period of 18-24 hours the medium was changed to remove unattached cells and then cells were maintained in complete medium with daily medium changes. For control experiments, cells were also seeded on Type I collagen (Vitrogen, Collagen Corp./Celltrix) which was either coated at 10 μg/cm^2 onto tissue culture polystyrene from a pH 9 carbonate buffer or formed into a gel containing about 3 mg/ml protein using the protocol provided with the product.

4.2.2.1. Non-Specific Interactions

Two types of control experiments were completed to assess the nonspecific interactions of cells with hydrogels. In the first set unmodified gels were seeded with either hepatocytes or 3T3 fibroblasts. Linear PEO and S3210 hydrogels (4 gels each) were seeded at 30,000 viable cells/cm^2. Typically, signs of spreading are observed within 3 hr for both hepatocytes and 3T3 cells on control collagen substrates, so cells were examined four hours after seeding and on each of the next two days. No signs of spreading were seen on the unmodified gels. Although this negative finding might be attributed to a toxic contaminant leaching from the gels, cells cultured in petri dishes in the presence of the gels were well-spread and exhibited a normal morphology when maintained directly underneath (and in close contact with) the gels. Thus, the lack of spreading on the unmodified gels can be attributed to the non-adhesive nature of the gel surfaces. After two days the gels were removed from the original wells, dipped gently in warm complete medium to remove unattached cells, and placed in a fresh dish or well to assess cell attachment. Fewer than 20 cells were observed on any surface.

The response of cells to nonspecifically modified gels was also tested. Cells were seeded on gels modified with ADGlu instead of ADGal (4 gels each, Table 3-7). ADGlu coupling is a negative control for the ADGal-PEO. Amino-glucose coupling would invoke an almost identical physico-chemical change to the hydrogel, but there is no receptor for glucose on hepatocytes so no adhesion is expected. Using the protocol

described above, no cell attachment was observed. Both control experiments (unmodified and ADGlu-modified) were repeated three times.

The *in vivo* biocompatibility of PEO hydrogels was examined by George Wu in our lab as part of his M.D. thesis work (Wu, 1993). Star 3509 PEO hydrogels were surgically implanted in the rat mesentery membrane with silica-free poly(dimethylsiloxane) (PDMS) as control. The PDMS has been highly purified and well characterized and is considered to be relatively nondegrading, nontoxic and biocompatible. It is suggested by the Devices and Technology Branch (DTB) of the National Heart, Lung and Blood Institute (NHLBI) as a primary reference material for biocompatibility testing. The peritoneal cavity is a well vascularized site with a large surface area for rapid fluid exchange and is an excellent site for future liver cell transplants, making it the choice location for biocompatibility studies of PEO hydrogels. To study the host inflammatory reaction more consistently and to avoid cross-reactions from the inevitable inflammatory response caused by the surgical incision, the implants were enclosed by the mesentery membrane rather than free floating in the peritoneal cavity. The procedure is very similar to that which would be used for hepatocyte transplantation.

Material samples (PDMS and PEO) were cut into 4x5x0.75 mm pieces. One of each was implanted into the mesentery of each of eight animals used in the study. At one and three weeks post-implantation, the implants and surrounding tissue in four animals was removed, fixed in formalin, processed and embedded in glycolmethacrylate for histologic sectioning. Sections were taken from three points cut horizontally through the block for eosin and hematoxylin staining. The morphology of the inflammatory response was observed on an inverted microscope and photographed. The inflammatory reaction observed on each implant was quantified by measuring the thickness of the fibrous capsule surrounding the implant. The measurements (ten per implant) were taken on an inverted microscope attached to a CCD camera (Hitachi Denshi model KP-M1U) and connected to a Macintosh IIsi, using the image analyzer program NIH Image 1.44. The inflammatory response to PEO hydrogels was not statistically different from the PDMS standard (Table 4-2).

4.2.2.2. Amino-Galactose Derivatized Hydrogels

The ADGal ligand immobilized on PEO hydrogels should interact specifically with hepatocytes through the asialoglycoprotein receptor, leading to cell adhesion. Hepatocytes were seeded onto ADGal modified hydrogels with ligand concentrations outlined in Tables 3-8 and 4-3. In contrast to underivatized and ADGlu-derivatized

Table 4-2. Inflammatory Response (from Wu, 1993)

Time	Fibrous Capsule Thickness (μm)	
	PDMS	S3509
1 week	63.6 ± 18.7	89.9 ± 26.4
3 weeks	89.2 ± 42.0	59.1 ± 24.4

hydrogels, hepatocytes adhere to all ADGal-derivatized hydrogels examined within 3 hours of seeding. Results reported previously in the literature show a threshold concentration of 3 mM galactose required for hepatocyte adhesion and a threshold value of 30-70 mM galactose required for spreading to occur on galactose-derivatized polyacrylamide gels (Weigel, 1979; Oka, 1986). Hepatocytes adhered to ADGal-derivatized star PEO hydrogels at ligand concentrations well below 1 mM (Table 4-3). Hepatocytes adherent to ADGal-derivatized PEO gels exhibit virtually no signs of spreading for times less than 3 hours after seeding, while spreading begins to occur on control collagen-coated substrates by this time. This is consistent with previous reports that hepatocyte attachment occurs within 45 min. on carbohydrate-derivatized surfaces of other types (Oka, 1986; Schnaar, 1989; Weisz, 1991a), whereas spreading requires at least 12 hr of incubation (Oka, 1986; Rotem, 1992). Once a threshold ligand concentration is surpassed, hepatocytes become well-spread on ADGal-derivatized star hydrogels by eighteen hours after seeding (Table 4-3, Figure 4-5). The critical minimum ligand concentration for hepatocyte spreading on star PEO hydrogels is below 5 mM – an order of magnitude lower than that reported by Oka. The precise threshold value varies with the type of star; hepatocyte spreading was observed on star 3498 and star 3510 hydrogels at ligand concentrations below 3 mM while hepatocytes remained rounded on star 3210 hydrogels with 4.1 mM ADGal (Table 4-3). Hepatocytes seeded onto ADGal-derivatized linear/oligomer hydrogels, though adherent, remained rounded throughout the duration of cell culture (4-6 days) (Table 4-3, Figure 4-6). The ligand on linear/oligomer hydrogels appear to interact with hepatocytes in a manner more similar to polyacrylamide gels than to star PEO gels; the PEO:TEG gels have a ligand concentration well within the range where spreading was observed on star hydrogels (Table 4-3) yet spreading was not observed, as would be predicted from literature results on polyacrylamide (Oka, 1986).

A

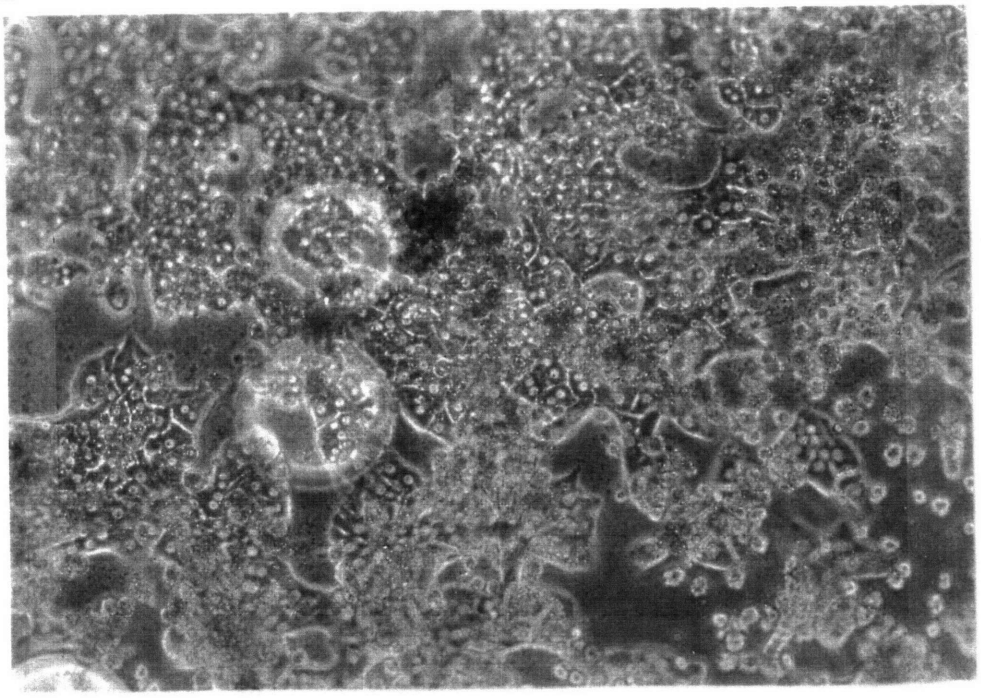

B

Figure 4-5. Hepatocytes on ADGal-Star PEO hydrogel. A. Spreading 18 hours post-seeding as observed by light microscopy, original magnification 100x. B. Morphological appearance of hepatocytes maintained for 4 days, as observed by scanning electron microscopy.

Table 4-3. Hepatocyte Behavior on ADGal-Derivatized Hydrogels

Polymer	Polymer Conc. (gm/L)[a]	Radiation Dose (Mrad)	Hydroxyl Conc. (mM)	ADGal Conc. (mM)	Hepatocyte Spreading
S3210 w/linear	58.4	8	7.2	3.8	Yes
	58.4	8	7.2	0.08[b]	No
S3210	69.0	8	19.0	14.1	Yes
	69.0	8	19.0	4.1[c]	No
	69.0	8	19.0	0.53[b]	No
	60.7	6	16.7	12.4	Yes
	64.5	8	17.7	12.3	Yes
S3498	56.6	8	5.7	3.7	Yes
	56.6	8	5.7	0.17[b]	No
	56.0	8	5.6	4.0	Yes
	44.1	4	4.4	2.6	Yes
S3509	72.8	10	7.0	5.5	Yes
S3510 w/linear	31.8	2	3.1	2.6	Yes
	31.8	2	3.1	0.11[b]	No
S3510	63.8	4	12.3	8.6	Yes
	72.7	8	14.0	9.3	Yes
PEO:PEG	40.6	18	8.4	2.4	No
PEO:TEG	32.3	20	11.1	9.9	No
Polyacrylamide[d]				30-70	Yes

a After equilibrium swelling.
b ADGal concentration calculated from the ratio of ADGal:ADGlu in the original coupling buffer, assuming equal coupling affinity for both ligands.
c A substoichiometric amount of ADGal added during the coupling stage reduced the final concentration.
d Galactose-modified polyacrylamide gel data from Oka, 1986.

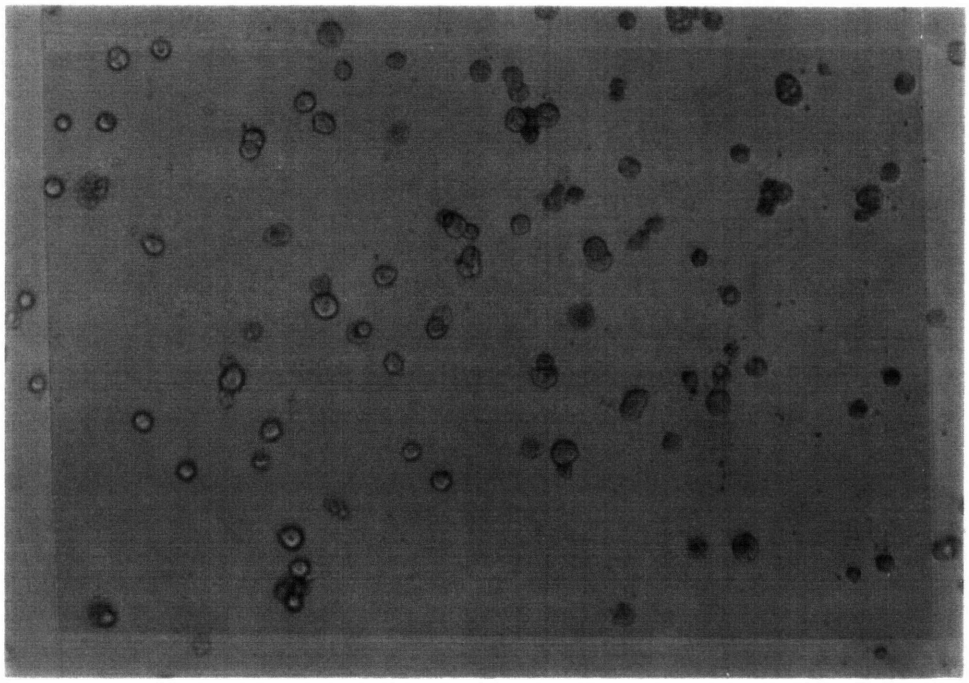

Figure 4-6. Hepatocytes on ADGal-Linear/Oligomer PEO hydrogel. Spreading 2 days post-seeding as observed by light microscopy, original magnification 100x.

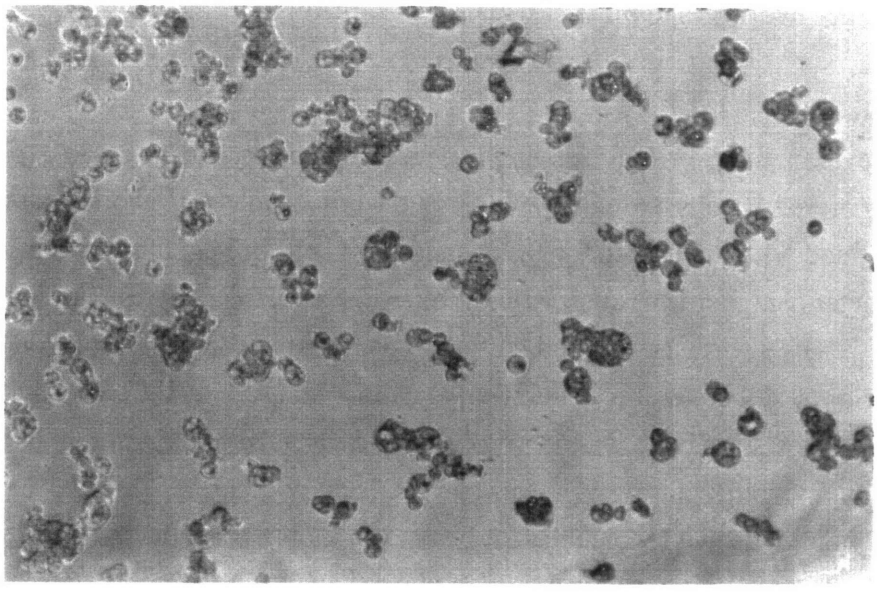

Figure 4-7. Hepatocytes on RGD-Linear/Oligomer PEO hydrogel. Spreading 24 hours post-seeding as observed by light microscopy, original magnification 100x.

The relationship between ligand concentration, ligand presentation and hepatocyte spreading is explored more fully in Chapter 5.

4.2.2.3. RGD Derivatized Linear/Oligomer Hydrogels

RGD immobilized on PEO hydrogels should bind to classical adhesion receptors on hepatocytes and other cells, leading to cell adhesion. Hepatocytes were seeded onto linear/oligomer hydrogels which had been derivatized with RGD (Table 3-4). The hydrogels used for RGD immobilization have low hydroxyl concentrations, yielding ligand concentrations on RGD-modified gels estimated to be 5-10 times lower than that of the ADGal-modified gels (compare Tables 3-4 and 3-7). While spreading was not observed on ADGal-modified linear/oligomer hydrogels, hepatocytes seeded onto RGD-modified gels were starting to spread within 24 hours (Figure 4-7) despite the low ligand concentration. Massia and Hubbell conducted a study to determine the minimum RGD concentration (maximum spacing) required for human foreskin fibroblast (HFF) adhesion and spreading onto RGD-modified glycophase glass (Massia, 1991a). They found a spacing of 440 nm sufficient for HFF spreading. Assuming even ligand distribution throughout the gel, the ligand spacing on the RGD-modified linear/oligomer hydrogels would be 15 nm, well below the maximum 440 nm RGD spacing. The linear/oligomer hydrogel results match RGD literature results and show there is nothing inherent in the linear/oligomer hydrogels to prevent hepatocyte spreading.

4.3 Hepatocyte Viability

Hepatocyte viability prior to seeding is determined by trypan blue dye exclusion - the membranes of viable cells exclude the ionic dye while dead cells become stained blue. Cells are treated with the dye and then live and dead cells are counted with a hemacytometer using a phase contrast light microscope. Hepatocytes with a minimum viability of 70-95% were used in cell culture experiments. While this method is quite adequate prior to cell culture, trypan blue dye cannot be used in culture on hydrogels, as the substrate takes up the dye, making it difficult to visualize the cells.

Hepatocyte viability during culture was visualized with a LIVE/DEAD Viability/Cytotoxicity Kit (Molecular Probes). The kit uses two probes: calcein AM, a fluorogenic substrate that is cleaved only in viable cells to form a green fluorescent membrane-impermeable product, and ethidium homodimer-1 (EthD-1), a high-affinity red fluorescent DNA stain that is only able to pass through the compromised membranes of dead cells (Molecular Probes). Both reagents are colorless until they react with the

cells. The assay is performed by adding the probes diluted in PBS to the culture dishes, allowing incubation (at room temperature or 37°C) to continue for 15-45 minutes, and examining the culture with fluorescent microscopy. The reagent concentrations in the medium are at levels generally innocuous to most cells (Molecular Probes), but the medium is changed after running the assay for assurance.

Hepatocyte viability was determined on 13 separate occasions (3-4 ADGal-derivatized hydrogels of each polymer type and ligand concentration). As expected, the viability of morphologically normal well spread hepatocytes adherent to star PEO hydrogels was nearly 100% as determined by the Molecular Probes LIVE/DEAD fluorescent assay. Rounded cells adherent on the linear/oligomer gels were seen to be 75–90% viable using the fluorescent viability assay.

4.4. Hepatocyte Culture

4.4.1. Morphology

Hepatocyte morphology on gels differ from that on flat dishes, with hepatocytes cultured on collagen gels maintaining a shape reminiscent of hepatocyte morphology *in vivo* (Michalopoulos, 1975; DiPersio, 1991). An inverted phase contrast light microscope was used to examine the morphology of hepatocytes on PEO hydrogels. Hepatocytes which spread on ADGal-derivatized star PEO hydrogels exhibit a physiological morphology, including birefringent areas between cells indicative of bile canaliculi (Figure 4-5 A), similar to that of cells on Type I collagen gels (Figure 4-8). The morphological appearance of hepatocytes maintained on these ADGal-modified gels for 4 days is shown in Figure 4-5 B. As observed by scanning electron microscopy, the surfaces of the cells exhibit abundant microvilli and cell-cell interlinkages. (Although the morphology of the cells has largely been preserved using the standard preparation technique, the cell-substrate interface and the surface of the gel have been distorted due to shrinkage of the gel, and the cell layer appears curled.) Hepatocytes maintained on ADGal-modified hydrogels retained a spread cuboidal morphology throughout the culture time as shown in Figure 4-5 A. In contrast, cells maintained on Type I collagen gels adopted a spread cuboidal morphology only in the early stages of culture, and formed trabecular structures and aggregates after 3-4 days (Figure 4-8). These differences in morphology at later times in culture perhaps reflect differences in the ability of cells to remodel the underlying substrate. Hepatocytes can extensively remodel Type I collagen

A

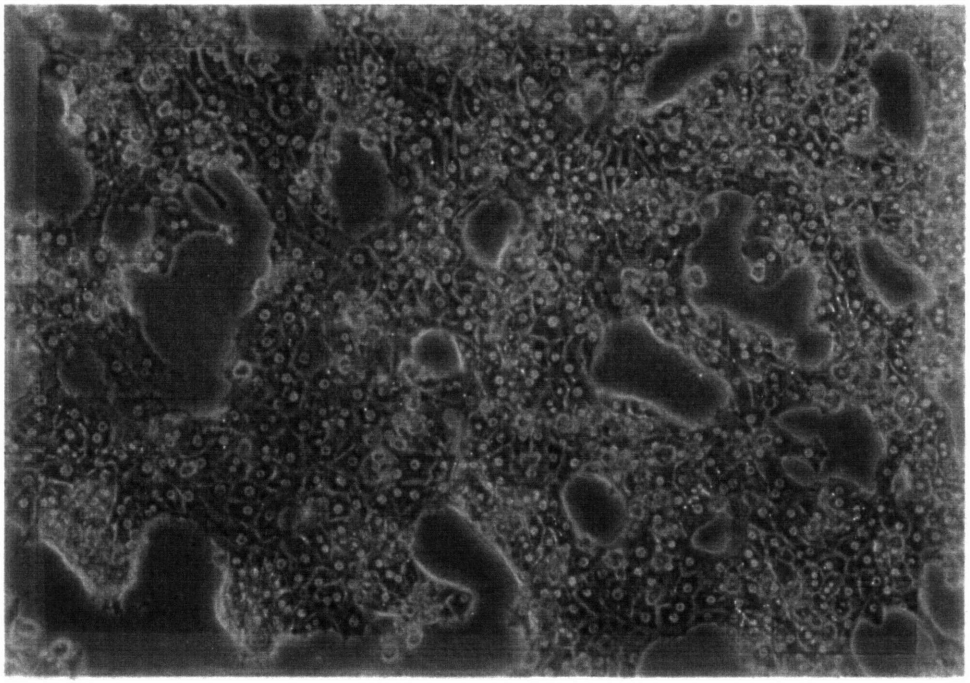

B

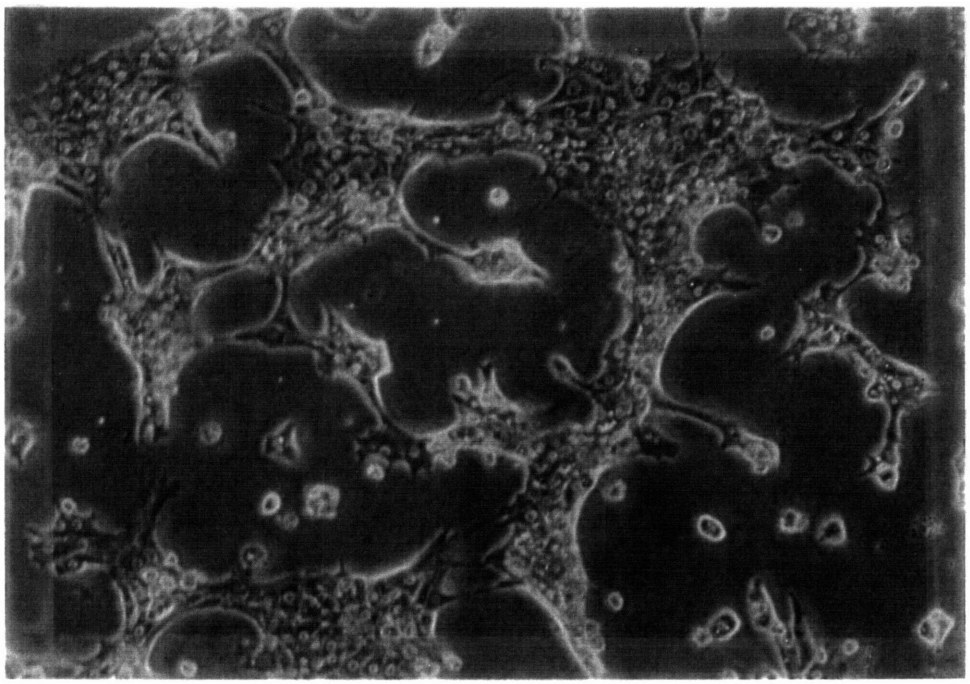

Figure 4-8. Hepatocytes on Type I collagen gel. A. Spreading 18 hours post-seeding as observed by light microscopy, original magnification 100x. B. Morphological appearance of hepatocytes maintained for 3 days as observed by light microscopy, original magnification 100x.

gels (Scheutz, 1988; Dunn, 1989), but the synthetic ADGal substrates are presumably resistant to cellular enzymes and remodeling processes.

4.4.2. Differentiated Function

Hepatocytes are highly differentiated cells, performing a variety of anabolic, catabolic, detoxifying, secretory and excretory functions. Differentiated function must be maintained when hepatocytes are cultured *in vitro*, whether the cells are cultured for future transplantation or to study cellular mechanisms. Most differentiated functions of hepatocytes are extremely labile in culture. The secretion rate of serum albumin, for example, declines by about 70% over five days when cells are culture on polystyrene coated with Type I collagen (Cima, 1991). Cells maintained on collagen gels exhibit greater retention of differentiated function compared to cells maintained on collagen adsorbed to polystyrene, presumably due to the less extensive spreading on the gel form (Ben-Ze'ev, 1988; Dunn, 1989; Mooney, 1992). The retention of differentiated function on a totally synthetic substrate such as the ADGal-modified PEO hydrogels is a desirable characteristic of a biomaterial.

Albumin secretion is one marker of differentiated function. Albumin synthesis occurs exclusively in the liver (Miller, 1951), and measurement of albumin in the culture medium gives a general indication of hepatocyte protein synthesis and secretion. Secretion rates were determined from reserved samples of culture medium which had been collected daily and stored frozen until analysis. An enzyme-linked immunosorbent assay (ELISA) double sandwich antibody technique can accurately measure albumin amounts in the ng/ml range (Schwerer, 1987). The technique is displayed schematically in Figure 4-9. Briefly, after ELISA microtiter plates (Immulon II flat plate) are coated with unconjugated rat albumin antibody (Cappel), a 1% gelatin blocking solution is used to prevent nonspecific albumin adsorption. Albumin standards (50 ng/ml, Cappel) and experimental samples (diluted to an estimated 10 ng/ml) are loaded into the first row of the plate, then serially diluted through the next six rows. The bottom row does not receive albumin, to provide a zero point (Figure 4-9 B). After the albumin has bound to the unconjugated antibody, peroxidase-conjugated rat albumin antibody (Cappel) is allowed to bind. The peroxidase enzyme reacts with a substrate solution of 0.35 mg/ml 2,2'-azino-di(3-ethyl-benzthiazoline-6-sulphonic acid) (ABTS, Sigma) and 0.01% hydrogen peroxide in citrate-phosphate buffer (pH 5.0) producing a dark green product. The reaction is stopped with a 0.32% sodium fluoride solution. Albumin concentration is determined from the extinction read with a double wavelength micro ELISA autoreader

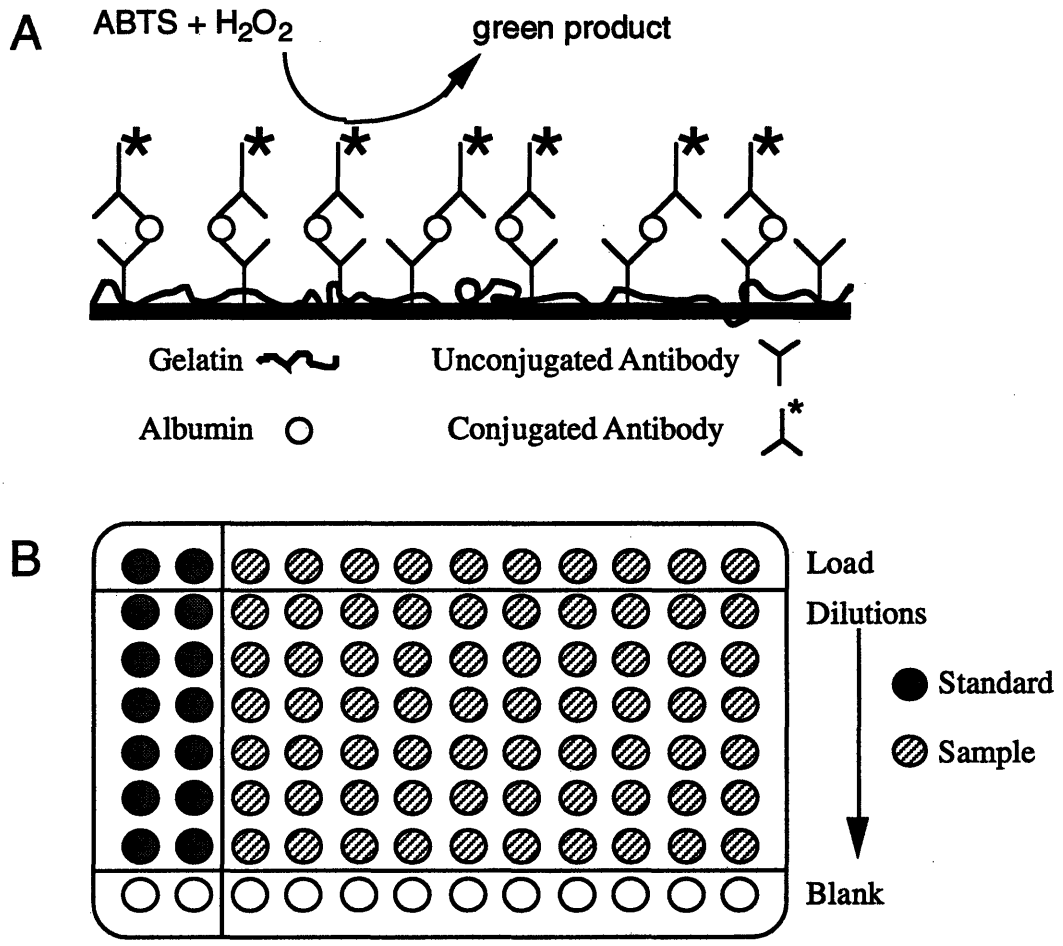

Figure 4-9. ELISA double sandwich antibody technique. A. Schematic representation of process. B. Experimental setup of microtiter test plate.

(Molecular Devices Maxline microplate auto reader with Vmax Software 2.0.1) at 405/490 nm. A detailed protocol can be found in Appendix B.

Functional viability of hepatocytes cultured on ADGal-modified PEO gels was assessed by measuring the rate of secretion of serum albumin as a function of time in culture, and comparing the rate to cells maintained on Type I collagen gels. Hepatocytes were seeded onto hydrogels set up in the tight well configuration to prevent cells from adhering to the bottom of the culture dish and obscuring results. Cells were maintained for 4-6 days in culture. Although it may be desirable to culture cells for more extended periods for some technological applications, the ability of a substrate to support differentiated function of hepatocytes in culture is clearly evident after 2-3 days (Ben-Ze'ev, 1988; Mooney, 1992). For each time point, medium samples from three or four

replicate cultures were saved for analysis. Each individual medium sample was then measured in duplicate or triplicate. Results are shown in Figure 4-10 and Table 4-4, expressed as a rate of secretion per square centimeter culture area. Cells cultured on ADGal gels could not be removed from the surfaces for counting, and other measures of cell number (protein content, microculture tetrazoliom (MTT) response) are unreliable for primary hepatocytes. Thus, secretion rates were not normalized for cell number. Qualitatively, very little cell debris was noted after the first medium change and the surface coverage appeared constant. The retention of differentiated function on a totally synthetic substrate such as the ADGal-modified PEO hydrogels is an important attribute.

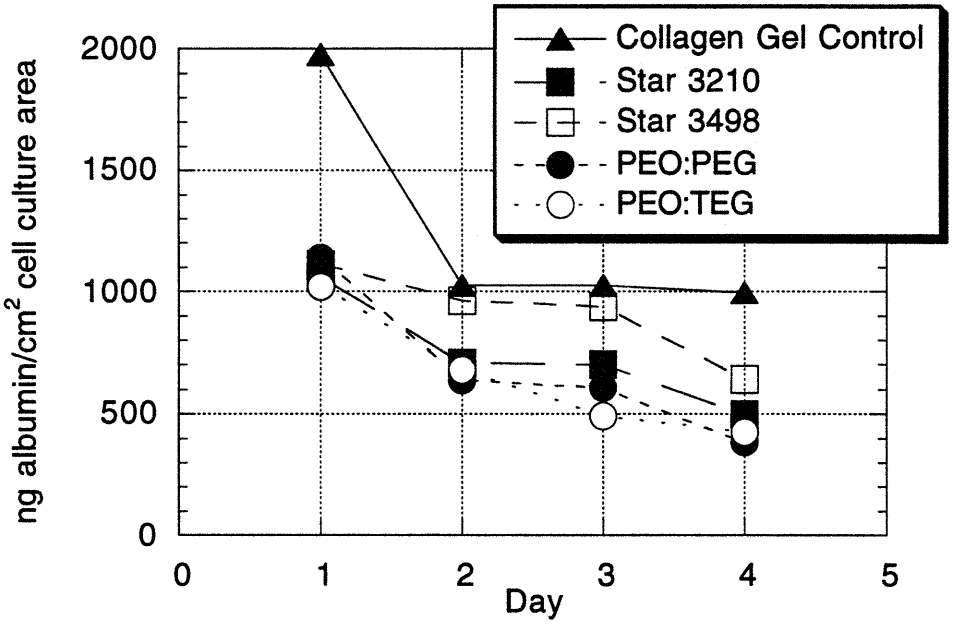

Figure 4-10. Hepatocyte albumin secretion rate on ADGal hydrogels. Average of 2-4 samples from each of duplicate experiments. Error bars were deleted for clarity.

Table 4-4. Hepatocyte albumin secretion rate on ADGal hydrogels.

Day	Scaffold				
	Collagen Gel	Star 3498	Star 3210	PEO:PEG	PEO:TEG
1	1977 ± 363	1059 ± 324	1114 ± 294	1139 ±191	1019 ± 315
2	1024 ± 267	706 ± 297	963 ± 306	638 ± 320	680 ± 193
3	1024 ± 223	701 ± 216	936 ± 297	607 ± 258	492 ± 180
4	995 ± 596	497 ± 277	641 ± 231	384 ± 126	426 ± 188

4.5. Characterization of the Nature of Adhesion

4.5.1. Trypsin Detachment

The number of hepatocytes adherent to a scaffold can be determined by detaching the cells and counting them in a hemacytometer or Coulter Counter. Generally, cells are removed from substratum with trypsin, a serine protease which acts by cutting proteins at lysine and arginine residues. However, the majority of hepatocytes adherent to ADGal-modified PEO hydrogels are not removed with trypsin. On carbohydrate derivatized materials the trypsin must act on the receptor because there are no amino-acid residues in the ligand. Resistance to trypsin may imply that the receptor is somehow buried in the cell membrane after it binds to the surface of the gel. If the ligand-receptor complex is partially internalized or the receptor is folded in such a way that prevents the trypsin from interacting with the cleavable amino-acids, trypsin would be ineffective in detaching cells. Isolated rabbit ASGP-R reconstituted in lipid bilayer membranes have been shown to undergo a conformational change causing them to cross the lipid bilayer upon binding a multi-valent ligand (Blumenthal, 1980). This phenomenon has not been demonstrated in intact cells, however. The ASGP-R is normally endocytosed via coated pits, so resistance to trypsin may alternatively represent a frustrated attempt at endocytosis. The thickness of the cell membrane lipid bilayer is about 4 nm and ligand tethers on star PEO hydrogels are 8 nm or greater, so the PEO chains could be dragged across the membrane at less than 50% of full-chain extension.

The hepatic ASGP-R is a member of the class of mammalian lectins designated C-type lectins, which exhibit an absolute requirement for Ca^{++} to bind carbohydrate ligands

(Geffen, 1992). Asialoglycoproteins bound to the ASGP-R from the solution state are rapidly released from the receptor in the presence of a divalent cation-free buffer containing a chelating agent (Tolleshaug, 1980; Weigel, 1984; Schwartz, 1984). Similar behavior might be expected of hepatocytes adherent to surfaces through the ASGP-R. Cells which had been allowed to attach to ADGal-star PEO hydrogels for 20 hr were incubated in Ca^{++}- and Mg^{++}-free PBS containing 30 mM EDTA, a chelating agent (pH 7.4). Only minimal cell rounding was observed after 1 hour, and no further detachment was observed over four more hours. Weisz and Schnaar reported a similar difficulty in removing rat hepatocytes bound to galactose-modified polyacrylamide gels using a chelating agent (Weisz, 1991b). This inability to remove adherent cells depends on the time of incubation on the substrate; for incubation times less than about 30 minutes cells can be released readily by a chelating agent (Weigel, 1978; 1980) but they become progressively more difficult to remove as the incubation time is increased (Weigel, 1978). Concomitant with the increase in difficulty of disrupting the bonds between the ASGP-R and immobilized ligands using a chelating agent, the strength of adhesion between the cells and the substrate, as assayed by centrifugal detachment, also increases over the first 45 minutes (Guarnaccia, 1982; Weisz, 1991b).

4.5.2. Competition with Galactose

Receptor-ligand binding is a noncovalent, reversible phenomena. Researchers have found that soluble ligand in the medium at a concentration 2 orders of magnitude lower than the ligand concentration in the gel will inhibit hepatocyte adhesion to carbohydrate modified materials (Schnaar, 1978; Weigel, 1979). Incubation of hepatocyte adherent hydrogels in excess galactose may cause cell detachment. Hepatocytes seeded onto ADGal-star PEO hydrogels at 30,000 cells/cm^2 were exposed to galactose solutions to compete for receptor binding sites. At 40 and 70 minutes post-seeding the media was removed from samples and replaced with 20 mM galactose solution. Samples were incubated for an additional 60 minutes at 37°C before removing the galactose solution for analysis. Cells removed with the collected media and galactose solutions were counted in a hemacytometer to quantify adhesion (Table 4-5). As expected, the number of adherent cells increases with incubation time, but it is noteworthy that the hepatocytes develop sugar resistant adhesion over time. Other researchers report similar results with hepatocyte adhesion on carbohydrate-modified polyacrylamide using 20-50 mM soluble ligand, including the reduced ability to remove cells over time (Schnaar, 1978; Guarnaccia, 1982). Adhesion-strengthening requires the concerted interactions of

Table 4-5. Galactose Competition

Minutes Post-Seeding	Percent Adherent Cells[a]	
	Before Galactose	After Galactose
40	73.1 ± 4.2	56.0 ± 8.8
70	81.1 ± 9.7	73.2 ± 4.8

a Percent of total viable cell seeded which are adherent.
± Standard Deviation of 4 samples.

cytoskeletal components, actin and microtubules, and of clathrin, a major component of coated pits (Weisz, 1991b). Based on these observations, Weisz and Schnaar proposed an interaction between the ligand-bound receptor and the cytoskeleton which required the participation of coated pit proteins (Weisz, 1991b) but did not describe a mechanism.

4.6. Cytoskeletal Interactions

The asialoglycoprotein receptor is not a classical adhesion receptor; it carries an endocytotic function to clear damaged glycoproteins from the blood stream. Yet, hepatocytes adhere and spread on carbohydrate derivatized scaffolds. Integrins, cell adhesion receptors, are shown to aggregate and co-localize with cytoskeletal elements such as talin, vinculin, actin, and microtubules in focal adhesion patches once the integrins bind to extracellular matrix proteins (Stamatoglou, 1990; Massia, 1991; Wang, 1993). Integrins are transmembrane receptors which physically link actin-associated proteins to the extracellular matrix (Beckerle, 1990; Otey, 1990; Turner, 1990). Through this direct link, bound integrins are able to transmit mechanical forces from the extracellular matrix to the cytoskeleton, affecting cell shape and function (Ingber, 1991). The development of sugar-resistant and chelating-resistant adhesion in hepatocytes seeded onto carbohydrate derivatized surfaces suggests a conformational change occurs in the receptor on ligand binding; the conformational change may include a cytoskeletal association with bound ASGP-R (Guarnaccia, 1982b, Weisz, 1991a). A specific molecular pathway for mechanical force transfer to the cytoskeleton could support hepatocyte spreading on ADGal surfaces.

The ability of the ASGP-R to transfer mechanical forces across the cell membrane was explored with a magnetic twisting device in which controlled mechanical loads are applied directly to cell surface receptors without producing a global cell shape change

(Wang, 1993). The viscosity of the cell membrane will impart some resistance to the applied load, but a nonlinear increase in resistance to increasing mechanical loads – cell stiffening – would imply force transfer through a mechanical link. Mechanical loads are applied to the receptors through ferromagnetic microbeads which are coated with the desired ligand and allowed to bind to plated cells. After bound beads are aligned through magnetization, the cellular response to stress applied through a twisting magnetic field is measured by quantifying changes in the rotation (angular strain) of the surface-bound magnetic microbeads using a sensitive in-line magnetometer (Figure 4-11). The hepatocyte response to ADGal beads through the ASGP-R was compared to the response to control beads coated with either RGD-containing peptides or acetylated low-density lipoprotein (AcLDL). RGD binds to integrins, which are known to transfer mechanical forces effectively across the cell membrane and through the CSK, leading to cell adhesion and spreading (Hughes, 1979; Ruoslahti, 1987; Singer, 1987). In contrast, AcLDL binds to scavenger receptors which are not involved in cell adhesion and do not transfer mechanical force to the cytoskeletal lattice (Wang, 1993).

ASGP-R specific microbeads were prepared by first coupling tresyl activated Star 3510 to the primary amine groups on the surface of ferromagnetic microbeads (4 μm diameter with polystyrene core; 80 μg/ml; Spherotech). PEO-coupled beads were then re-tresylated and coupled with a 10-fold excess of ADGal as described for star PEO in Chapter 3. XPS examination of coupled beads showed a strong C-O peak, indicating

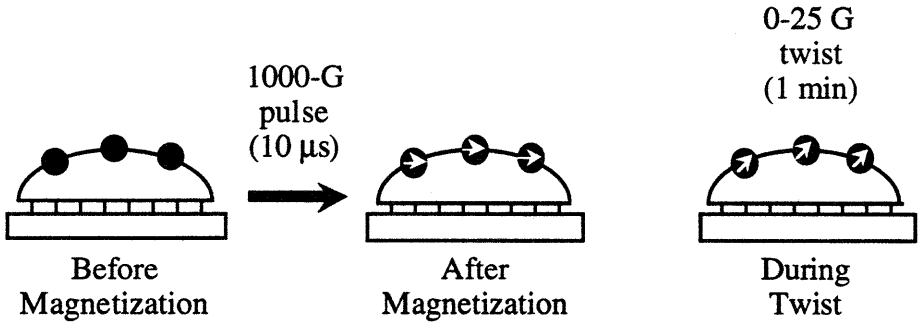

Figure 4-11. Magnetic twisting device. A brief pulse from a strong magnetic field (1000 G for 10 μs) magnetizes and aligns the beads. Angular rotation of the beads induced during a weak "twisting" field (0-25 G for 1 minute) is measured with a magnetometer. (Redrawn from Wang, 1993.)

successful PEO coupling. Ferromagnetic control beads (5.5 μm diameter with solid ferromagnetic core) coated with RGD-containing peptides (Peptite 2000; Telios) or acetylated low-density lipoprotein (AcLDL: Biomedical Technologies) were provided by N. Wang of the Harvard School of Public Health. ADGal is thus chemically coupled to the beads via long PEO tethers while the control ligands are coated directly onto the beads (Figure 4-12).

Hepatocytes were plated in complete medium at a concentration of 30,000 viable cells/cm^2 culture surface area on 96 well plates (Removawells, Immulon II Dynatech, Chantilly VA) which were coated with Type I collagen (Vitrogen, Collagen corp./Celltrix) at 10 μg/cm^2. Following an attachment period of 18-24 hours the medium was exchanged for complete medium with 1% BSA (Sigma) and 20 mM HEPES (Gibco) to remove unattached cells. This supplemented medium, which will subsequently be referred to as "BSA/complete medium," is required to control pH since the cytometry equipment in not in a CO_2 controlled atmosphere. The BSA blocks nonspecific bead adsorption.

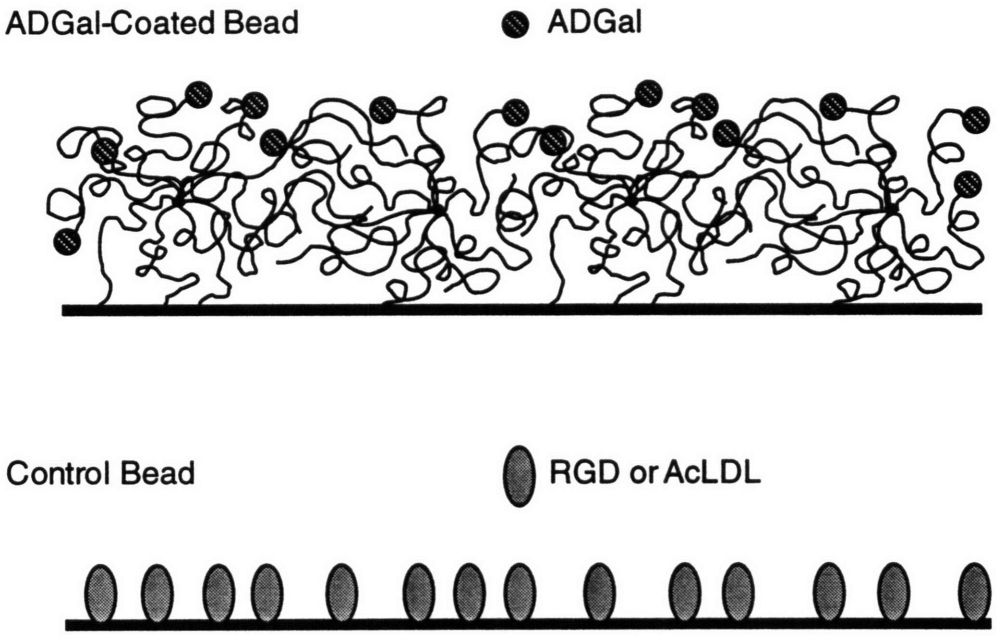

Figure 4-12. Ligand-coated ferromagnetic beads. ADGal is tethered to the bead surface via star PEO while control ligands (RGD and AcLDL) are coated directly onto the bead surface.

Magnetic twisting cytometry (Wang, 1993) was used to assess receptor-cytoskeletal linkages. Ligand-coated/coupled beads were suspended in BSA/complete medium. Suspended beads were added to cells which had been adherent to collagen-coated wells for 45-50 hours (5-10 beads/cell). After 15-60 minutes, unbound beads were washed away with BSA/complete medium. Nonspecific binding was checked with beads lacking coupled ligand. BSA in the medium blocked the nonspecific binding, as fewer than 5% of the beads bind to hepatocytes in the presence of BSA while greater than 50% bind in its absence (experiments repeated twice).

After ligand-coupled beads bound to adherent hepatocytes, individual wells were placed into the magnetic twisting device and maintained at 37°C. Application of a brief (10 μs) but strong (1000 gauss) homogeneous magnetic pulse magnetized all surface-bound beads in the horizontal direction. Twenty seconds after bead magnetization, a twisting torque was produced by applying a weaker magnetic field (0-25 gauss) perpendicular to the original field for 1 minute. This field was too small to realign the bead magnetic moments; rather, it rotated beads in place in the same direction.

The extent of bead rotation is measured by an in-line magnetometer that continuously detects the magnitude of the bead magnetic vector in the horizontal direction. The torque of the applied twisting field is proportional to the twisting field, bead magnetization, and the sine of the angle between the twisting field vector and the bead magnetization vector. Angular strain (ϕ) and applied stress (σ) are determined from the remnant magnetic field (B) in both the relaxed and twisting mode.

$$\phi(t) = \cos^{-1}\left(\frac{B(t)_{twist}}{B(t)_{relax}}\right) \tag{4-2}$$

$$\sigma(t) = cH_a\left(\frac{B(t)_{twist}}{B(t)_{relax}}\right) \tag{4-3}$$

where H_a is the external magnetic twisting field and c is a calibration constant determined by twisting beads in a known viscosity standard (Wang, 1994). For the solid magnetic beads c=2.72 dyne/cm^2/gauss (Wang, 1994) and for the ferromagnetic bead with polystyrene core c=0.51 dyne/cm^2/gauss (Wang, unpublished results). Apparent stiffness (E) is defined here as the ratio of stress to strain (i.e., rather than the derivative of stress with respect to strain) (Wang, 1994).

$$E = \sigma/\phi \tag{4-4}$$

Ligand-coupled ferromagnetic beads were twisted using applied magnetic fields yielding stresses from 0-40 dyne/cm^2. The ASGP-R exhibited a non-linear stress-strain relationship (Figure 4-13) similar to that observed with RGD-beads on endothelial cells (Wang, 1993; Wang 1994). The ultimate angular deformation of ADGal-beads on hepatocytes (38° at 15.2 dyne/cm^2) was intermediate between that exhibited by RGD-beads (21° at 40 dyne/cm^2) and AcLDL-beads (71° at 40 dyne/cm^2) bound to plated hepatocytes (Figure 4-13). The fact that control beads are solid ferromagnetic materials leads to a higher applied stress for a given magnetic field. The response of hepatocytes to RGD-coated beads at 40 dyne/cm^2 matches that of spread bovine capillary endothelial (BCE) cells (Wang, 1994). BCE data is plotted with the hepatocyte data for comparison (Figure 4-13). RGD and AcLDL coated beads are used as controls. While both ligands bind to specific transmembrane receptors, the receptors exhibit different mechanical interactions with the CSK. RGD binds to integrins, which are known to transfer mechanical forces effectively across the cell membrane and through the CSK, leading to cell adhesion and spreading (Hughes, 1979; Ruoslahti, 1987; Singer, 1987). In contrast, AcLDL binds to scavenger receptors that are not involved in cell adhesion and do not transfer mechanical force to the cytoskeletal lattice (Wang, 1993). The behavior of the ADGal beads intermediate between the two different types of control beads suggests the existence of a mechanical link between the ASGP-R and the CSK.

Mechanical properties were measured again after the CSK was disrupted with a combination of cytochalasin D (Cyt-D, 0.5 μg/ml) which disrupts actin microfilaments, and nocodazole (Noc, 5 μg/ml) which disrupts microtubules and intermediate filaments, to test the hypothesis that the resistance to bead rotation is due to interaction between the ASGP-R and the CSK. A combination of drugs was used as it was observed that both actin and tubulin must be disrupted to reduce strong hepatocyte adhesion to carbohydrate-derivatized polyacrylamide surfaces (Weisz, 1991b). Mechanical testing was repeated after hepatocytes with ligand-coupled beads were incubated at 37°C in BSA/complete medium containing the above concentrations of drugs for 30 minutes. A 60% increase in angular deformation was observed at an applied stress of 15.2 dyne/cm^2. A similar increase in angular deformation (80%) was observed when hepatocytes with RGD-beads were treated in a similar manner, both on hepatocytes and BCE cells (Figure 4-13).

Stress-induced stiffening, with apparent stiffness defined as the ratio of effective stress to strain, increased linearly with applied stress (Figure 4-14). The stiffening

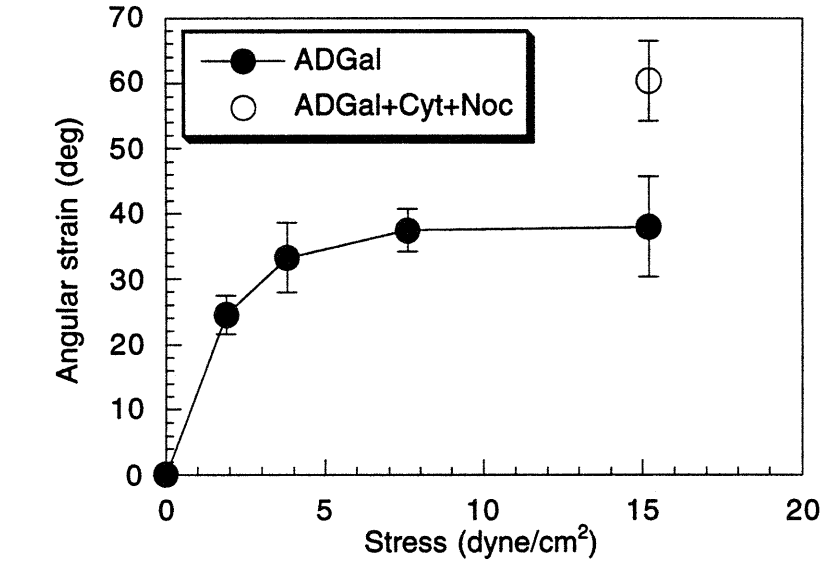

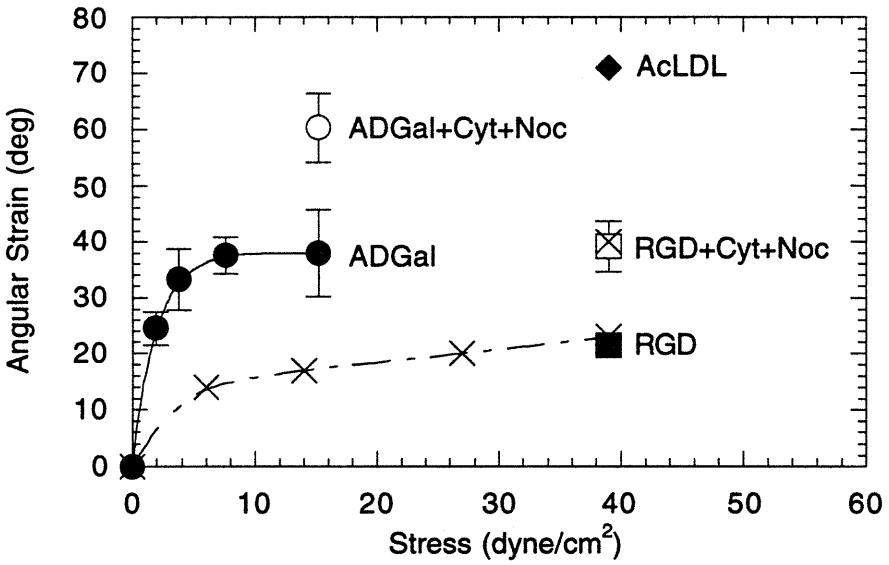

Figure 4-13. Angular strain of ligand coated microbeads in response to an applied stress. Data designated by (X) from Wang, 1994 - response of spread bovine capillary endothelial cells to RGD-coated beads

response (slope of stiffness versus stress) compares favorably with the literature value for RGD-beads on spread endothelial cells (Wang, 1994). Twisting of the ASGP-R receptor through ADGal beads yields a stiffening response of 1.5 (curve fitting $r^2 = 0.99$) as compared to a stiffening response of 1.9 for the integrin receptor (Wang, 1994).

Disruption of the cytoskeleton through incubation with Cyt-D and Noc led to a 60% decrease in stiffness of the ASGP-R at a stress of 15.2 dyne/cm^2 (Figure 4-14).

Cell adhesion, cytoskeletal stiffness, and force transfer between the cell and the extracellular matrix via integrins are closely related (Wang, 1994). The same relationship can be inferred from the cytoskeletal stiffness and force transfer measured through the asialoglycoprotein receptor. The resistance to bead rotation measured with ADGal-coupled ferromagnetic beads lies at least partially in the cytoskeleton, because when hepatocytes were incubated with drugs which disrupt actin and microtubules, the major components of the CSK, a 60% decrease in CSK stiffness was observed. The linear stiffening response observed is an inherent mechanical property of the CSK which can be predicted by the tensegrity model of cytoskeletal architecture (Ingber, 1993; Wang, 1993). Although the ASGP-R is an endocytotic receptor, it also interacts with the cytoskeleton in a manner which induces cell spreading onto carbohydrate derivatized surfaces.

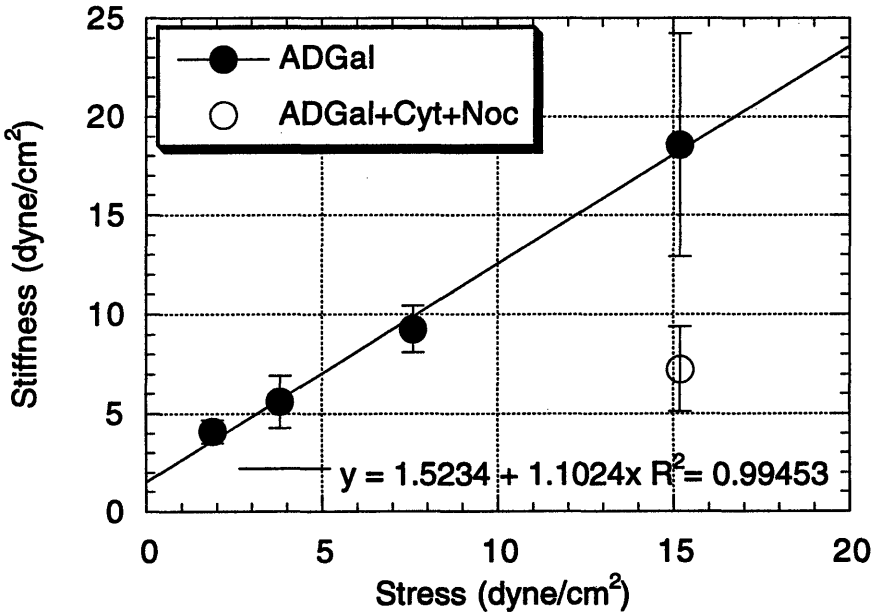

Figure 4-14. Cytoskeletal stiffening response to stress applied through the ASGP-R.

5. Relationship Between Ligand Tether Length and Concentration for Hepatocyte Spreading

Hepatocyte attachment to galactose-modified surfaces is presumably mediated by the galactose-specific asialoglycoprotein receptor. The results observed on ADGal-modified PEO hydrogels are qualitatively similar to those reported previously in terms of the ability of cells to spread on the galactose-modified surfaces and the inability to remove bound cells using chelating agents, but there is a significant quantitative difference which may illuminate important features of the receptor/cytoskeletal interactions. In the Weisz and Schnaar experiments cells were seeded onto polyacrylamide gels containing sufficient ligand to induce cell spreading (although many of the experiments were performed before such spreading – which requires approximately 12 hours – had occurred) (Schnaar, 1978; Weisz, 1991a,b). Both adhesion and spreading of rat hepatocytes on galactose-modified polyacrylamide have been described as threshold phenomena. The critical ligand concentration for adhesion was reported as 3 mM; the critical ligand concentration for spreading 30-70 mM (Weigel, 1979; Oka, 1986). In contrast, cells spread on the PEO star hydrogels at ligand concentrations as low as 3 mM, an order of magnitude less than that required for spreading on polyacrylamide and equal to the polyacrylamide threshold for adhesion. The known binding affinities of the ASGP-R for multivalent *(i.e.*, branched) ligands and the known requirements for participation by the different subunits of the receptor in high affinity binding suggest a mechanistic interpretation of the varying results.

5.1. Asialoglycoprotein Receptor Subunit Clustering

The ASGP-R is a hetero-oligomer composed of two related polypeptide chains designated HL-1 and HL-2 (Lodish, 1991). Receptor binding affinity in intact hepatocytes increases by five orders of magnitude as the ligand valency increases from a single galactose to a tri-branched form (Connolly, 1982; Rice, 1993). Binding affinity for the isolated receptor does not vary with ligand valency, suggesting an organizational or structural difference between the isolated receptor and the intact receptor in the membrane. Intact receptors may undergo a conformational change on triantennary binding which induces cytoskeletal interactions (Baenziger, 1980; Connolly, 1982). Both receptor subunits have been cloned and expressed in fibroblasts and hepatoma cells; from these studies it has been demonstrated that the subunits HL-1 and HL-2 cooperate to enable high-affinity binding of trivalent ligands. HL-1 by itself is unable to bind and internalize trivalent ligands, while HL-2 functions to enable high affinity binding of

trivalent ligands without affecting endocytosis of bound ligand-receptor complexes (Shia, 1989). Evidence points to a structure of the fully functional ASGP-R as comprising at least one HL-2 chain and at least three HL-1 chains (Lodish, 1991, Rice 1993). The optimal spacing of sugar moieties in tri-branched ligands (*i.e.*, the spacing giving the highest affinity binding) is consistent with the spacing between the binding sites of a [(HL-1)$_3$(HL-2)] receptor structure as described by Lodish (Lodish, 1991) and shown in Figure 5-1.

Cell spreading may occur in response to tethered galactose when the tethers allow a fully-functional receptor, simultaneously binding three galactose moieties, to form; *i.e.*, when the substrate can mimic a triantennary oligosaccharide. Formation of a fully functional receptor may be accompanied by a conformational change in the receptor that enhances interactions of the receptor with the cytoskeleton (Baenziger, 1980).

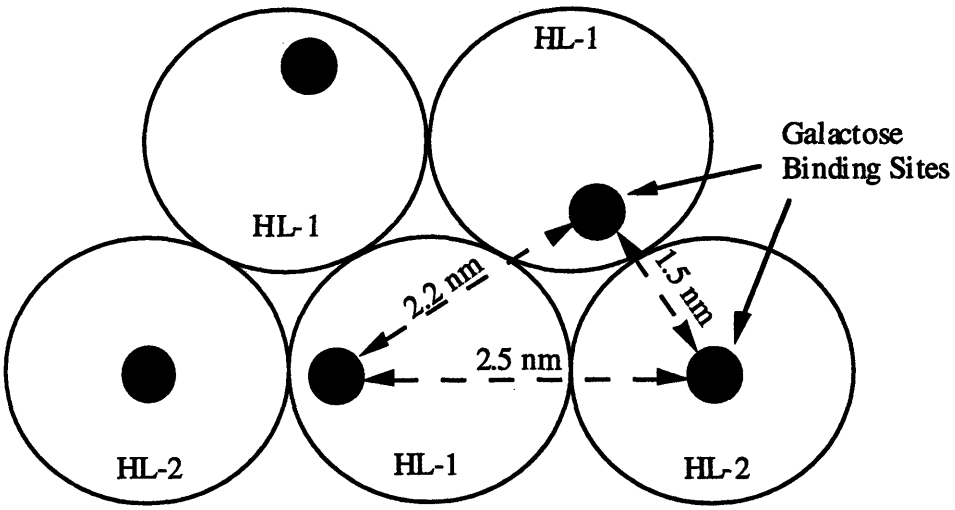

Figure 5-1. En-face view of asialoglycoprotein receptor illustrating spacing of sugar moieties in tri-branched ligands. (Redrawn from Lodish, 1991.)

5.2 Ligand Distribution and Tether Length

To explore this hypothesis, consider the relative spacing and mobility of ligands in the PEO hydrogel systems and the literature polyacrylamide system. The positions of individual ligand molecules are not static because the polymer chains which tether them to the gel undergo random thermal motion. The range of motion of the ligand around some time-averaged position will depend on the length and mobility of the tether which

links it to the gel. For short polyacrylamide tethers, the range is on the order of 1 nm. For long PEO tethers, the range of motion is many times greater. To assess whether three neighboring ligands could assume positions which mimic the ligand spacing in a high-affinity trivalent oligosaccharide, compare the range of motion of the ligand molecules to that necessary to form a trivalent bond.

First, consider the average ligand spacing. From the volumetric concentration of ligand in the gels, and an assumption that the average positions of all ligands are distributed uniformly in space in a cubic array, a reference length, d_0, between the centers of adjacent ligands can be calculated. At any specific instant in time, neighboring ligands may be much closer or much more distant than d_0, but they will be separated by the distance d_0 on average. The values of d_0 for star PEO hydrogels which support hepatocyte spreading are shown in Table 5-1. The shortest average distance between two adjacent ligands in these PEO hydrogels, 4.9 nm, is still far greater than the distance between adjacent galactose binding sites in the ASGP-R, which is about 2 nm. However, PEO chain mobility can allow instantaneous local positions sufficiently close given the tether lengths available on the star hydrogels. The free energy driving force for aggregation of the subunit chains in the cell membrane may then overcome the entropic cost associated with restricting the ligands to positions in the binding site of the receptor.

Next, an estimate of the distance three neighboring ligands would have to move from their "unperturbed states" to form a triangle with sides of 1.5 nm, 1.5 nm and 2.1 nm (*i.e.*, a triangle slightly smaller than the high affinity binding triangle) is required. In order to estimate this "stretching distance", designated d_S, consider the ligands to be located on springs at the positions of the crosslinks, as illustrated in Figure 5-2. The springs must be stretched a distance d_s in order to position the ligands in the binding sites. Then d_s can be calculated as shown in Figure 5-3 according to:

$$d_s = \sqrt{2}\left(d_0 - 1.5\right)/2 \tag{5-1}$$

Values for d_s are also shown in Table 5-1.

Now compare the values of d_S with the length of the ligand tethers. Ligand is coupled to the terminal hydroxyl of PEO; tethered to the hydrogel macrostructure by a length of polymer. The average molecular weight between crosslinks is also the average molecular weight between a crosslink and the chain end, therefore, for linear and star gels, M_c defines the average ligand tether length. For linear/oligomer gels, 70-90% of ligand is linked to the ends of the oligomers, thus the tether length for these gels is closer to 0.5

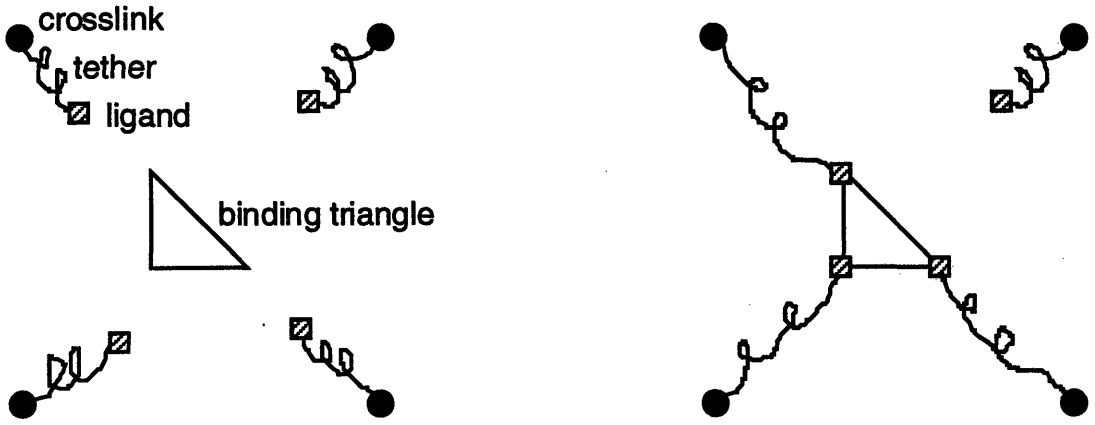

Figure 5-2. Tether stretch. In order to estimate the "stretching distance", consider the ligands to be located on springs at the positions of the crosslinks. The springs must be stretched a distance d_s in order to position the ligands in the binding sites of a fully functional receptor binding a trivalent ligand.

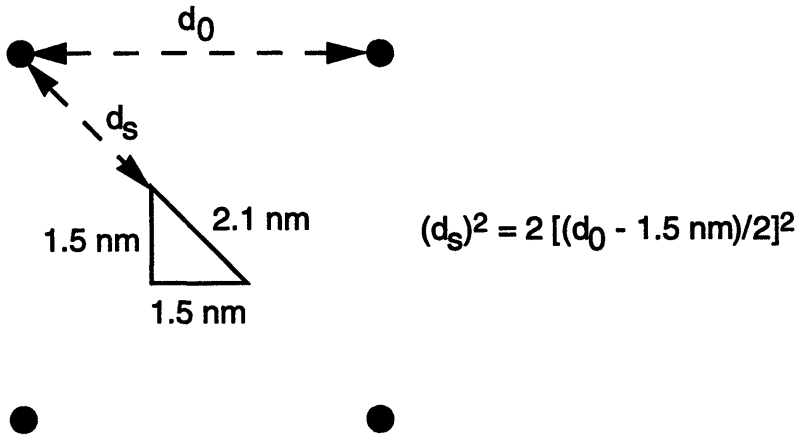

Figure 5-3. Tether stretching distance estimated from simplified geometry.

$MW_{oligomer}$. The molecular weight between crosslinks (tether length) can be calculated from equilibrium swelling measurements as detailed in Chapter 2. The length of a fully-extended PEO tether, the polymer contour length, is aN where a is the monomer size and N is the number of monomer units in the chain . For PEO a = 2.78Å (Jeon, 1991a) and N = $M_c/44$ (the monomer molecular weight is 44). The lengths of the fully-extended PEO tethers are shown in Table 5-1.

The gel d_s corresponds to less than 35% of the fully-extended tether length on all PEO hydrogels which supported hepatocyte spreading (Tables 4-3 and 5-1). To assess whether the ligands would likely occupy these positions due to thermal motions of the chains, a second measure of the tether length is used: the root mean square (rms) end to end distance, $\langle r^2 \rangle^{1/2}$, as described by polymer physics. If the crosslinks are considered to be fixed points which immobilize one end of the tether, the likely position of the other end of the tether (where the ligand is attached) will be a distance $\langle r^2 \rangle^{1/2}$ away from the crosslink, in any direction. Monte Carlo simulations have shown that in aqueous solutions, PEO chains tethered at one end follow the same scaling laws as free chains if the chains contain at least 30 bonds (Sarmoria, 1992); these chains exhibit Gaussian behavior at extensions of up to 1/3 of the fully extended length (Flory, 1953). The root-mean-square end-to-end distance of these tethers is approximately 2-4 nm (Sarmoria, 1992), or about 20-30% of the fully extended chain length. Since $\langle r^2 \rangle^{1/2}$ is comparable in magnitude to the d_s on hydrogels which support hepatocyte spreading, the ligand-bearing ends of three neighboring chains on these gels could occupy the binding positions shown in Figure 5-1.

In previous studies with polyacrylamide, spacers of 10 bonds were used (Oka, 1986). The length of a CH_2-CH_2 unit in an alkane chain is 0.127 nm (Israelachvili, 1992), so the spacers must have been roughly 1.3 nm. Short polymer chains of 30 bonds or less, tethered at one end, are expected to have a more extended conformation (Sarmoria, 1992); it is reasonable to expect they may stretch beyond 1/3 of the fully extended chain length to achieve trivalent receptor binding. Consequently, according to the same analysis described above for PEO tethers, a fully functional receptor could form in the polyacrylamide system for ligand concentrations between 30 and 70 mM – the observed threshold range for hepatocyte spreading.

5.3. Hepatocyte Spreading

Hepatocyte spreading appears to occur in response to tethered galactose when the tethers simultaneously bind three galactose moieties, mimicking a triantennary oligosaccharide, thus forming a fully functional receptor. Star PEO hydrogels which would cross the rounded/spread cell threshold – where the tether must stretch to greater than 1/3 of its end-to-end distance to achieve trivalent binding – were prepared by reducing the ADGal concentration. Tether lengths could not be shortened sufficiently via increased radiation dose, because once the molecular weight between crosslinks (which

Table 5-1. Tether Extension

Polymer	ADGal Conc. (mM)	Ligand Spacing (d_0, nm)	Tether Stretch (d_s, nm)	Tether MW	Tether Length (nm)	Tether Extension (% Length)
S3210 w/linear	3.8	7.6	4.3	3500	22.1	19.5
	0.08[a]	27.5	18.4	3500	22.1	83.1
S3210	14.1	4.9	2.5	2100	13.3	18.8
	4.1[b]	14.6	9.3	2100	13.3	69.9
	0.53[a]	7.4	4.2	2100	13.3	31.6
	12.4	5.1	2.6	1600	10.1	25.7
	12.3	5.1	2.6	1300	8.2	31.7
S3498	3.7	7.7	4.4	5100	32.2	13.7
	0.17[a]	21.4	14.0	5100	32.2	43.5
	4.0	7.5	4.2	4600	29.1	14.4
	2.6	8.6	5.0	4100	25.9	19.3
S3509	5.5	6.7	3.7	3000	19.0	19.5
S3510 w/linear	2.6	8.7	5.1	5200	32.9	15.5
	0.11[a]	24.7	16.4	5200	32.9	49.9
S3510	8.6	5.8	3.0	2500	15.8	19.0
	9.3	5.6	2.9	1800	11.4	25.5
PEO:PEG	2.4	8.8	5.2	500	3.2	162.5
PEO:TEG	9.9	5.5	2.8	100	0.6	466.7
Polyacrylamide[c]	30-70	2.9-3.8	1.0-1.6		1.3	76.9

a ADGal concentration calculated from the ratio of ADGal:ADGlu in the original coupling buffer, assuming equal coupling affinity for both ligands.
b A substoichiometric amount of ADGal added during the coupling stage reduced the final concentration.
c Polyacrylamide data from Oka and Weigel, 1986.

corresponds to tether length) falls below 1500, chain scission dominates over crosslinking (Dennison, 1986). Instead, star PEO hydrogels with low ligand concentrations were prepared by coupling a mixture of ADGal and ADGlu to yield the desired active ligand (ADGal) concentration (Tables 3-8 and 5-1). Hepatocytes did not spread on Star PEO hydrogels with low ligand concentrations.

5.3. Hepatocyte Spreading

Short tether arms produced in the linear/oligomer hydrogels provide pairs of ligands which cannot physically reach all three binding sites in the high affinity binding triangle (Table 5-1). As would be predicted by the ligand tether length/concentration relationship outlined above, adherent hepatocytes remained rounded throughout the duration of culture. The linear/oligomer hydrogel results compare favorably to literature results where adhesion was observed at 3 mM galactose, but a threshold value of 30-70 mM galactose was required for spreading to occur on galactose-derivatized polyacrylamide gels (Weigel, 1979; Oka, 1986).

Hepatocytes were examined visually with a Diaphot inverted phase contrast light microscope equipped with a Nikon 35 mm camera. Hepatocyte spreading could not be quantified with the video camera assembly used with grafted PEO. The three dimensional nature of the hydrogel scaffold led to shadowing and shades of gray which the thresholding software could not resolve. Instead, 35-mm photographs were taken through the microscope at 24, 48 and 72 hours post-seeding. Viable hepatocytes (determined with the Molecular Probes Live/Dead assay) were carefully traced from the photographs onto Académie Tracing Paper which was then scanned into a Macintosh IIsi computer. The scanned images were analyzed with Image 1.49 software (NIH) which calculated the area of adherent hepatocytes (Table 5-2, Figure 5-4). Between 100 and 500 cells from 1-4 experiments were averaged for each measurement. A cutoff between rounded and spread hepatocytes occurs around 550 μm^2. Note that rounded cell growth remains stagnant while spread cells grow slightly in area over the duration of the experiment. As predicted, hepatocytes spread when ligands can reach the trivalent high affinity binding triangle, *i.e.* when the tethers need stretch less than 1/3 their end-to-end distance (Figures 5-5, 5-6).

The phenomenon observed for the ASGP-R has broad implications for the design of biomaterials based on controlling receptor-mediated phenomena. Many receptors are believed to require precise spatial arrangements within the plane of the cell membrane in order to function properly, and thus the *spatial distribution* of a ligand on a biomaterial surface is perhaps as important as its average *concentration* on the surface. The PEO star hydrogels provide a versatile system for exploring this phenomenon.

Table 5-2. Spread area of hepatocytes on ADGal-modified PEO hydrogels.

Polymer	Tether Extension (% Length)	Hepatocyte Area (μm^2)		
		Day 1	Day 2	Day 3
S3210 w/linear	19.5	880 ± 88	737 ± 379	1093 ± 463
	83.1	510 ± 146	425 ± 78	402 ± 95
S3210	18.8	819 ± 125	602 ± 249	981 ± 433
	25.7	637 ± 215	634 ± 217	934 ± 478
	31.6	415 ± 151	436 ± 105	426 ± 128
	31.7	776 ± 201	860 ± 395	1008 ± 465
	69.9	478 ± 104	382 ± 69	448 ± 149
S3498	13.7	755 ± 230	741 ± 367	1073 ± 457
	14.4	859 ± 99	704 ± 270	1014 ± 484
	19.3	629 ± 183	601 ± 173	937 ± 442
	43.5	420 ± 116	527 ± 90	426 ± 73
S3509	19.0	837 ± 459	747 ± 255	904 ± 457
S3510 w/linear	15.5	844 ± 104	1094 ± 165	1167 ± 197
	49.9	464 ± 129	472 ± 65	418 ± 90
S3510	19.0	626 ± 246	846 ± 372	1082 ± 343
	25.5	873 ± 108	916 ± 368	1176 ± 511
PEO/PEG	162.5	494 ± 112	495 ± 125	495± 97
PEO/TEG	466.7	463 ± 116	473 ± 114	472 ± 92

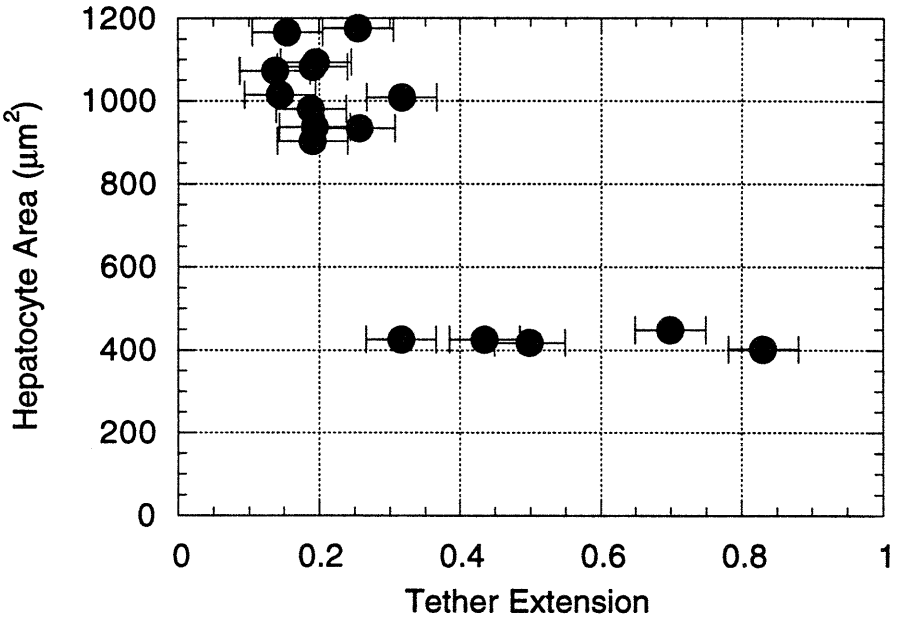

Figure 5-4. Hepatocyte area on ADGal-PEO hydrogels, 72 hours post seeding. Vertical error bars have been excluded for clarity.

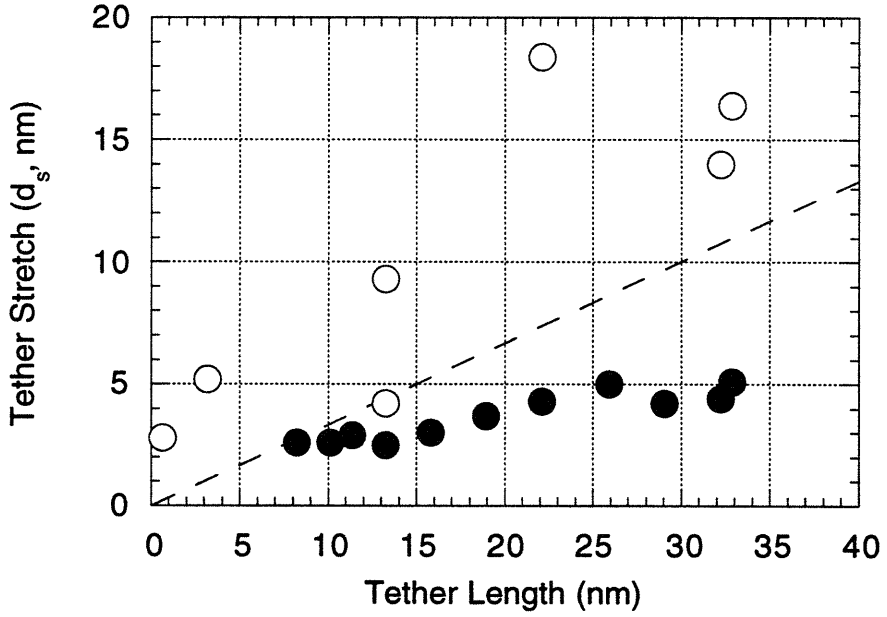

Figure 5-5. Tether length vs. tether stretch. Solid circles represent materials which support hepatocyte spreading while open circles represent materials with rounded cells. The line marks where tether extension equals 1/3 of the end to end distance.

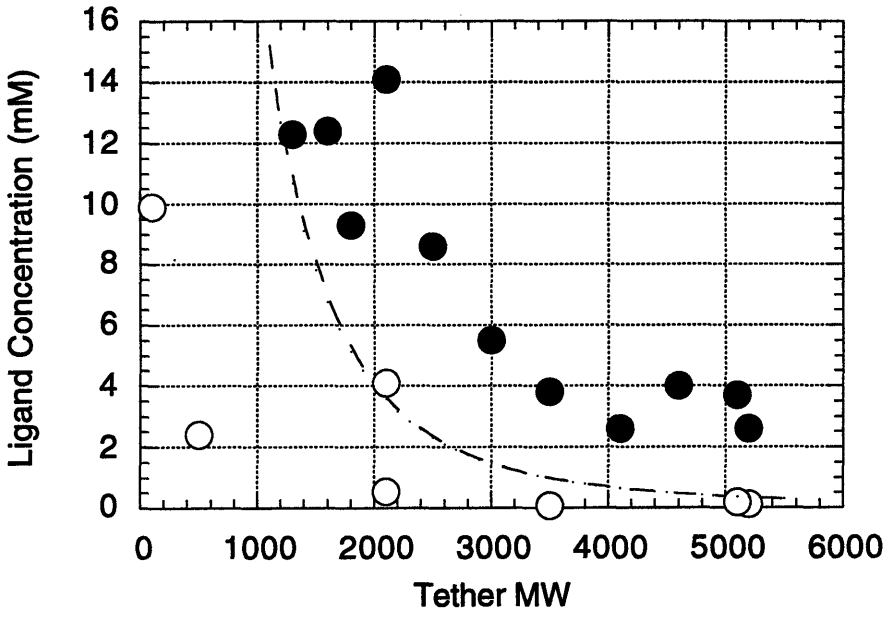

Figure 5-6. Tether MW vs. ligand concentration. Solid circles represent materials which support hepatocyte spreading while open circles represent materials with rounded cells. The line marks where tether extension equals 1/3 of the end to end distance. Hepatocytes spread on PEO hydrogels when the tethers need stretch less than 1/3 their end-to-end distance to reach the high affinity binding triangle of the ASGP-R.

6. Conclusions

One of the goals in the field of biomaterials is development of synthetic implantable materials with surfaces which remain bland and inert towards the adsorption of proteins and cells. Elucidation of molecular-level events involved in receptor-mediated cell interactions with their natural environments has made such inert materials even more sought after as substrates for immobilizing ligands which foster highly specific cell interactions and precise control of cell behavior from the substrate. This thesis concerns the development of a scaffold material for hepatocyte (liver cell) transplantation, a proposed alternative to whole organ transplantation.

A series of radiation-crosslinked poly(ethylene oxide) (PEO) hydrogels which span a range of free chain end concentrations and tether lengths were synthesized, characterized and modified with bioactive ligands to create a scaffold for hepatocyte adhesion. The derivatized materials were seeded with hepatocytes to analyze the cellular response. Several conclusions can be drawn from each aspect of this work, from materials development through derivatization and cellular interactions.

6.1. PEO Hydrogels

Stable PEO hydrogels can be produced from aqueous solutions through high energy electron beam irradiation which creates covalent crosslinks between polymer backbone chains while preserving endgroup functionality for further derivatization. Homogeneous hydrogels, lacking bubbles which can be created from hydrogen radical recombination, are assured by considering diffusion characteristics. Irradiation doses were staged (2 Mrads at a time) to limit the amount of gas produced; sufficient time elapsed between irradiation doses for the hydrogen to escape the developing gel (20 hours). No functionalities which may compromise the inert qualities sought in biomaterial design are created by the irradiation of aqueous PEO solutions which have first been degassed to minimize oxygen content. No unsaturation or carbonyl formation was observed by means of Fourier Transform Infra-Red spectroscopic analysis of PEO hydrogels.

Hydrogels produced from linear PEO, while maintaining structural properties suitable for implantation, are limited in the number of endgroups available for derivatization. Star PEO, made up of PEO chains emanating from a poly(divinyl benzene) core, provides an excellent starting material for producing biomaterials with a large range of endgroup concentrations and tether arm lengths. Irradiation of an aqueous solution locks the star structure in place; the resulting network reflects aspects of the relative proximity of

interchain and intrachain segments. Analysis of the network structure through swelling and compression measurements confirms that highly overlapping solutions of stars behave in a similar fashion to solutions of linear molecules, although the polymer-solvent interaction parameter for star PEO in water is approximately 10% higher than that of linear PEO, reflecting an exclusion zone close to the star core. Modification of the Flory swelling equation to account for the bimodal distribution of crosslinks (f-functional crosslinks at the star core where f is the number of PEO arms; and tetra-functional crosslinks throughout the hydrogel, created through irradiation) makes a small contribution to the calculation of the molecular weight between crosslinks whose effect decreases with increasing star functionality.

An alternate means of creating PEO hydrogels with increased endgroup concentrations is by irradiating solutions which contain a combination of relatively high molecular weight linear PEO to provide the hydrogel macrostructure and low molecular weight PEO oligomers to increase the endgroup concentration. Oligomer crosslinks provide pairs of endgroups for further derivatization. The degree of oligomer incorporation can be determined from swelling measurements and an empirically derived mobility factor which accounts for the increased probability of oligomer-main chain crosslinks over main chain crosslinks due to the oligomer mobility through the hydrogel network.

underivatized PEO hydrogels, and PEO hydrogel implantation into the mesentery of rats caused a minimal biological response as compared to poly(dimethyl siloxane) (PDMS), the NIH standard. Radiation-crosslinked PEO hydrogels possess the inert character of the ideal biomaterial while providing a range of endgroup concentrations and tether lengths for derivatization with bioactive molecules.

6.2. Hydrogel Derivatization

The hydroxyl endgroup can be activated with tresyl chloride chemistry to provide a leaving group for efficient ligand coupling through amines or thiols. Ligand is thereby tethered to the hydrogel through a length of PEO equal to the molecular weight between crosslinks (for linear or star hydrogels) or equal to approximately half the oligomer length (for linear/oligomer hydrogels). Anhydrous conditions are required for high yield tresylation and can be achieved through extended solvent exchange with a graded series of acetone and use of dried reagents (activation yield >75%). Coupling can be achieved under a range of conditions, depending on the constraints of the ligand or substrate, but is

optimal when completed at room temperature in a solution with good buffering capabilities at pH 8.5-9.5 (coupling yield >95%). Thorough washing of the coupled hydrogels removes any residual tresyl chloride. Fluorescent lectin binding confirms uniform ligand distribution throughout the hydrogel. Ligand concentration can be determined via a colorimetric assay. PEO hydrogels adsorb less than 10% monolayer coverage of fibronectin both before and after derivatization, confirming that the addition of specific bioactivity does not alter protein adsorption characteristics of the PEO hydrogels.

6.3. Hepatocyte Adhesion

Primary rat hepatocytes seeded onto test materials adhere to 1-amino-1-deoxy-ßD-galactose (ADGal) derivatized PEO hydrogels through the asialoglycoprotein receptor (ASGP-R), a receptor unique to hepatocytes which binds galactose moieties on damaged proteins for endocytosis and degradation. Neither hepatocytes nor fibroblast 3T3 cells adhere to underivatized PEO hydrogels. Hepatocytes do not adhere to negative controls of glucose-derivatized hydrogels, which have similar physicochemical characteristics as galactose-derivatized hydrogels but do not interact specifically with hepatocytes.

Binding affinity for the ASGP-R increases five orders of magnitude as the ligand valency increases from a single galactose to a tri-branched form. The optimal tri-branched ligand spacing has been determined by others and described as a high affinity binding triangle. The ability of hepatocytes to spread on ADGal-derivatized PEO hydrogels correlates with the ease of achieving a trivalent ligand form. Spreading was observed on hydrogels in which the ligand tethers would need to stretch less than 1/3 their end-to-end distance to reach the three corners of the high affinity binding triangle. On star PEO hydrogels, the long tether arms can stretch to achieve trivalent ligand binding at low ligand concentrations; providing a scaffold for spread hepatocytes which maintain normal cuboidal morphology for at least six days in culture. Adherent hepatocytes remain viable, whether rounded or spread, and maintain differentiated function as measured by albumin secretion.

Hepatocytes bound to ADGal-derivatized hydrogels for more than two hours can not be removed using trypsin, chelating agents, or sugar competition. Resistance to trypsin may imply that the receptors are somehow buried in the cell membrane after binding ligands. If the ligand-receptor complex is partially internalized or the receptor is folded in such a way that prevents the trypsin from interacting with the cleavable amino-acids,

trypsin would be ineffective in detaching cells. Development of chelating-agent-resistant and sugar-resistant adhesion suggests conformational changes of the ligand-bound receptor. The ability of the ASGP-R to transfer mechanical forces across the cell membrane to the cytoskeleton was confirmed with a magnetic twisting device in which controlled mechanical loads are applied directly to cell surface receptors without producing a global cell shape change. Resistance to an applied load was reduced by 60% after cytoskeletal components were disrupted by drugs. Receptor conformational changes (induced by trivalent ligand binding) could lead to cytoskeletal interactions which would allow hepatocytes to spread on ADGal-derivatized star PEO hydrogels.

6.4. Star PEO Applications

In addition to hepatocyte specific ligands such as ADGal, other bioactive moieties can be immobilized onto PEO scaffolds to elicit a desired cellular response. In particular, immobilization of growth factors to polymer films may stimulate *in vitro* cell growth without allowing the factors to be degraded by the cells. Such a material would be advantageous in cell culture by eliminating the need to add expensive growth factors to medium. Also, the mechanism by which growth factors stimulate cells could be studied with the help of variable tethers to the polymer substrate. When immobilizing bioactive molecules such as hormones or growth factors, complete surface coverage may not be necessary or even desired as surface adsorbed proteins may be required for cell adhesion before the immobilized ligands can take affect. Star PEO grafting offers advantages over linear PEO in that ligands are immobilized in clusters which will facilitate receptor clustering often required to stimulate intracellular signaling. Initial investigations into this application using PEO hydrogels with immobilized epidermal growth factor (EGF) has demonstrated the validity of the approach (appendix A).

The phenomenon observed for the ASGP-R has broad implications for the design of biomaterials based on controlling receptor-mediated phenomena. Many receptors are believed to require precise spatial arrangements within the plane of the cell membrane in order to function properly, and thus the *spatial distribution* of a ligand on a biomaterial surface is perhaps as important as its average *concentration* on the surface. Star PEO hydrogels provide a versatile system for exploring this phenomenon.

Star PEO hydrogels encompass many of the ideals for engineered biomaterials. Irradiation crosslinking leaves polymer endgroups intact, which may be activated and coupled with bioactive ligands. A large range of ligand concentrations or ligand tether

lengths can be achieved by tailoring the star configuration or the irradiation conditions. The underivatized material does not adsorb significant amounts of protein or cause nonspecific cell adhesion; these properties are retained after derivatization. Hepatocytes bind immobilized ligands which induce desired cellular responses. Other bioactive ligand/receptor systems may also be amenable to exploitation by PEO hydrogel immobilization.

7. References

Abuchowski, A., van Es, T., Palczuk, N. C., and Davis, F. F. "Alteration of immunological properties of bovine serum albumin by covalent attachment of polyethylene glycol." *Journal of Biological Chemistry* **252** (1977) pp. 3578-3581.

Adam, M., Fetters, L.J., Graessley, W.W., Witten, T.A. "Concentration dependence of static and dynamic properties for polymeric stars in a good solvent." *Macromolecules* **24** (1991) pp. 2434-2440.

Altieri, D. C. "Occupancy of CD11b/CD18 (Mac-1) divalent ion binding site(s) induces leukocyte adhesion." *Journal of Immunology* **147** (1991) pp. 1891-1898.

Andrade, J. D. "Interfacial phenomena and biomaterials." *Medical Instrumentation* **7** (1973) pp. 110-120.

Andrade, J. D., Nagaoka, S., Cooper, S., Okano, T., and Kim, S. W. "Surfaces and blood biocompatibility. Current hypothesis." *Transactions of the American Society of Artificial Internal Organs,* **10** (1987) pp. 75-84.

Andrade, J. D., Hlady, V., Wei, A. P., Ho, C. H., Lea, A. S., Jeon, S. I., Lin, Y. S., and Stroup, E. "Proteins at interfaces: principles, multivariate aspects, protein resistant surfaces, and direct imaging and manipulation of adsorbed proteins." Clinical Materials Elsevier Science Publishers Ltd. England. (1992) pp. 1-18.

Ashwell, G. "Colorimetric analysis of sugars." *Methods in Enzymology* **3** (1957) pp. 73-105.

Atha, D. H., and Ingham, K. C. "Mechanism of precipitation of proteins by polyethylene glycols." *Journal of Biological Chemistry,* **256** (1981) pp. 12108-12117.

Baenziger, J. U., and Fiete, D. "Galactose and N-acetylgalactosamine-specific endocytosis of glycopeptides by isolated rat hepatocytes." *Cell* **22** (1980) pp. 611-620.

Bailey, F. E., Jr., and Callard, R. W. "Some properties of poly(ethylene oxide) in aqueous solution." *Journal of Applied Polymer Science* **1** (1959) pp. 56-62.

Balaji, P. V., Qasba, P. K., and Rao, V. S. R. "Molecular dynamics simulations of asialoglycoprotein receptor ligands." *Biochemistry* **32** (1993) pp. 12599-12611.

Beckerle, M. C., Yeh, R. K. "Talin: role at sites of cell-substratum adhesion." *Cell Motil Cytoskeleton* **16** (1990) pp. 7-13.

Benguinot, L., Lyall, R. M., Willingham, M. C., Pastan, I. "Down-regulation of the epidermal growth factor receptor in KB cells is due to receptor internalization and subsequent degradation in lysosomes." *Proceedings of the National Academy of Science USA* **81** (1984) pp. 2384-2388.

Ben-Ze'ev, A., Robinson, G. S., Bucher, N. L. R., and Farmer, S. R. "Cell-cell and cell-matrix interactions differentially regulate the expression of hepatic and cytoskeletal genes in primary cultures of rat hepatocytes." *Proceeding of the National Academy of Science USA* **85** (1988) pp. 2161-2165.

Berg, T., Boman, D., Seglen, P. O. "Induction of tryptophan oxygenase in primary rat liver cell suspensions by glucocorticoid hormone." *Experimental Cell Research* **72** (1972) pp. 571-574.

Bergström, K., Holmberg, K., Safranj, A., Hoffman, A. S., Edgell, M. J., Kozlowksi, A., Hovanes, B. A., and Harris, J. M. "Reduction of fibrinogen adsorption on PEG-coated polystyrene surfaces." *Journal of Biomedical Materials Research* **26** (1992) pp. 779-790.

Bessos, H., Appleyard, C., Micklem, L. R., and Pepper, D. C. *Prep. Chromatography* **1** (1987) p. 207.

Bethell, G. S., Ayers, J. S., Hancock W. S., and Hearn, M. T. W. "Novel methods of activation of cross-linked agaroses with 1,1'-carbonyldiimadazole which gives a matrix for affinity chromatography devoid of additional charged groups." *Journal of Biological Chemistry* **254** (1979) p. 2572.

Bieze, T. W. N., van der Maarel, J. R. C., Eisenbach, C. D., and Leyte, J. C. "Polymer dynamics in aqueous poly(ethylene oxide) solutions. An NMR study." *Macromolecules* **27** (1994) pp. 1355-1366.

Birshtein, T. M. and Zhulina, E. B. "Conformations of star-branched macromolecules." *Polymer* **25** (1984) pp. 1453-1461.

Birshtein, T. M., Zhulina, E. B. and Borisov, O. V. "Temperature-concentration diagram for a solution of star-branched macromolecules." *Polymer* **27** (1986) pp. 1078-1086.

Blumenthal, R., Klausner, R. D., and Weinstein, J. N. "Voltage-dependent translocation of the asialoglycoprotein receptor across lipid membranes." *Nature* **288** (1980) pp.333-341.

Bottenstein, J., Hayashi, I., Hutchings, S., Masui, H., Mather, J., McClure, D. B., Ohasa, S., Rizzino, A., Sato, G., Serrero, G., Wolfe, R., and Wu, R. "The growth of cells in serum-free hormone-supplemented media." *Methods in Enzymology* **58** (1979) pp. 94-109.

Brandley, B. K., Shaper, J. H., and Schnaar, R. L. "Tumor cell haptotaxis on immobilized N-acetylglucosamine gradients." *Developmental Biology* **140** (1990) pp. 161-171.

Bray, J. C., and Merrill, E. W. "Poly(vinyl alcohol) hydrogel. Formation by electron beam irradiation of aqueous solutions and subsequent crystallization." *Journal of Applied Polymer Science* **17** (1973) pp. 3779-3794.

Bridges, K., Harford, J., Ashwell, G., and Klausner, R. D. "Fate of receptor and ligand during endocytosis of asialoglycoproteins by isolated hepatocytes." *Proceedings of the National Academy of Science USA* **79** (1982) pp. 350-354.

Bucher, N. L. R., Patel, U., and Cohen, S. "Hormonal factors concerned with liver regeneration." *Ciba Foundation Symposium* **55** (1977) pp. 95-107.

Buck, C., Albelda, S., Damjanovich, L., Edelman, J., Shih, D. T., and Solowska, J. "Immunohistochemical and molecular analysis of β_1 and β_3 integrins." *Cell Differentiation and Development* **32** (1990) pp. 189-202.

Buckley, A., Davidson, J. M., Kamerath, C. D., Wolt, T. B., and Woodward, S. C. "Sustained release of epidermal growth factor accelerates wound repair." *Proceedings of the National Academy of Science USA* **82** (1985) pp. 7340-7344.

Cailleau, R. M. Human Tumor Cells in Vitro. J. Fogh, ed. Plenum, New York (1975) p. 70.

Canalis, E., and Raisz, L. G. "Effect of epidermal growth factor on bone-formation *in vitro." Endocrinology* **104** (1979) pp. 862-869.

Carpenter, G., and Cohen, S. "Epidermal growth factors." Biochemical Actions of Hormones. Vol. V G. Litwack, ed. Academic Press, NY (1978) pp. 203-247.

Castillo, E. J., Koenig, J. L., Anderson, J. M., and Lo, J. "Protein adsorption on hydrogels." *Biomaterials* **6** (1985) pp. 338-345.

Chaikof, E. L., Merrill, E. W., Callow, A. D., Connolly, R. J., Verdon, S. L., and Ramberg, K. "PEO enhancement of platelet deposition, fibrinogen deposition and complement C3 activation." *Journal of Biomedical Materials Research* **26** (1992) pp. 1163-1168.

Chapiro, A. Radiation Chemistry of Polymeric Systems. Interscience, New York (1962).

Cima, L., Vacanti, J. P., Vacanti, C., Ingber, D., Mooney, D., and Langer, R. "Tissue engineering by cell transplantation using degradable polymer substrates." *Journal of Biomechanical Engineering,* **113** (1991) pp. 143-151.

Comfort, A. R., Albert, E. C., Langer, R. "Immobilized enzyme cellulose hollow fibers: I. Immobilization of heparinase." *Biotechnology and Bioengineering* **34** (1989) pp. 1366-1373.

Connolly, D. T., Townsend, R. R., Kawaguchi, K., Bell, W. R., and Lee, Y. C. "Binding and endocytosis of cluster glycosides by rabbit hepatocytes." *Journal of Biological Chemistry* **257** (1982) pp. 939-945.

Cornell, R. P. "Gut-derived endotoxin elicits hepatotrophic factor secretion for liver regeneration." *American Journal of Physiology* **249** (1985) pp. R551-R562.

Crossland, R. K., Wells, W. E., and Shiner, Jr., V. J. "Sulfonate leaving groups, structure and reactivity. 2,2,2-trifluorethanesulfonate." *Journal of the American Chemical Society* **93** (1971) pp. 4217-4219.

Cuatrecasas, P. and Parikh, I. "Adsorbents for affinity chromatography - use of N-hydroxysuccinimide esters of agarose." *Biochemistry* **11** (1972) pp. 2291-2299.

Dan, N. and Tirrell, M. "Polymers tethered to curved interfaces. A self-consistent-field analysis." *Macromolecules* **25** (1992) pp. 2890-2895.

Daoud, M. and Cotton, J. P. "Star shaped polymers: a model for the conformation and its concentration dependence." *Journal de Physique* **43** (1982) pp. 531-538.

Davis, F. F., Abuchowski, A., van Es, T., Palczuk, N. C., Savoca, K., Chen, R. H-L., and Pyatak, P. "Soluble, nonantigenic polyethylene glycol-bound enzymes." Biomedical Polymers: Polymeric Materials and Pharmaceuticals for Biomedical Use. E. P. Goldberg and A. Nakajima, eds. Academic Press, Inc. (1980) pp. 441-452.

de Gennes, P. G. Scaling Concepts in Polymer Physics, Cornell University Press, Ithaca, New York, NY, (1979).

de Gennes, P. G. "Conformation of polymers attached to an interface." *Macromolecules* **13** (1980) pp. 1069-1075.

Demetriou, A. A "Intraperitoneal transplantation of hepatocytes attached to dextran beads: future promises." *Gastroenterology,* **92** (1987) pp. 548-549.

Demetriou, A. A., Reisner, A., Sanchez, J., Levenson, S. M., Moscioni, A. D., and Roy-Chowdhury, J. "Transplantation of microcarrier-attached hepatocytes into 90% partially hepatectomized rats." *Hepatology,* **8** (1988) pp. 1006-1009.

Demiroglou, A., Jennissen, H. P., "Synthesis and protein-binding properties of spacer-free thioalkyl agaroses." *Journal of Chromatography* **521** (1990) pp. 1-17.

Dennison, K. A. "Radiation crosslinked poly(ethylene oxide) hydrogel membranes." Ph.D. Thesis. Massachusetts Institute of Technology (1986).

Desai, N. P., and Hubbell, J. A. "Solution technique to incorporate polyethylene oxide and other water-soluble polymers into surfaces of polymeric biomaterials." *Biomaterials,* **12** (1991a) pp. 144-153.

Desai, N. P., and Hubbell, J. A. "Biological responses to polyethylene oxide modified polyethylene terephthalate surfaces." *Journal of Biomedical Materials Research* **25** (1991b) pp. 829-843.

DiMilla, P. A., Albelda, S. M., Quinn, J. A. "Adsorption and elution of extracellular matrix proteins on non-tissue culture polystyrene petri dishes." *Journal of Colloid and Interface Science* **153** (1992) pp. 212-225.

DiPersio, C. M., Jackson, D. A., and Zaret, K. S. "The extracellular matrix coordinately modulates liver transcription factors and hepatocyte morphology." *Molecular and Cellular Biology* **11** (1991) pp. 4405-4414.

Dossin, L. M. and Graessley, W. W. "Rubber elasticity of well-characterized polybutadiene networks." *Macromolecules* **12** (1979) pp. 123-130.

Drickamer, K. "Two distinct classes of carbohydrate-recognition domains in animal lectins." *Journal of Biological Chemistry* **263** (1988) pp. 9557-9560.

Drumheller, P. D., and Hubbell, J. A. "Densely crosslinked polymer networks of poly(ethylene glycol) in trimethylolpropane triacrylate for cell-adhesion-resistant surfaces." *Journal of Biomedical Materials Research* **29** (1995) pp. 207-215.

Dunn, J. C. Y., Yarmush, M. L., Koebe, H. G., and Tompkins, R. G. "Hepatocyte function and extracellular-matrix geometry - long-term culture in a sandwich configuration." FASEB **3** (1989) pp. 174-177.

Ferry, J. D. and Kan, H. C. "Interpretation of deviations from neo-hookean elasticity by a two-network model with crosslinks and trapped entanglements." *Rubber Chemistry and Technology* **51** (1978) pp. 731-737.

Flory, P. J. "Statistical mechanics of swelling network structures." *The Journal of Chemical Physics* **18** (1950) pp. 108-111.

Flory, P. J. Principles of Polymer Chemistry. Cornell University Press, Ithaca, NY (1953).

Flory, P. J. "Statistical thermodynamics of random networks." *Proceedings of the Royal Society of London, A* **351** (1976) pp. 351-380.

Flory, P. J. "The elastic free energy of dilation of a network." *Macromolecules* **12** (1979) pp. 119-122.

Flory, P. J. "Elastic activity of imperfect networks." *Macromolecules* **15** (1982) pp. 99-100.

Freeman, H. J., Lotan, R. and Kim, Y. S. "Application of lectins for detection of goblet cell glycoconjugate differences in proximal and distal colon of the rat." *Laboratory Investigation* **42** (1980) pp. 405-412.

Fuhrer, C., Geffen, I., Spiess, M. "Endocytosis of the ASGP receptor H1 is reduced by mutation of tyrosine-5 but still occurs via coated pits." *Journal of Cell Biology* **114** (1991) pp. 423-431.

Gasanov, E. K., Sergeeva, I. P., Sobolev, V. D., Zorin, Z. M., and Churaev, N. V. "Investigation of adsorbed layers of polyethylene oxide on quartz surface by means of capillary electrokinetics and ellipsometry." *Colloid Journal* **53** (1991) pp. 522-528.

Geffen, I., and Speiss, M "Asialoglycoprotein receptor." *International Review of Cytology* **137B** (1992) pp. 181-219.

Gin, H., Dupuy, B., Bonnemaison-Bourignon, D., Bordenave, L., Bareille, R., Latapie, M. J., Baque, C., Bezian, J., and Ducassou, D. "Biocompatibility of polyacrylamide microcapsules implanted in peritoneal cavity or spleen of the rat. Effect on various inflammatory reactions *in vitro*." *Biomaterials, Artificial Cells, Artificial Organs* **18** (1990) pp. 25-42.

Gjessing, R., and Seglen, P. O. "Adsorption, simple binding and complex binding of rat hepatocytes to various in vitro substrata." *Experimental Cell Research* **129** (1980) pp. 239-249.

Goldstein, I. J., Poretz, R. D., "Isolation, physicochemical characterization, and carbohydrate-binding specificity of lectins." The Lectins: Properties, Functions and Applications in Biology and Medicine. I. E. Liener, N. Sharon, I. J. Goldstein, eds. Academic Press, Inc., Harcourt Brace Javonovich, Publishers (1986) pp. 33-247.

Gombotz, W. R., Guanghui, W., and Hoffman, A. S. "Immobilization of poly(ethylene oxide) on poly(ethylene terephthalate) using a plasma polymerization process." *Journal of Applied Polymer Science* **37** (1989) pp. 91-107.

Gnanou, Y., Hild, G., and Rempp, P., "Molecular structure and elastic behavior of poly(ethylene oxide) networks swollen to equilibrium." *Macromolecules* **20** (1987) pp. 1662-1671.

Gnanou, Y., Lutz, P., and Rempp, P. "Synthesis of star-shaped poly(ethylene oxide)." *Makromol. Chem.* **189** (1988) pp. 2885-2892.

Graham, B. "Electron irradiation of organic polyethers." US Patent No. 2,964,455 (1960).

Grest, G. L., Kremer, K. and Witten, T. A. "Structure of many-armed star polymers: a molecular dynamics simulation." *Macromolecules* **20** (1987) pp. 1376-1383.

Guarnaccia, S. P., and Schnaar, R. L. "Hepatocyte adhesion to immobilized carbohydrates. I. Sugar recognition is followed by energy-dependent strengthening." *Journal of Biological Chemistry* **257** (1982) pp. 14288-14292.

Guarnaccia, S. P., Kuhlenschmidt, M. S., Slife, C. W. and Schnaar, R. L. "Hepatocyte adhesion to immobilized carbohydrates. II. Cellular modification of the carbohydrate surface." *Journal of Biological Chemistry* **257** (1982) pp. 14293-14299.

Gutsche, A. T., Zurlo, J., Lo, H. and Leong, K. "Synthesis and characterization of polymer substrates for rat hepatocyte culture." MRS Symposium Proceedings, Vol. (1994)

Han, D. K., Park, K. D., Ahn, K. D., Jeong, S. Y., Kim, Y. H. "Preparation and surface characterization of PEO-grafted and heparin-immobilized polyurethanes." *Journal of Biomedical Materials Research: Applied Biomaterials* **23** (1989) pp. 87-104.

Harris, J. M., Struck, E. C., Case, M. G., Paley, M. S., Yalpani, M., van Alstine, J. M., and Brooks, D. E. "Synthesis and characterization of poly(ethylene glycol) derivatives." *Journal of Polymer Science: Polymer Chemistry Edition* **22** (1984) pp. 341-352.

Hiatt, C. W., Shelokov, A., Rosenthal, E.J., Galimore, J. M. "Treatment of controlled pore glass with poly(ethylene oxide) to prevent adsorption of rabies virus." *Journal of Chromatography,* **56** (1971) pp. 362-364.

Hill-West, J. L., Chowdhury, S. M., Slepian, M. J., Hubbell, J. A. "Inhibition of thrombosis and intimal thickening by *in situ* photopolymerization of thin hydrogel barriers." *Proceedings of the National Academy of Science, USA* **91** (1994) pp. 5967-5971.

Hjerten, S. "Hydrophobic interaction chromatography of proteins nucleic acids, viruses, and cells on noncharged amphiphilic gels." *Methods of Biochemical Analysis* **27** (1981) pp. 89-108.

Hu, D. S. G., Liu, H. J., and Pan, I. L. "Inhibition of bovine serum albumin adsorption by poly(ethylene glycol) soft segment in biodegradable poly(ethylene glycol)/poly(L-lactide) copolymers." *Journal of Applied Polymer Science* **50** (1993) pp. 1391-1396.

Hubbell, J. A., Massia, S. P., Desai, N. P., and Drumheller, P. D. "Endothelial cell-selective materials for tissue engineering in the vascular graft via a new receptor." *Bio/Technology* **9** (1991) pp. 568-572.

Hughes, R. C., Pena, S. D. J., Clark, J., and Dourmashkin, R. R. "Molecular requirements for the adhesion and spreading of hamster fibroblasts." Experimental *Cell Research* **121** (1979) pp. 307-314.

Ingber, D. E. "Fibronectin controls capillary endothelial cell growth by modulating cell shape." *Proceedings of the National Academy of Science: USA* **87** (1990) pp. 3579-3583.

Ingber, D. E. "Integrins as mechanochemical transducers." *Current Opinion in Cell Biology* **3** (1991) pp. 841-848.

Ingber, D. E. "Cellular tensegrity: defining new rules of biological design that govern the cytoskeleton." *Journal of Cell Science* **104** (1993) pp. 613-627.

Israelachvili, J. Intermolecular and Surface Forces. Academic Press, London (1992).

Ito, Y., Liu, S.-Q., Nakabayashi, M. and Imanishi, Y. "Cell growth on immobilized cell-growth factor. II. Adhesion and growth of fibroblast cells on poly(methyl methacrylate) membrane immobilized with proteins of various kinds." *Biomaterials* **13** (1992) pp. 789-794.

Jackson, D. S., Kamp, L., Sheffield, W. D., and Matlaga, B. "Effect of angiogenic factors on the vascularization of Ivalon sponge implants." Soft and Hard Tissue Repair. T. K. Shint, R. B. Heppenstull, E. Pines, D. Rovee, eds. Praeter Press, NY (1984) pp. 190-201.

James, H. M. and Guth, E. "Theory of the increase in rigidity of rubber during cure." *Journal of Chemical Physics* **15** (1947) pp. 669-683.

Jauregui, H. O., Hayner, N. T., Driscoll, J. L., Williams-Holland, R., Lipsky, M. H., and Galletti, P. M. "Trypan blue dye uptake and lactate dehydrogenase in adult rat hepatocytes - freshly isolated cells, cell suspensions, and primary monolayer cultures." *In Vitro* **17** (1981) pp. 1100-1110.

Jauregui, H. O., Naik, S., Solomon, B. A., Duffy, R. L., Lipsky, M. H., and Galletti, P. M. "Attachment of adult rat hepatocytes to modified Amicon XM-50 membranes." *Transactions of the American Society of Artificial Internal Organs* **B29** (1983) pp. 698-703.

Jauregui, H. O., McMillan, P. N., Driscoll, J. and Naik, S. "Attachment and long term survival of adult rat hepatocytes in primary monolayer cultures: comparison of different substrata and tissue culture media formulation." *In Vitro Cellular and Developmental Biology* **22** (1986) pp. 13-22.

Jeon, S. I., Lee, J. H., Andrade, J. D., and de Gennes, P. G. "Protein-surface interactions in the presence of polyethylene oxide. I. Simplified theory." *Journal of Colloid and Interface Science* **142** (1991a) pp. 149-158.

Jeon, S. I., and Andrade, J. D. "Protein-surface interactions in the presence of polyethylene oxide. II. Effect of protein size." *Journal of Colloid and Interface Science* **142** (1991b) pp. 159-166.

Jirtle, R. L., Biles, C., and Michalopoulos, G. "Morphologic and histochemical analysis of hepatocytes transplanted into syngenic hosts." *American Journal of Pathology,* **101** (1980) pp. 115-126.

King, P. A. "Radiation modification of poly(ethylene oxide)." Irradiation of Polymers. Advances in Chemistry Series **66**, ACS , Washington, DC (1967) pp. 113-126.

King, P. A. and Ward, J. A. "Radiation chemistry of aqueous poly(ethylene oxide) solutions. I." *Journal of Polymer Science, Part A-1* **8** (1970) pp. 253-262.

Kishida, A., Mishima, K., Corretge, E., Konishi, H., and Ikada, Y. "Interactions of poly(ethylene glycol)-grafted cellulose membranes with proteins and platelets." *Biomaterials* **13** (1992) pp. 113-118.

Knauer, D. J., Wiley, H. S., and Cunningham, D. D. "Relationship between epidermal growth-factor receptor occupancy and mitogenic response - quantitative-analysis using a steady-state model system." *Journal of Biological Chemistry* **259** (1984) pp. 5623-5631.

Kobayashi, K. and Sumitomo, H. "Oligosaccharide-carrying styrene-type macromers. Polymerization and specific interactions between the polymers and liver cells." *Journal of Macromolecular Science Chemistry* **A24** (1988) pp.655-667.

Kornberg, L. J., Earp, H. S., Turner, C. E., Prockop, C. and Juliant, R. L. "Signal transduction by integrins: Increased protein tyrosine phosphorylation caused by clustering of beta-1 integrins." *Proceedings of the National Academy of Science USA* **88** (1991) pp. 8392-8396.

Korsmeyer, R. W.; Peppas, N. A. "Effect of the morphology of hydrophilic polymeric matrices on the diffusion and release of water soluble drugs." *Journal of Membrane Science* **9** (1981) pp. 211-227.

Kreamer, B. L., Staeckler, J. L., Sawada, N., Sattler, G. L., Hsia, M. T., Pitot, H. C. "Use of a low-speed, iso-density pecoll centrifugation method to increase the viability of isolated rat hepatocyte preparations." *In Vitro Cellular and Developmental Biology* **22** (1986) pp. 201-207.

Kühn, K., and Eble, J. "The structural bases of integrin-ligand interactions." *Trends in Cell Biology* **4** (1994) pp. 256-261.

Lee, E. M., Simister, E. A., and Thomas, R. K. "Neutron and X-ray reflectivity from polymers at the air water interface." *Molecular Crystals and Liquid Crystals* **179** (1990) pp. 151.

Lee, J. H., Kopecek, J., and Andrade, J. D. "Protein-resistant surfaces prepared by PEO-containing block copolymer surfactants." *Journal of Biomedical Materials Research* **23** (1989) pp. 351-368.

Lee, J. H., Kopeckova, P., Kopecek, J., and Andrade, J. D. "Surface properties of copolymers of alkyl methacrylates with methoxy(polyethylene oxide) methacrylates and their application as protein-resistant coatings." *Biomaterials,* **11** (1990) pp. 455-464.

Lee, R. T., and Lee, Y. C. "Affinity labeling of the galactose/N-acetylgalactosamine-specific receptor of rat hepatocytes: preferential labeling of one of the subunits." *Biochemistry* **26** (1987) pp. 6320-6329.

Lee, S. H., and Ruckenstein, E. "Adsorption of proteins onto polymeric surfaces of different hydrophilicities - a case study with bovine serum albumin." *Journal of Colloid and Interface Science* **125** (1988) pp. 365-379.

Lee, Y. C., Townsend, R. R., Hardy, M. R., Lönngren, J., and Bock, K. "Binding of synthetic clustered ligands to the Gal/GalNac lectin on isolated rabbit hepatocytes." Biochemical and Biophysical Studies of Proteins and Nucleic Acids. Lo, Liu, and Li, eds. Elsevier Science Publishing (1984) pp. 349-360.

Lee, Y. C. "Binding modes of mammalian hepatic Gal/GalNAc receptors." *CIBA Foundation Symposium* **145** (1989) pp. 80-95.

Lin, H. B., and Cooper, S. L. "Polyurethane copolymers containing covalently attached RGD-peptide: synthesis and cell adhesion studies." MRS Symposium Proceedings, Vol. 252, Tissue Inducing Biomaterials. L. G. Cima and E. S. Ron, eds. (1992) pp. 185-192.

Lodish, H. F. "Recognition of complex oligosaccharides by the multi-subunit asialoglycoprotein receptor." *TIBS* **16** (1991) pp. 374-377.

Luckham, P. F., and Klein, J. "Interactions between smooth solid surfaces in solutions of adsorbing and nonadsorbing polymers in good solvent conditions." *Macromolecules* **18** (1985) pp. 721-728.

Malcom, B. N. and Rowlinson, J. S. *Transactions of the Faraday Society* **53** (1957) p. 921.

March, S. C., Parikh, I. and Cuatrecasas, P. "Simplified methods for cyanogen-bromide activation of agarose for affinity chromatography." *Analytical Biochemistry* **60** (1974) pp. 149-152.

Marti, U., Burwen, S. J., and Jones, A. L. "Biological effects of epidermal growth factor, with emphasis on the gastrointestinal tract and liver: an update." *Hepatology* **9** (1989) pp. 126-138.

Massia, S. P., and Hubbell, J. A. "RGD spacing of 440 nm is sufficient for integrin $\alpha_V\beta_3$-mediated fibroblast spreading and 140 nm for focal contact and stress fiber formation." *Journal of Cell Biology* **114** (1991a) pp. 1089-1100.

Massia, S. P., and Hubbell, J. A. "Human endothelial cell interactions with surface-coupled adhesion peptides on a nonadhesive glass substrate and two polymeric biomaterials." *Journal of Biomedical Materials Research* **25** (1991b) pp. 223-242.

Matas, A. J., Sutherland, D. E. R., Steffes, M. W., Mauer, S. M., A. Lowe, Simmons, R. L., and Najarian, J. S. "Hepatocellular transplantation for metabolic deficiencies - decrease of plasma bilirubin in Gunn rats." *Science* **192** (1976) pp. 892-894.

McGary, Jr., C. W. "Degradation of poly(ethylene oxide)." *Journal of Polymer Science* **46** (1960) pp. 51-57.

McGowan, J. A., and Bucher, N. L. R. "Pyruvate promotion of DNA synthesis in serum-free primary cultures of adult rat hepatocytes." *In Vitro* **19** (1983) pp. 159-166.

Merrill, E. W., and Salzman, E. W. "Polyethylene oxide as biomaterial." *American Society for Artificial Internal Organs,* **6** (1983) pp. 60-64.

Merrill, E. W. "Distinctions and correspondences among surfaces contacting blood." *Annals of the New York Academy of Science* **516** (1987) pp. 1926-203.

Merrill, E. W., Wright, K. A., Sagar, A., Pekala, R. W., Dennison, K. A., Tay, S-W., Sung, C., Chaikof, E., Rempp, P., Lutz, P., Sadron, C., Callow, A. D., Connolly, R., Ramberg, K., Verdon, S. "Versions of immobilized polyethylene oxide for medical applications." Presented at the Fourth International Conference of Polymers in Medicine, (1990).

Merrill, E. W., Dennison, K. A., and Sung, C. "Partitioning and diffusion of solutes in hydrogels of poly(ethylene oxide)." *Biomaterials* **14** (1993) pp. 1117-1126.

Michalopoulos, G., and Pitot, H. C. "Primary culture of parenchymal liver cells on collagen membranes." Experimental *Cell Research* **94** (1975) pp. 70-78.

Miller, L. L., Bly, C. G., Watson, M. L., and Bale, W. F. "The dominant role of the liver in plasma protein synthesis. A direct study of the isolated perfused rat liver with the aid of lysine-ε-C^{14}." *Journal of Experimental Medicine* **94** (1951) pp. 431-453.

Minkova, L., Stamenova, R. Tsvetanov, C., and Nedkov, E. "Structural studies of radiation-crosslinked poly(ethylene oxide)." *Journal of Polymer Science* **27** (1989) pp. 621-642.

Mito, M., Ebata, H., Kusano, M., Onishi, T., Siato, T., and Sakamoto, S. "Morphology and function of isolated hepatocytes transplanted into rat spleen." *Transplantation* **28** (1979) pp. 499-505.

Mochitate, K., Pawelek, P. and Grinnell, F. "Stress relaxation of contracted collagen gels: disruption of actin filament bundles, release of cell surface fibronectin, and down-regulation of DNA and protein synthesis." *Experimental Cell Research* **193** (1991) pp. 198-207.

Mooney, D., Hansen, L., Vacanti, J., Langer, R., Farmer, S., and Ingber, D. "Switching from differentiation to growth in hepatocytes: control by extracellular matrix." *Journal of Cellular Physics* **151** (1992a) pp. 497-505.

Mooney, D. "Control of hepatocyte morphology and function by the extracellular matrix" Ph.D. Thesis. Massachusetts Institute of Technology (1992b).

Mori, Y., Nagaoka, S.; Takiuchi, H., Kikuchi, T., Noguchi, N., Tanzawa, H., and Noishiki, Y. "A new antithrombogenic material with long polyethyleneoxide chains." *Transactions of the American Society for Artificial Internal Organs* **28** (1982) pp. 459-463.

Moscioni, A. S., Roy-Chowdhury, J., Barbour, R., Brown, L. L., Roy-Chowdhury, N., Competiello, L. S., Lahiri, P., and Demetriou, A. A. "Human liver cell transplantation." *Gastroenterology,* **96** (1989) pp. 1546-1551.

Nakamura, K., Toyoda, K., and Kato, Y. "Preparation of adsorbents for affinity chromatography using TSKgel Tresyl-Toyopearl 650M." *Journal of Chromatography* **478** (1989) pp. 159-167.

Nakamura, K., Hashimoto, T., Kato, Y., Shimura, K., and Kasai, K. I. "Effect of type and concentration of coupling buffer on coupling yield in the coupling of proteins to a tresyl-activated support for affinity chromatography." *Journal of Chromatography* **513** (1990) pp. 367-369.

Nagaoka, S., Mori, Y., Takiuchi, H., Yokota, K. Tanzawa, H., and Nishiumi, S. "Interactions between blood components and hydrogels with poly(oxyethylene) chains." Polymers as Biomaterials. S. W. Shalaby, A. W. Hoffman, B. D. Ratner and T. A. Horbet, eds. Plenum Press, NY (1984) pp. 361-374.

Nagaoka, S. and Nakao, A. "Clinical application of antithrombogenic hydrogel with long poly(ethylene oxide) chains." *Biomaterials* **11** (1990) pp. 119-121.

Nakao, A., Ohkura, K., Nonami, T., Harada, A., Takagi, H., and Mori, Y. "Effect of a hydrogel with long polyethyleneoxide chains on blood coagulation and fibrinolysis." *Transactions of the American Society of Artificial Organs,* **32** (1986) pp. 319-322.

Needham, D., McIntosh, T. J., and Lasic, D. D. "Repulsive interactions and mechanical stability of polymer-grafted lipid membranes." *Biochimica et Biophysica Acta* **1108** (1992) pp. 40-48.

Nilsson, K. and Mosbach, K. "Immobilization of enzymes and affinity ligands to various hydroxyl group carrying supports using highly reactive sulfonyl chlorides." *Biochemical and Biophysical Research Communications* **102** (1981) pp. 449-457.

Nilsson, K. and Mosbach, K. "Immobilization of ligands with organic sulfonyl chlorides." *Methods in Enzymology* **104** (1984) pp. 56-69.

Norde, W. "Energy and entropy of protein adsorption." *Journal of Dispersion Science and Technology* **13** (1992) pp. 363-377.

Nuzzo, R. G., Dubois, L. H., Allara, D. L. "Fundamental studies of microscopic wetting on organic surfaces. 1. Formation and structural characterization of a self-consistent series of polyfunctional organic monolayers." *Journal of the American Chemical Society* **112** (1990) pp. 558-569.

Oka, J. A., Weigel, P. H. "Binding and spreading of hepatocytes on synthetic galactose surfaces occur as distinct and separable threshold responses." *Journal of Cell Biology* **103** (1986) pp. 1055-1060.

Orlando, R. A., and Cheresh, D. A. "Arginine-glycine-aspartic acid binding leading to molecular stabilization between integrin $\alpha_V\beta_3$ and its ligand." *Journal of Biological Chemistry* **266** (1991) pp. 19543-19550.

O'Shannessey, D. "Hydrazido-derivatized supports in affinity-chromatography." *Journal of Chromatography* **510** (1990) pp. 13-21.

Otey, C. A., Pavalko, F. M., Burridge, K. "An interaction between α-actin and the β_1 subunit *in vitro*." *Journal of Cell Biology* **111** (1990) pp. 721-729.

Pale-Grosdemange, C., Simon, E. S., Prime, K. L, and Whitesides, G. M. "Formation of self-assembled monolayers by chemisorption of derivatives of oligo(ethylene glycol) of structure $HS(CH_2)_{11}(OCH_2CH_2)_m$ on gold." *Journal of the American Chemical Society* **113** (1991) pp. 12-20.

Pedley, D. G. and Tighe, B J. "Water binding properties of hydrogel polymers for reverse osmosis and related applications." *British Polymer Journal* **11** (1979) pp. 130-136.

Pekala, R. W., Rudoltz, M., Lang, E. R., Merrill, E. W., Lindon, J., Kushner, L., McManama, G., and Salzman, E. W. "Crosslinked polyether/polysiloxane networks for blood-interfacing applications." *Biomaterials,* **7** (1986a) pp. 372-378.

Pekala, R. W., Merrill, E. W., Lindon, J., Kushner, L., and Salzman, E. W. "Fibrinogen adsorption and platelet adhesion at the surface of modified polypropylene glycol/polysiloxane networks." *Biomaterials,* **7** (1986b) pp. 379-385.

Peppas, N. A. and Merrill, E. W. "PVA hydrogels: determination of interaction parameter χ for PVA-water gels crosslinked from solutions." *Journal of Polymer Science, Polymer Chemistry* **14** (1976) pp. 459.

Peppas, N. A., and Mikos, A. G. "Preparation methods and structure of hydrogels." Hydrogels in Medicine and Pharmacy. N. A. Peppas, ed. CRC Press, Boca Ratton (1986) pp. 1-25.

Peppas, N. A., and Langer, R. "New challenges in biomaterials." *Science* **263** (1994) pp. 1715-1720.

Perez, E. P. "Bilayer composite hydrogels for corneal prostheses." Ph.D. Thesis. Massachusetts Institute of Technology (1995).

Porath, J., Lass and, T., Janson, J. C. "Agar derivatives for chromatography, electrophoresis and gel-bound enzymes. 3. Rigid agarose gels crosslinked with divinyl sulfone (DVS)." *Journal of Chromatography* **103** (1975) pp.49-62.

Prime, K. L., and Whitesides, G. M. "Adsorption of proteins onto surfaces containing end-attached oligo(ethylene oxide): a model system using self-assembled monolayers." *Journal of the American Chemical Society* **115** (1993) pp. 10714-10721.

Raja, R. H., Herzig, M., Grissom, M., and Weigel, P. H. "Preparation and use of synthetic cell culture surfaces. A new reagent for the covalent immobilization of proteins and glycoproteins on a nonionic inert matrix." *The Journal of Biological Chemistry* **261** (1986) pp. 8505-8513.

Ratner, B. D., and Hoffman, A. S. "Synthetic hydrogels for biomedical application." Hydrogels for Medical and Related Applications. J. D. Andrade, ed. ACS Symposium Series #31 (1976) pp. 1-36.

Ratner, B. D. "Biomedical applications of hydrogels: review and critical appraisal." Biocompatibility of Clinical Implant Materials. Vol. II. D. F. Williams, ed. CRC Press. (1981) pp. 145-175.

Ratner, B. D. "New ideas in biomaterials science - a path to engineered biomaterials." *Journal of Biomedical Materials Research* **27** (1993) pp. 837-850.

Reinhart, C. T. and Peppas, N. A. "Solute diffusion in swollen membranes. Part II. Influence of crosslinking on diffusive properties." *Journal of Membrane Science* **18** (1984) pp. 227-239.

Rempp, P., Lutz, P., and Merrill, E. W. "Anionically polymerized star macromolecules having divinyl benzene cores with grafted poly(ethylene oxide) arms as biomaterials." Presented at the American Chemical Society Symposium, Polymer Division (1990).

Rice, K. G., Lee, Y. C. "Oligosaccharide valency and conformation in determining binding to the asialoglycoprotein receptor of rat hepatocytes." *Advanced Enzymology and Related Areas of Molecular Biology* **66** (1993) pp. 41-83.

Richman, R. A., Claus, T. H., Plikis, S. J., Friedman, D. L. "Hormonal stimulation of DNA synthesis in primary cultures of adult rat hepatocytes." *Proceedings of the National Academy of Science, USA* **73** (1976) pp. 3589-3593.

Roovers, J., Zhou, L. L., Toporowski, P. M., van der Zwan, M., Iatrou, H., Hadjichristidis, N. "Regular star polymers with 64 and 128 arms. Models for polymeric micelles." *Macromolecules* **26** (1993) pp. 4324-4331.

Rotem, A., Toner, M., Tompkins, R. G., Yarmush, M. L. "Oxygen uptake rates in cultured rat hepatocytes." *Biotechnology and Bioengineering* **8** (1992) pp. 227-232.

Ruoslahti, E., and Pierschbacher, M. D. "New perspectives in cell adhesion: RGD and integrins." Science **238** (1987) pp. 491-497.

Sarkar, M., Liao, J., Kabat, E. A., Tanabe, T., and Ashwell, G. "The binding site of rabbit hepatic lectin." *Journal of Biological Chemistry* **254** (1979) pp. 3170-3174.

Sarmoria, C., Blankschtein, D. "Conformational characteristics of short poly(ethylene oxide) chains terminally attached to a wall and free in aqueous solution." *Journal of Physical Chemistry* **96** (1992) pp. 1978-1983.

Sato, G. H., Zaroff, L., and Mills, S. "Tissue culture population and their relation to the tissue of origin." *Proceedings of the National Academy of Science, USA* **46** (1960) pp. 963-972.

Sato, H., Kidaka, T. and Hori, M. "Leakage of immobilized IgG from therapeutic immunoadsorbents." *Applied Biochemistry and Biotechnology* **15** (1987) pp. 145-158.

Sawhney, A. S., and Hubbell, J. A. "Poly(ethylene oxide)-graft-poly(L-lysine) copolymers to enhance the biocompatibility of poly(L-lysine)-alginate microcapsule membranes." *Biomaterials* **13** (1992) pp. 863-870.

Sawyer, J. T., Sanford, J. P., and Doyle, D. "Identification of a complex of the three forms of the rat liver asialoglycoprotein receptor." *Journal of Biological Chemistry* **263** (1988) pp. 10534-10538.

Schakenraad, J. M. and Busscher, H. J. "Cell-polymer interactions: the influence of protein adsorption." *Colloids and Surfaces* **42** (1989) pp. 331-343.

Scheutz, E. G., Li, D., Omiecinski, C. J., *et. al.* "Regulation of gene expression in adult rat hepatocytes cultured on a basement membrane matrix." *Journal of Cellular Physics* **134** (1988) pp. 309-323.

Schnaar, R. L., Weigel, P. H., Kuhlenschmidt, M. S., Lee, Y. C., and Roseman, S. "Adhesion of chicken hepatocytes to polyacrylamide gels derivatized with N-acetylglucosamine." *The Journal of Biological Chemistry* **253** (1978) pp. 7940-7951.

Schnaar, R. L., Brandley, B. K., Needham, L. K., Swank-Hill, P., Blackburn C. C. "Adhesion of eucaryotic cells to immobilized carbohydrates." *Methods in Enzymology* **179** (1989) pp. 542-558.

Schreiber, A. B., Libermann, T. A., Lax, I., Yarden, Y., Schlessinger, J. "Biological role of epidermal growth factor-receptor clustering - investigation with monoclonal anti-receptor antibodies." Journal *of Biological Chemistry* **258** (1983) pp. 846-853.

Schwartz, A. L., Fridovich, S. E., and Lodish, H. F. "Kinetics of internalization and recycling of the asialoglycoprotein receptor in a hepatoma cell line." *Journal of Biological Chemistry* **257** (1982) pp. 4230-4237.

Schwartz A., L. "The hepatic asialoglycoprotein receptor." *CRC Critical Review of Biochemistry* **16** (1984) pp. 207-233.

Schwerer, B., Bach, M. and Bernheimer, H. "ELISA for determination of albumin in the nanogram range: assay in cerebrospinal fluid and comparison with radial immunodiffusion." *Clinica Chimica Acta* **163** (1987) pp. 237-244.

Seglen, P. O. "Preparation of isolated rat liver cells." *Methods of Cell Biology* **13** (1976) pp. 29-83.

Shaltiel, S. Chromatography of Synthetic and Biological Polymers, Vol. 2, Hydrophobic, Ion Exchange and Affinity Methods. R. Epton, ed; Ellis Horwood, Chichester (1976) pp. 13-41.

Shia, M. A., and Lodish, H. F. "The two subunits of the human asialoglycoprotein receptor have different fates when expressed alone in fibroblasts." *Proceedings of the National Academy of Science USA* **86** (1989) pp. 1158-1162.

Simpson, R. J., Smith, J. A., Moritz, R. L., *et. al.* "Rat epidermal growth factor: complete amino acid sequence. Homology with the corresponding murine and human proteins; isolation of a form truncated at both ends with full in vitro biological activity." *European Journal of Biochemistry* **153** (1985) pp. 629-637.

Singer, I. I., Kawka, D. W., Scott, S., Mumford, R. A., and Lark, M. W. "The fibronectin cell attachment sequence arg-gly-asp-ser promotes focal contact formation during early fibroblast attachment and spreading." *Journal of Cell Biology* **104** (1987) pp. 573-584.

Soni, N. N., Whitehurst, V. E., Knight, R. S., and Sinkford, J. C. "Long-range effects of Ivalon sponge containing isobutyl cyanoacrylates on rat tissue." Oral *Surgery,* **39** (1975) pp. 197-202.

Spiess, M. "The asialoglycoprotein receptor: a model for endocytic transport receptors." *Biochemistry* **29** (1990) pp. 10009-10018.

Stamatoglou, S. C., Hughes, R. C., Lindahl, U. "Rat hepatocytes in serum-free primary culture elaborate an extensive extracellular matrix containing fibrin and fibronectin." *The Journal of Cell Biology* **105** (1987) pp. 2417-2425.

Stamatoglou, S. C., Sullivan, K. H., Johansson, S., Bayely, P. M., Burdett, I. D., and Hughes, R. C. "Localization of two fibronectin-binding glycoproteins in rat liver and primary hepatocytes. Co-distribution *in vitro* of integrin ($\alpha_5\beta_1$) and non-integrin (AGp110) receptors in cell-substratum adhesion sites." *Journal of Cell Science* **97** (1990) pp. 595-606.

Stenger, D. A., Georger, J. H., Dulcey, C. S., Hickman, J. J., Rudolph, A. S., Nielsen, T. B., McCort, S. M., and Calvert, J. M. "Coplanar molecular assemblies of amino- and perfluorinated alkylsilanes: characterization and geometric definition of mammalian cell adhesion and growth." *Journal of the American Chemical Society* **114** (1992) pp. 8435-8442.

Streuli, C. H., and Bissell, M. J. "Expression of extracellular matrix components is regulated by substratum." *The Journal of Cell Biology* **110** (1990) pp. 1405-1415.

Sun, Y., Hoffman, A. S., Gombotz, W. R. "Non-fouling biomaterial surfaces: II. Protein adsorption on radiation grafted polyethylene glycol methacrylate copolymers." *ACS Polymer Preprints* **28** (1987) pp. 292-294.

Sundberg, L. and J. Porath "Preparation of adsorbents for biospecific affinity chromatography. 1. Attachment of group-containing ligands to insoluble polymers by means of bifunctional oxiranes." *Journal of Chromatography* **90** (1974) pp. 87-98.

Thompson, J. A., Maciag, T., Haudenschild, C. C., Anderson, K. D., DiPietro, J. M., and Anderson, W. F. "Implantable bioreactors: modern concepts of gene therapy." Therapeutic Peptides and Proteins. D. Marshak and D. Liu, eds. (1989a) pp. 143-147.

Thompson, J. A., Haudenschild, C. C., Anderson, K. D., DiPietro, J. M., Anderson, W. R., and Maciag, T. "Heparin-binding growth factor 1 induces the formation of organoid neovascular structures *in vivo*." *Proceedings of the National Academy of Science USA*, **86** (1989b) pp. 7928-7932.

Tolleshaug, H., Berg, T. "Investigtion of the uptake of asialoglycoproteins by isolated rat hepatocytes." *Hoppe Seyler's Z. Physiol. Chem.* **361** (1980) pp. 1155-1164.

Townsend, R. R., Hardy, M. R., Wong, T. C., and Lee, Y. C. "Binding of N-linked bovine fetuin glycopeptides to isolated rabbit hepatocytes: Gal/GalNAc hepatic lectin discrimination between Galß(1,4)GlcNAc and Galß(1,3)GlcNAc in a triantennary structure." *Biochemistry* **25** (1986) pp. 5716-5725.

Treloar, L. R. G. The Physics of Rubber Elasticity. 3rd Ed., Clarendon Press, Oxford (1975).

Truce, W. E., and Norell, J. R. "Thietane dioxide derivatives via the interaction of sulfonyl chlorides with ketene diethylacetal." *Journal of the American Chemical Society* **85** (1963) pp. 3231-3236.

Tseng, Y. C., and Park, K. "Synthesis of photoreactive poly(ethylene glycol) and its application to the prevention of surface-induced platelet activation." *Journal of Biomedical Materials Research* **26** (1992) pp. 373-391.

Turner, C. E., Glenney, J. R. Jr., Burridge, K. "Paxillin: a new vinculin-binding protein present in focal adhesions." *Journal of Cell Biology* **111** (1990) pp. 1059-1068.

Ubrich, N., Hubert, P., Regnault, V., Dellacherie, E., Rivat, C. "Compared stability of sepharose-based immunoadsorbents prepared by various activation methods." *Journal of Chromatography* **584** (1992) pp. 17-22.

United Network for Organ Sharing, National Organ Procurement and Transplantation Network.

Vagberg, L. J. M., Cogan, K. A. and Gast, A. P. "Light-scattering study of starlike polymeric micelles." *Macromolecules* **24** (1991) pp. 1670-1677.

van Sommeren, A. P. G., Machielsen, P. A. G. M., and Gribnau, T. C. J. "Comparison of three activated agaroses for use in affinity chromatography: effects on coupling performance and ligand leakage." *Journal of Chromatography* **639** (1993) pp. 23-31.

van Wachem, P. B., Hogt, A. H., Biugeling, T., Feijen, J., Bantjes, A., Detmers, J. P., van Aken, W. G. "Adhesion of cultured human endothelial cells onto methacrylate polymers with varying surface wettability and charge." *Biomaterials* **8** (1987) pp. 323-328.

Verdon, S. L., Chaikof, E. L., Coleman, J. E., Hayes, L. L., Connolly, R. J., Ramberg, K., Merrill, E. W., and Callow, A. D. "Scanning electron microscopy analysis of polyethylene oxide hydrogels for blood contact." *Scanning Microscopy* **4** (1990) pp. 341-350.

Wall, D. A. and Hubbard, A. L. "Galactose-specific recognition system of mammalian liver: receptor distribution on the hepatocyte cell surface." *Journal of Cell Biology,* **90** (1981) pp. 687-696.

Wang, N., Butler, J. P., and Ingber, D. E. "Mechanitransduction across the cell surface and through the cytoskeleton." *Science* **260** (1993) pp. 1124-1127.

Wang, N., and Ingber, D. E. "Control of cytoskeletal mechanics by extracellular matrix, cell shape, and mechanical tension." *Biophysical Journal* **66** (1994) pp. 2181-2189.

Wang, N., Planus, E., Pouchelet, M., Fredberg, J. J., and Barlovatz-Meimon, G. "Urokinase receptor mediates mechanical force transfer across the cell surface." *American Journal of Physiology* **268** (1995) C1062-C1066.

Wasiewsik, W., Fasco, W. J., Martin, B. M., Detwiler, T. C., and Fenton, J. W., II "Thrombin adsorption to surfaces and prevention with polyethylene glycol 6,000." *Thrombosis Research,* **8** (1976) pp. 881-886.

Weigel, P. H., Schmell, E., Lee, Y. C., Roseman, S. "Specific adhesion of rat hepatocytes to ß-galactosides linked to polyacrylamide gels." *Journal of Biological Chemistry* **253** (1978) pp. 330-333.

Weigel, P. H., Schnaar, R. L., Kuhlenschmidt, M. S., Schmell, E., Lee, R. T., Lee, Y. C., and Roseman, S. "Adhesion of hepatocytes to immobilized sugars. A threshold phenomena." *Journal of Biological Chemistry* **21** (1979) pp. 10830-10838.

Weigel, P. H. "Characterization of the asialoglycoprotein receptor on isolated rat hepatocytes." *Journal of Biological Chemistry* **255** (1980a) pp. 6111-6120.

Weigel, P. H. "Rat hepatocytes bind to synthetic galactose surfaces via a patch of asialoglycoprotein receptors." *Journal of Cell Biology* **87** (1980b) pp. 855-861.

Weigel, P. H., Oka, J. A. "Recycling of the hepatic asialoglycoprotein receptor in isolated rat hepatocytes." *Journal of Biological Chemistry* **259** (1984) pp. 1150-1154.

Weisz, O. A., Schnaar, R. L. "Hepatocyte adhesion to carbohydrate-derivatized surfaces. I. Surface topography of the rat hepatic lectin." *Journal of Cell Biology* **115** (1991a) pp. 485-493.

Weisz, O. A., Schnaar, R. L. "Hepatocyte adhesion to carbohydrate-derivatized surfaces. II. Regulation of cytoskeletal organization and cell morphology." *Journal of Cell Biology* **115** (1991b) pp. 495-504.

Williams, E. C., Jammey, P.A., Ferry, J. D., and Mosher, D. F. "Conformational states of fibronectin - effects of pH, ionic-strength, and collagen binding." *Journal of Biological Chemistry* **257** (1982) pp. 4973-4978.

Willner, L., Jucknischke, O., Richter, D., Roovers, J., Zhou, L.-L., Toporowski, P.M., Fetters, L.J., Huang, J.S., Lin, M.Y., Hadjichristidis, N., "Structural investigation of star polymers in solution by small angle neutron scattering." *Macromolecules* **24** (1994) pp. 3821-3829.

Witten, T. A., Pincus, P. A. and Cates, M. E. "Macrocrystal ordering in star polymer solutions." *Europhysics Letters* **2** (1986) pp. 137-140.

Wu, G. "Characterizations of the *in vitro* and *in vivo* biocompatibility of galactose-derivatized poly(ethyleneoxide) as a model material for hepatocyte transplantation." Harvard-MIT Division of Health Sciences and Technology M.D. Thesis (1993).

Yoshioka, H. "Surface modification of haemoglobin-containing liposomes with polyethylene glycol prevents liposome aggregation in blood plasma." *Biomaterials,* **12** (1991) pp. 861-864.

Zipf, R. E., and Waldo, A. L. "Spectrophotometric analysis of carbohydrates and study of anthrone reagent." *Journal of Laboratory and Clinical Medicine* **39** (1952) pp. 497-502.

Appendix A. Alternate Example: Bound EGF Promotes Cell Growth

In addition to hepatocyte specific ligands such as ADGal, other bioactive moieties can be immobilized onto PEO scaffolds to elicit a desired cellular response. In particular, immobilization of growth factors to polymer films may stimulate *in vitro* cell growth without allowing the factors to be degraded by the cells. Such a material would be advantageous in cell culture by eliminating the need to add expensive growth factors to medium. Also, the mechanism by which growth factors stimulate cells could be studied with the help of variable tethers to the polymer substrate. Initial investigations into this application using PEO hydrogels with immobilized epidermal growth factor (EGF) has shown the validity of the approach.

A.1. Motivation: Hepatocyte Response to Epidermal Growth Factor

Epidermal growth factor (EGF), a 6-kDa polypeptide, plays a role in the regulation of a variety of physiological processes in many cell types including fibroblasts (Carpenter, 1978), bone cells (Canalis, 1979) and hepatocytes (Richman, 1976). The biological effects of EGF on hepatocytes are summarized in a review by Marti (Marti, 1989). EGF is most noted for its stimulation of DNA synthesis and cell growth (Richman, 1976), but it has also been implicated as a hepatotrophic factor during liver regeneration (Bucher, 1977; Cornell, 1985), suggesting that the presence of EGF during cultured hepatocyte transplantation may stimulate the desired regeneration. To take advantage of its mitogenic properties, EGF is usually added to serum-free cell culture medium at 10-50 ng/ml (Bottenstein, 1979; McGowan, 1983). Once bound, EGF is internalized and degraded in the lysosomes (Beguinot, 1984), so EGF must be continuously replenished in the medium. Immobilizing EGF to the culture dish or transplantation scaffold will obviate the need to add the growth factor to the medium and may provide regenerative stimulus once implanted. Preventing receptor internalization may further stimulate cells to divide, since the number of persistently occupied receptors determines the degree of mitogenic stimulation (Knauer, 1984). Buckley and coworkers found that implantation of a controlled-release EGF pellet within a poly(vinyl alcohol) sponge resulted in a much more dramatic stimulation of wound repair than did sequential daily EGF injections (Buckley, 1985), which suggests an implantation scaffold with immobilized EGF may be even more effective. While the mechanism for EGF signaling is not precisely known, bound receptors migrate to coated pits and there is some evidence receptor clustering is required for signal transduction (Schreiber, 1983). Immobilization of EGF via flexible

tethers would allow bound receptors to move freely within the cell membrane. PEO grafted chains or PEO hydrogels are ideally suited for this application.

A.2. EGF Coupling to PEO Hydrogels

Mouse EGF used in this study is nearly homologous to human and rat EGF and exhibits activity in rat hepatocytes (Simpson, 1985). Mouse EGF contains only one primary amine, at the N-terminus, which was used to immobilize the growth factor to tresyl chloride activated PEO hydrogels in the same manner as amino-carbohydrate ligands (Chapter 3). The EGF binding site is far enough from the N-terminus that immobilization should not affect protein folding or activity (Simpson, 1985). EGF was coupled to linear PEO hydrogels at a nominal concentration of 10 μg/ml. PEO hydrogels inhibit protein adsorption and nonspecific cell adhesion, so Type I collagen was co-immobilized on some samples to provide hepatocyte binding sites.

A.3. Hepatocyte Response

Hepatocytes were seeded at a nominal concentration of 30,000 viable cells/cm^2 onto linear PEO hydrogels derivatized as outlined in Table A-1. Hepatocytes were cultured in chemically defined serum-free medium lacking soluble EGF (William's E with 20 mU/ml insulin (Gibco, Grand Island, NY), 5 nmol/L dexamethasone (Sigma, St. Louis, MO), 20 mmol/L pyruvate (Gibco), and 100 U/ml penicillin/streptomycin (Gibco)) with daily medium changes. Controls included hepatocytes seeded onto collagen gels cultured in serum-free medium with or without soluble EGF. A cell proliferation assay which stains the nuclei of growing cells as the DNA takes up 5-bromo-2'-deoxyuridine (BrdU) was used to visualize cell stimulation. As an internal control, hepatocytes which rolled off the hydrogels and adhered to the tissue culture dish bottom were also assayed for cell growth. No EGF should be available to these cells, so any growth would indicate EGF leaching from the hydrogel.

Hepatocytes were examined daily with an inverted phase contrast light microscope. Few cells adhered to hydrogels without collagen, confirming the need for an adhesion mechanism. Adherent cells exhibited little spreading on the derivatized hydrogels, with or without the presence of co-immobilized collagen. Adherent hepatocytes were stained for DNA synthesis 48 hours after seeding. As expected, BrdU staining indicated cell growth on controls cultured with EGF in the medium, but not on controls cultured in EGF-free medium. No cell growth was apparent on PEO hydrogels derivatized with EGF or collagen alone (EGF-free medium), but DNA synthesis was evident on PEO hydrogels

with EGF and collagen co-immobilized (EGF-free medium). Hepatocytes adherent to the bottom of the culture dishes did not stain, assuring no EGF was leaching from the hydrogels. These results suggest immobilized EGF is effective in stimulating mitogenesis, as long as cells are provided with a mechanism for adhesion to the substrate, and point to the general validity of immobilizing bioactive ligands with long, flexible PEO tethers.

Table A-1. Immobilized Epidermal Growth Factor.

Substrate	Medium	Cell Number	BrdU Staining (% of Cells Stained)	
Collagen Gel Control	with EGF	+++++	++++	(> 50%)
Collagen Gel Control	no EGF	+++++	+	(< 5%)
PEO + EGF	no EGF	+	–	
PEO + Collagen	no EGF	+++	–	
PEO + EGF + Collagen	no EGF	+++	+++	(≈ 35%)

Appendix B. Protocols

B.1. Carbohydrate Measurement with Acidic Anthrone

(Ashwell, 1957)

Set Up

Materials:
- incubator
- test tubes/ rack
- parafilm
- rubber gloves
- pipet
- ice water bath
- timer
- vortexer

Reagents:
- 0.2% Anthrone in H_2SO_4
- calibration solutions in a range 0 - 1 mM in PBS (assuming fresh anthrone, else span range 0 - 2 mM)

Procedure

Note: **The timing between steps in the assay is critical.** Samples will be prepared in batches of 6.

1. Preheat incubator to 90 C. Be sure the heating oil has reached temperature set point before starting incubation.
2. Place 6 test tubes in rack in ice water bath (10-15 C).
3. Start timer. Add 2 ml Anthrone to each tube. Record finish time.
4. At 5 minutes, add 1 ml sample or calibration solution. (Include a 0 point in the calibration curve by adding 1 ml PBS in place of calibration solution.) Record finish time.
5. At 10 minutes mix each tube with the vortexer. Replace tube in ice water bath after mixing. Record finish time.
6. Cover tubes with parafilm.
7. Incubate for 16 minutes. Record start and stop times of incubation.
8. After cooling, measure absorbance at 625 nm. Note: The color will remain stable for several hours.

B.2. ELISA Protocol Step-By-Step

(Schwerer, 1987; prepared by A. Park)

Day 1

Make up **bicarbonate buffer coating solution**: (100 ml bottle/lid)
- 0.159 g Na_2CO_3 (sod. carb. anhyd.)
- 0.293 g $NaHCO_3$ (sod. bicarb.)
- 0.2 g sodium azide (small tin can)
- 100 ml DI water

Check pH (9.6)

Make up **PBS-Tween washing solution**: (4 L Erlenmeyer or beaker+stirbar)
- 32 g NaCl
- 0.8 g NaH_2PO_4 (monobasic)
- 5.64 g Na_2HPO_4 (sod. phosphate)
- 0.80 g KCl
- 2 ml Tween-20 (0.05%)
- 4 L DI water

Check pH (7.4)

Coat plates with **unconjugated rat albumin antibody** (2 µg/ml)
- obtain 1 microfuge tube of antibody from freezer. (1 tube=100 µl; goal=8 µg/ml)
- add 80 µl of antibody to 4 ml bicarbonate buffer solution
- add 125 µl of resulting solution to 10 ml buffer (once for each plate)
- add 100 µl to each well
- cover plates with parafilm and place in refrigerator

Make up **substrate buffer** (100 ml--need 40 ml/4 plates)
- 1.28 g citrate
- 1.09 g Na_2HPO_4
- 100 ml DI water

Check pH (5.0)

Make up **stop solution** (100 ml--need 10 ml/plate)
- 0.32 g NaF
- 100 ml DI water

Day 2

Aspirate antibody coating solution.
Add PBS-Tween solution and aspirate 3x.
Add PBS-Tween solution to keep plates from dehydrating if for use on another day.

B.2. ELISA Protocol Step-By-Step

(continued)

Day 2 up to Day 9

Make **1% gelatin blocking solution** in PBS-Tween: (100 ml bottle/lid=20 ml/plate)
1 g gelatin
100 ml PBS-Tween
Heat with stirring to dissolve.
Cool.
Add 200 µl to each well.

Incubate at 37°C for 30 minutes.
Wash 3x with PBS-Tween.
Refill with 100 µl PBS-Tween per well.

Prepare **standard albumin sample**:
obtain 1 microfuge tube from Cima lab freezer (1 tube=100 µl of 14.2 µg/ml; goal=50 ng/ml)
add 1.32 ml of PBS-Tween to 100 µl tube and mix well
add 100 µl of resulting solution to 10 ml PBS-Tween and mix well
add 100 µl of resulting solution to 10 ml PBS-Tween
add 100 µl to 2 wells per plate (columns 1 & 2)

Prepare **experiment albumin samples**:
add 10 µl of sample (guess ≈ 10 µg/ml) to 1 ml PBS-Tween in microfuge tube
mix well
add 100 µl of resulting solution to appropriate row A well

Dilute samples:
using multichannel pipettor set at 100 µl, mix row A wells several times
pick up 100 µl of resulting solution and add to row B wells; mix 3x
pick up 100 µl of resulting solution and add to row C wells; mix 3x
pick up 100 µl of resulting solution and add to row D wells; mix 3x
pick up 100 µl of resulting solution and add to row E wells; mix 3x
pick up 100 µl of resulting solution and add to row F wells; mix 3x
pick up 100 µl of resulting solution and add to row G wells; mix 3x
pick up 100 µl of resulting solution and discard
add nothing new to row H (blank).

Incubate at 37°C for 1 hour
Wash 3x with PBS-Tween

B.2. ELISA Protocol Step-By-Step

(continued)

Prepare **conjugated antibody**: (1 tube/2 plates)
add 950 µl PBS-Tween to one tube (50 µl/tube)
add 900 µl of resulting solution to 22 ml PBS-Tween
add 100 µl to each well

Incubate at 37°C for 1 hour
Wash 3x with PBS-Tween

Prepare **substrate solution**: (0.25 mg/ml ABTS, 0.01% H_2O_2 in substrate buffer)
add (1) 10 mg tablet from desiccator to 40 ml substrate buffer
just before you need it, add 13.2 µl of 30% H_2O_2 to 40 ml of final solution
cover with foil
add 100 µl to each well

Cover with foil
Incubate at room temperature for 45 minutes exactly
Add 100 µl **stop solution** to each well without aspirating

Read plates in ELISA plate reader within one hour.

Set dual endpoints L1=405, L2=490.

B.3. Fluorescein-Labeled Lectin Binding

(Freeman, 1980)

1. Prepare 0.05% Tween-20 in MilliQ water (washing solution), refrigerate.
2. Place a small piece of each gel (≈ 0.4 cm^2) in a small scintilation vial.
3. Add PBS to cover gels.
4. Add appropriate amount of lectin *Ricinus communis* I (RCA-120) to achieve the desired concentration of 0.1 mg/cm^2. Do this in the dark so that the lectin is not bleached out.
5. Incubate on a shaker in a dark, humid environment for 12-24 hours.
6. Remove gels from lectin solution and place each in a scintillation vial.
7. Add enough washing solution to cover gels (≈ 2 ml).
8. Incubate on shaker in the dark for 30 minutes.
9. Remove washing solution from gels by pouring the contents of the vial through filter paper.
10. Replace gel in scintillation vial.
11. Repeat this procedure (steps 7-19) 7 more times (8 total washes).
12. View with fluorescent microscope using fluorescein excitation filter (485 nm) and emission filter (520-560 nm).
13. Take photographs as desired using 1600 speed color film. Film should be pushed twice during development to pick up dim fluorescence.

B.4. Live/Dead Viability Assay

Set Up

Materials:
- Fluorescence filter: fluorescein excitation filter (485 nm)w/ long pass emission filter (530 and 590 nm)
- Fuji 1600 speed color push film
- 20 µl pipet
- 15 ml sterile centrifuge tube
- vortexer

Reagents:
- Sterile PBS
- Live/Dead kit from Molecular Probes, Inc (L-3224)

OR
- Aliquots of EthD-1 (ethidium homodimer, 2 mM in DMSO/H_2O 1:4 (v/v))
- Aliquots of calcein AM (4 mM in anhydrous DMSO)

Procedure

1. Remove the LIVE/DEAD reagent stock solutions (one of calcein and one of EthD-1) from freezer and allow to warm to room temperature.
2. Measure 10 ml sterile PBS into sterile centrifuge tube.
3. Add 20 µl of EthD-1 to 10 ml sterile PBS; vortex.
4. To above solution, add 5 µl calcein AM; vortex.
5. If using fresh stock solution, aliquot remaining reagent into sterile aliquot tubes (25 µl per tube)
6. Remove cells from incubator and wash with PBS.
7. Add sufficient working solution to cover dish (1 ml for 35 mm dishes, 150 µl for 24 well plate).
8. Incubate (room temperature or in incubator) for 30-45 minutes.
9. Observe with fluorescent microscope using designated filter. Take photographs as desired.
10. Calcein AM is subject to hydrolysis, but working solution may be effective for 1-5 days.

B.5. Scanning Electron Microscopy

Materials:

- 25% EM grade glutaraldehyde (use in hood)
- 0.1 M cacodylate buffer, pH 7.4 (use in hood)
- 1% osmium tetroxide in cacodylate buffer (use in hood)
- 1% tannic acid

Procedure:

1. Fix cells in 2% warm glutaraldehyde for 30 min.
   Take dish from the incubator to the fume hood – wear gloves to handle glutaraldehyde. Add 25% gluteraldehyde to make 2% solution in culture medium and leave in hood during fixation.
2. Rinse in 0.1 M cacodylate buffer (in hood, with gloves) 3 times, 3-5 min. each rinse.
3. Post fix for 30 min in 1% osmium tetroxide in cacodylate buffer.
4. Post fix for 30 min in 1% tannic acid.
5. Rinse with distilled water 3 times
6. Dehydrate in graded series of alcohols to 100% ethanol (twice each for 10 min).
7. Critical point dry with CO_2.
8. Sputter-coat dried gels with gold (Denton Vacuum Desk II) for 60 s at 40 mA prior to examination with a Hitachi S-530 scanning electron microscope.

B.6. Tresyl Chloride Activation - PEO Hydrogels

(Nilsson, 1981; Harris, 1984; Demiroglou, 1990)

Materials:

- PEO hydrogels
- sterile MilliQ water
- reagent grade acetone
- dry reagent grade acetone (dried over molecular sieve beads)
- doubly distilled dry triethylamine (stored over KOH for not more than one month)
- tresyl chloride (new ampoule)
- 1 mM hydrochloric acid (HCl)
- reaction beaker
- parafilm
- aluminum foil
- convection oven
- roto-stir table
- Reagent grade acetone

B.6. Tresyl Chloride Activation - PEO Hydrogels

(continued)

Procedure:

1. Rehydrate PEO hydrogel in sterile water, and carefully weigh hydrated gel.
2. Dry reaction beaker and transfer pipets in 120°C convection for 24+ hours. Remove, seal in aluminum foil and refrigerate (4°C).
3. Place gels in a clean, dry beaker.
4. Wash gels (3x, 30 min. each wash) successively in the following solutions:
   a. Refrigerated sterile water
   b. Refrigerated 70/30 solution MilliQ water/acetone.
   c. Refrigerated 40/60 solution MilliQ water/acetone.
   d. Refrigerated 20/80 solution MilliQ water/acetone.
   e. Reagent grade acetone.
   f. Dry acetone.
5. Transfer dried hydrogels to dried reaction beaker. Add sufficient dry acetone to cover and seal with parafilm, leaving a small entrance for the pipette tip.
6. Place on roto-stir table, with stirring to create a slight vortex.
7. Slowly drip in 250 µl dry triethylamine.
8. Slowly drip in 250 µl dry tresyl chloride (0.05 M or 50% excess).
9. Allow reaction to proceed for 105 minutes at room temperature.
10. Wash gels (3x, 30 min. each wash) successively in the following solutions:
    a. Reagent grade acetone.
    b. Refrigerated 30/70 solution 1 mM HCl/acetone.
    c. Refrigerated 50/50 solution 1 mM HCl/acetone.
    d. Refrigerated 70/30 solution 1 mM HCl/acetone.
    e. Refrigerated 85/15 solution 1 mM HCl/acetone.
    f. 1 mM HCl (sterile).
11. Carefully weigh hydrogel to obtain final activated weight.
12. Store in 1 mM HCl at 4°C.

B.7. Tresyl Chloride Activation - PEO in Solution

(Nilsson, 1984; Harris, 1984; Demiroglou, 1990)

Materials:

- molecular sieve beads (4 Å)
- PEO
- methylene chloride
- doubly distilled dry triethylamine (stored over KOH for not more than one month)
- tresyl chloride (new ampoule)
- methanol (MeOH)
- conc. hydrochloric acid (HCl)
- reaction flask
- glass transfer pipets
- magnetic stir bar
- parafilm
- aluminum foil
- convection oven
- stir plate
- -20°C freezer
- refrigerated centrifuge

Procedure:

1. Dry reaction flask and transfer pipets in 120°C convection for 24+ hours. Remove, seal in aluminum foil and refrigerate (4°C).
2. Dissolve 1g PEO in 11 ml (14.6 g) methylene chloride.
3. Add 1g molecular sieve beads. After bubbles dissipate, cover and refrigerate (4°C) overnight.
4. Decant polymer solution into dried reaction vessel, add magnetic stir bar and stir to obtain slight vortex.
5. Slowly drip in 100 µl dry triethylene.
6. Slowly drip in 100 µl dry tresyl chloride (0.05 M or 50% excess).
7. Seal with parafilm, allow reaction to proceed for 105 minutes at room temperature.
8. Draw off the methylene chloride and collect in a vacuum trap for proper disposal.
9. Redissolve polymer in 50 ml MeOH and 250 µl HCl.
10. Place in -20°C freezer overnight to allow polymer to precipitate out.
11. Centrifuge at -20°C, 7000 RPM for 30 minutes.
12. Decant supernatant, redissolve polymer in 50 ml MeOH and 50 µl HCl.
13. Repeat steps 10-12 five times, the final precipitation in MeOH without HCl.
14. Dry the final residue under vacuum (45 mm Hg, gauge).
15. Lyophilize (8-10 µm Hg; condenser temperature -50°C) and store with desiccant under nitrogen in 0°C freezer.